



**UNIVERSITY OF
KWAZULU-NATAL**

**INYUVESI
YAKWAZULU-NATALI**

**TECHNOLOGIES FOR A USER-FRIENDLY
MICROFLUIDIC SYSTEM FOR PORTABLE
APPLICATIONS**

TAFARA T.R. KUNOTA

2015

Submitted as the dissertation component in partial fulfilment for the degree of Master

of Medical Science (MMDSC) in the School of Laboratory Medicine and Medical

Sciences, University of KwaZulu-Natal.

Preface

“The urge to miniaturize electronics did not exist before the space program. I mean our grandparents had radios that was furniture in the living room. Nobody at the time was saying, 'Gee, I want to carry that in my pocket.' Which is a non-thought.” - Neil deGrasse Tyson

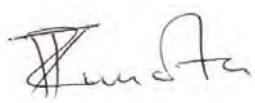
There are many reasons to believe that miniaturized microfluidic chip-based systems, which can perform most of the functions of laboratory technicians – will soon become a powerful tool in the effort to combat infectious disease in resource-limited settings. Just like integrated circuits that shrank and by so doing, democratized computing technology, microfluidics has the potential to bring the miracle of miniaturization to medical diagnostics and research.

The work described in this project is an example of innovation in bring the power of miniaturization to the several microfluidic systems that are currently suffering from technological challenges that limit their use as effective point-of-care medical diagnostic devices.

Declaration


The experimental work described in this dissertation was carried out at the KwZulu-Natal Research Institute for Tuberculosis and HIV (K|RITH), situated at the University of KwaZulu-Natal in the School of Laboratory Medicine and Medical Sciences under the supervision of Dr Frederick K. Balagadde from January 2014 to September 2015.

I Tafara Takunda Remigio Kunota declare that the work reported herein to be my own research, unless specifically indicated to the contrary in the text.

Signed:..... 

On this13thday of.....NOVEMBER.....2015.

I hereby certify that this statement is correct


.....

Dr Frederick K. Balagadde (Supervisor)

Dedications

I dedicate this work to my beloved

Mother, Mrs S.R. Kunota,

Brother, T.R. Kunota,

Cousin, A. Chifamba,

And to my

Late Father, Mr M.R. Kunota,

For their faith and unwavering support in my life.

“Now faith is the substance of things hoped for, the evidence of things not seen.”

- Hebrews 11:1

Acknowledgements

I wish to extend my gratitude to the following people:

1. My supervisor, Dr Frederick K. Balagadde, for consistently imparting his knowledge, advice and guidance for the duration of this project.
2. Yashveer Ramlakhan, for assisting me with the initial multilayer soft-lithography fabrication training and some of the technical advice.
3. Ashmika Surujdeen, for assisting me with the photolithography training.
4. Tawanda Mandizvo and Precious Dzapatsva, for the prayers, encouragement and support.
5. Members of the Balagadde Research Group, for their advice, support and entertaining group meetings and lunches for the duration of this project.

I would also like to thank the KwaZulu-Natal Research Institute for Tuberculosis and HIV (K|RITH) (for the years 2014 and 2015) and the National Research Foundation (NRF) (for the year 2015) for the financial support of this project.

My sincerest thanks goes to all those people whom I have failed to mention here for their contribution in this project.

Abstract

In the same way that the HIV virus subdues the human immune system, the HIV/AIDS epidemic has severely overloaded the health service infrastructure in resource limited countries and threatens to systematically suppress societies' capacity to cope with killer diseases. The epidemic has also directly impacted the health workforce, causing absenteeism, attrition (due to illness and death), and increased demand for provider time and skills. Advanced and miniaturized microfluidic systems can perform complex biotechnological functions such as growing bacteria, sequencing DNA and identifying disease causing pathogens. As a technology, microfluidics offers so many advantages but it also suffers from a variety of technological drawbacks that limit its wide spread practical application in hospitals and patient setting. Microfluidic systems require a lot of time (6 hours to an entire work-day) to set up and the set-up process requires the meticulous attention of highly trained personnel. We proposed the development of an automated, time conservative and user-friendly fluid-transport system (off-chip to on-chip) for Microfluidic Large Scale Integration platform based microfluidic devices. Using multilayer soft-lithography, micro-electric actuators and a LabVIEW graphical user-interface, a user-friendly automated microfluidic fluid transport system was developed. In comparison to the conventional manual loading system, the developed system can save at least 60% of the total chip preparation time required during the off-chip to on-chip fluid loading process. This system can be extended and made compatible with other devices that require complex off-chip to on-chip loading processes in microfluidic large scale integration platform based systems.

Table of Contents

Preface	i
Declaration	ii
Dedications	iii
Acknowledgements	iv
Abstract	v
List of Figures	4
List of Tables	6
List of Acronyms	7
CHAPTER 1: INTRODUCTION	9
Scope of Dissertation	11
CHAPTER 2: LITERATURE REVIEW	12
2.1 Background and Significance.	12
2.1.1 The Impact of HIV/AIDS, Tuberculosis on the Health Service Infrastructure and the Health Workforce in Sub-Saharan Africa.....	15
2.2 Current Point-of-Care Diagnostics for HIV/AIDS and TB.....	17
2.2.1 HIV POC Diagnostics and the Need for Portable, Automated, Cost Effective, High Volume and Rapid Sample Processing Diagnostic Systems.	18
2.2.2 TB POC Diagnostics and the Need for Portable, Automated, Cost Effective, High Volume and Rapid Sample Processing Diagnostic Systems.	22
2.3 Global Investment in HIV/AIDS and TB Management Programs and the Unmet Needs in HIV/AIDS and TB POC Diagnostics.....	25
2.4 Microfluidics.....	27
2.4.1 Historical Background of the Development of Microfluidic Systems.	27
2.4.2 Basic Principles of Microfluidics.....	28
2.4.3 Microfluidic Platforms and Channel Fabrication Processes.	30
2.4.4 Fluid Control Systems.....	34
2.5 Microfluidic Large Scale Integration (MLSI).....	40

2.5.1 Background.....	40
2.5.2 Device Fabrication.....	41
2.5.3 General Principle: Microvalve, Micropump and Micromixer.....	47
2.6 Point-Of-Care (POC) Testing Using Microfluidic Large Scale Integration.....	52
2.6.1 Barriers to adoption POC technologies in Resource Limited Countries.....	52
2.6.2 The Promise of Using Microfluidic Large Scale Integration systems in POC clinical diagnostic Testing.....	55
CHAPTER 3: RESEARCH AIMS AND OBJECTIVES.....	59
3.1 Problem Identification.....	59
3.2 Research Aims and Objectives.....	60
3.3 Specific Aims.....	60
3.4 Conceptual Framework.....	61
CHAPTER 4: METHODOLOGY.....	66
4.1 Materials.....	66
4.1.1 Microscopy.....	66
4.1.2 Multilayer Soft-Lithography.....	66
4.2 Chip Designs.....	74
4.3 Plug Designs.....	86
4.4 Auto-loading System.....	91
4.4.1 Background and Significance.....	91
4.4.2 Automation (Auto-loading) Characterization.....	93
4.5 Graphical User Interface Software.....	96
CHAPTER 5: RESULTS AND DISCUSSION.....	99
5.1 Microfluidic Plugs.....	99
5.2 Auto-loading System Version 1.0.....	101
5.2.1 System Characterization.....	101
5.2.2 Results and Discussion.....	103
5.3 Auto-loading System Version 2.0.....	106
5.3.1 System Characterization.....	106

5.3.2 Results and Discussion.....	108
5.4 Auto-loading System Version 3.0.....	111
5.4.1 System Characterization.	111
5.4.2 Results and Discussion.....	113
5.5 Microfluidic Chips.....	115
CHAPTER 6: CONCLUSION.....	120
CHAPTER 7: FUTURE WORK.....	121
APPENDICES.....	125
Appendix A: Single Port, Dual Port, Hybrid Dual Port Microfluidic Device Master Mold Protocol and Single Port and Dual Port PDMS Microfluidic Device Fabrication Protocol.....	125
Appendix B: Hybrid Dual Port PDMS Microfluidic Device Fabrication Protocol	130
REFERENCES.....	133

List of Figures

Figure 2.1: The distribution of the world’s population and the number of doctors according to regions in 2010.	13
Figure 2.2: The distribution of the number of nurses in the world and the doctors and nurse density per 1000 people of the population according to regions in 2010.	14
Figure 2.3: A schematic diagram showing various available TB diagnostic.	23
Figure 2.4: The different types of microvalves.	35
Figure 2.5: The different types of pumps and micropumps.	37
Figure 2.6: The different types of micromixers.	39
Figure 2.7: Process flow of microfluidic device fabrication using soft-lithography.	42
Figure 2.8: The photolithography and soft-lithography process.	44
Figure 2.9: The master mold fabrication and the replica molding processes in soft-lithography.	45
Figure 2.10: Microfluidic device architectural designs.	48
Figure 2.11: Side view illustrating the functionality of the two-layer PDMS push-down and two-layer PDMS push-up valves.	49
Figure 2.12: Linear pneumatic peristaltic micropump.	51
Figure 2.13: Rotary pneumatic peristaltic micropump.	51
Figure 2.14: Diversity of Target Product Profile (TPP), users and settings within the spectrum of POC testing.	54
Figure 2.15: A hypothetical sketch showing how a MLSI based system would perform an ELISA. .	56
Figure 3.1: A microfluidic chip connected to luer-tygon-tube connections.	62
Figure 3.2: 8 luer stubs attached to an 8-port pneumatic pressure manifold.	63
Figure 3.3: Diagram showing the new approach of using microfluidic plugs.	64
Figure 3.4: The pressure and valve control module.	65
Figure 4.1: Dual port microfluidic device geometry.	76
Figure 4.2: The individual layers of the dual port microfluidic chip.	77
Figure 4.3: Rotary and Linear pneumatic peristaltic micropumps architecture.	78
Figure 4.4: Microfluidic chip geometry with a combination of the linear and rotary peristaltic micropumps.	79
Figure 4.5: Single port microfluidic device geometry.	81
Figure 4.6: The individual layers of the single port microfluidic chip.	82
Figure 4.7: Hybrid dual port microfluidic device geometry.	84
Figure 4.8: The individual layers of the hybrid dual port microfluidic chip.	85

Figure 4.9: The proposed new system of using microfluidic plugs to insert pins into the microfluidic device	88
Figure 4.10: Diagram showing the trimmed sections of the PDMS microfluidic device’s control layer used to make PDMS plugs.	89
Figure 4.11: Epoxy adhesive microfluidic plugs.	90
Figure 4.12: 8 position dead-ended flow path – SD configuration valve schematic	94
Figure 4.13: 8 position flow-through flow path – SF configuration valve schematic	95
Figure 4.14: A screenshot image showing the front panel of the main LabVIEW VI (MagicElf) used for the SD and SF valve control.....	97
Figure 4.15: A screenshot image showing the sub-VI control board that controls the automated fluid transport system from off-chip to on-chip	98
Figure 5.1: Simple schematic illustration of the Auto-loading System v1.0 using 4 multi-position SF and SD valves.	104
Figure 5.2: Pressure and valve control module.....	105
Figure 5.3: Simple schematic illustration of the Auto-loading System v2.0 using 4 multi-position SF and SD valves.	109
Figure 5.4: Tee-pins inserted into the single port microfluidic chip.....	110
Figure 5.5: Simple schematic illustration of the Auto-loading System v3.0 using 4 multi-position SF and SD valves.	114
Figure 5.6: A rotary pneumatic peristaltic micropumps within a working PDMS microfluidic chip.	116
Figure 5.7: A linear pneumatic peristaltic micropumps within a working PDMS microfluidic chip .	117
Figure 5.8: ‘Open’ microvalves in a working microfluidic chip.	118
Figure 5.9: ‘Closed’ microvalves in a working microfluidic chip.....	119
Figure 7.1: Proposed new punch.....	123
Figure 7.2: Proposed new hybrid dual port microfluidic device geometry.....	124

List of Tables

Table 2.1: HIV-1 and HIV-2 Diagnostic Testing and Monitoring Landscape..... 20

Table 2.2: Microfluidic Channel Fabrication Processes or Methods 33

List of Acronyms

μ-TAS	micro-Total Analysis Systems
AIDS	Acquired Immune Deficiency Syndrome
APDS	Autonomous Pathogen Detection System
ART	Anti-Retroviral Therapy
CAD	Computer-Aided Design
DARPA	Defence Advanced Research Projects Agency
DNA	Deoxyribonucleic Acid
EID	Early Infant Diagnosis
ELISA	Enzyme-Linked Immunosorbent Assay
HBV	Hepatitis B
HCV	Hepatitis C
HIV	Human Immunodeficiency Virus
HPLC	High Pressure Liquid Chromatography
ID	Inner Diameter
LabVIEW	Laboratory Virtual Instrumentation Engineering Workbench
LED	Light-Emitting Diode
LOC	Lab-On-a-Chip
MDGs	Millennium Development Goals
MDR-TB	Multidrug Resistant Tuberculosis
MEMS	Microelectromechanical Systems
MSI	Microfluidic Large Scale Integration
MSL	Multilayer Soft-Lithography
MTB	Mycobacterium Tuberculosis

OD	Outer Diameter
o-PEP	post exposure prophylaxis
PCR	Polymerase Chain Reaction
PDMS	Polydimethylsiloxane
PMMA	Polymethylmethacrylate
PMTCT	Prevention of Mother-To-Child Transmission
POC	Point-Of-Care
RDT	Rapid Diagnostic Testing
RIF	Rifampin
RIPA	Radio Immunoprecipitation Assay
SAV	Surface Area to Volume ratio
TPP	Target Product Profile
UK	United Kingdom
USA	United States of America
UV	Ultraviolet light
WHO	World Health Organization
XDR-TB	Extensively Drug Resistant Tuberculosis

CHAPTER 1: INTRODUCTION

The growing demand within the global health community to find new and improved efficient medical diagnostic methods for HIV/AIDS and TB without diminishing the quality of patient care has led to the development of various point-of-care technologies. The emergence of microfluidics technology and the demand of point-of-care (POC) diagnostic solutions in the health care system stimulated an interest in further research and development of miniaturized laboratory equipment and processes with the capability of clinical diagnostics.

Point-of-care technology for medical diagnostic testing has the possibility of bringing about improved health care service delivery in resource limited settings where there has been poor management of infectious diseases due to weak health care infrastructures that do not provide the necessary access to high-quality and timely medical care. POC technology offers rapid tests enabling ample time for initiating the appropriate treatment plan of action and provide medical decisions such as referrals without requiring fixed laboratory infrastructures. Developments in the microfabrication industry have allowed clinical diagnostics to be miniaturized for use in POC medical diagnostic testing.

In the same way that cell phones shrink computer technology, microdevices shrink medical laboratories onto an iPhone sized cartridge. Microdevices, as a product of the various available microfabrication processes especially in the category of microelectromechanical systems (MEMS) or commonly referred to as lab-on-a-chip (LOC) systems can be composed by an integration of microchannels, microvalves, micropumps, microfilters and microelectronics and other mechanical and electrical components. The same fabrication processes such as photolithography and soft-lithography used in the electronics industry brought about the establishment of what has become the potentially suited and the core technology used in the fabrication of microdevices for clinical diagnostics. This rising technological platform is Microfluidic Large Scale Integration (MLSI).

Microfluidic large scale integration refers to the development of microfluidic chips with thousands of integrated microvalves and fluidic control modules [1]. Basically, microfluidics is the science and technology of systems that process or manipulate small amounts of fluids (micro- to nano-liters), using channels with dimensions of tens to hundreds of micrometres [2]. MLSI is a microfluidic platform that specifically uses an extension of soft-lithography microfabrication process developed by the Quake group in the early 2000s called Multilayer Soft-Lithography (MSL) [3]. MLSI technology can only be created in a highly maintained and equipped clean room facility. A clean room is a specially designed laboratory where the size and the number of airborne particulates are highly controlled, together with the temperature, air pressure, humidity, vibration and lighting [4].

Analogous to the manner at which computer viruses and malware affect the operating system of a computer, and the way that the HIV virus subdues the human immune system, the HIV/AIDS epidemic has severely overloaded the health service infrastructure in resource limited countries and threatens to systematically suppress societies' capacity to cope with killer diseases. One approach that addresses challenges in the health care systems in resource limited countries is research and development of new POC technologies.

Many have expressed doubts that today's global health system is remotely adequate for meeting the emerging challenges of the 21st century [5]. A groundswell of opinion suggests that a new way of thinking is needed to improve the global health systems' ability to deal with the emerging challenges and one such way is by ensuring sufficient long-term investment in health research and development [5]. We, as part of the health research and development industry are expectant of an era of powerful, low cost, portable point-of-care (POC) diagnostic devices that will help combat infectious diseases in South Africa as well as in sub-Saharan Africa as a whole where these diseases progress the most. This is where Microfluidic Large Scale Integration (MLSI) microfluidic systems come into effect. Development of advanced and miniaturized microfluidic systems that can perform complex biotechnological functions such as growing bacteria, sequencing DNA and identifying disease causing germs under the automated control of a multi-tasking computer with minimal human involvement will thereby provide the ultimate low cost, portable POC medical diagnostics tools.

Microfluidic large scale integration technology offers many advantages making it a possible suitable platform to develop POC clinical diagnostic tools that specifically address the barriers existing in the health care delivery systems in resource limited countries. Just like integrated circuits that shrank and by doing so, democratized computing technology, microfluidics has the potential to bring the miracle of miniaturization to medical diagnostics and research. For example:

- The ability to combine patient sample preparation and analysis processes onto a single, integrated microfluidic device creates benefits such as the need for less sample (therefore less time needed to grow-up microbes and less risk of exposure to infectious doses of pathogens); less reagents (therefore lower cost); automation (therefore minimal human labour costs); and small size (possible portability).
- The self-contained nature of microfluidic systems is ideal for clinical analysis and research, especially when technologists need to be insulated from the potentially hazardous pathogens such as HIV and Mycobacterium Tuberculosis (MTB).
- Automation – performance of complex biological tasks hitherto done by humans. Particularly, the microfluidic approach can multiply the output of clinical technologists by allowing them to perform hundreds or thousands of tests simultaneously on a single microfluidic chip controlled by a multitasking computer.

Scope of Dissertation

The ultimate goal of the work presented in this dissertation is the design, development and characterization of a portable, automated fluid transport system for the microfluidic large scale integration platform.

To highlight the importance of developing such systems, **Chapter 2** presents the literature available on the effect of HIV and TB on the health care infrastructure, the available point-of-care diagnostics methods and instrumentation and the unmet needs of point-of-care diagnostic testing in resource limited settings. This chapter also introduces microfluidics technology, the underlying principle and the critical components that make on-chip automation possible. The importance of research and development in new medical diagnostics which meet the necessary requirements for point-of-care testing in resource limited settings is also discussed. The chapter also presents the promise of microfluidic large scale integration systems.

Chapter 3 describes the research aims and objectives. The conceptual framework to achieve the project goals is presented at the end of this chapter.

Chapter 4 presents the methodology. The methodology presented involves the fabrication methods and protocols followed in developing the microfluidic devices. This chapter also states the development of a one-of-a-kind microfluidic plug. It also presents the user-friendly developed graphical user operating system for off-chip to on-chip automation.

Chapter 5 presents the results, analysis and discussion. In this chapter the developed automated fluid transport systems are described and the systems' strengths and weaknesses are analysed and discussed. Each system designed after the initial design was developed as a solution to the identified problems in achieving a complete, automated off-chip to on-chip fluid transport system.

Chapter 6 presents the conclusion. This chapter will provide a summary of the results obtained and how this system can be improved.

Chapter 7 presents the future work. In this chapter, proposed solutions to the final system developed will be recommended. These recommendations aim to eliminate some design flaws identified during the development, and also enhance the efficiency of the system in automating the fluid transportation.

At the end of the dissertation is the appendix section.

CHAPTER 2: LITERATURE REVIEW

2.1 Background and Significance.

Sub-Saharan Africa, is characterized as the region with the heaviest burden of disease as a result of poor health care systems, limited resources and inadequate skilled clinical personnel [6]. In 2010, as shown by Figure 2.1 (a), 12 % of the world's population resided in sub-Saharan Africa.

According to World Health Organization (WHO) statistics, represented by Figure 2.1 (b) and Figure 2.2 (a), in 2010 there were about 9.2 million doctors and 18.1 million nurses worldwide. Of all the regions in the world, sub-Saharan Africa has the least number of doctors and nurses yet it has the largest disease burden. A more revealing statistic of the inadequacy of health care personnel in sub-Saharan Africa is illustrated using Figure 2.2 (b), which shows the doctor and nurse density per 1000 of the population, and it shows that sub-Saharan Africa region has the least doctors and nurse density per 1000 people of the population. Using the data presented in Figure 2.1 and Figure 2.2, it can be seen that, regions like the Americas and Europe have a better health workforce capable of handling their population whereas regions like South East Asia and sub-Saharan Africa do not have enough doctors and nurses to provide adequate health care to their people.

Unfortunately, the inadequacy of the health workforce in sub-Saharan Africa is further worsened by the current state of affairs and challenges such as poverty, famine, infrastructure decay, political instability and other debilitating diseases [6, 7].

With critical shortages of health personnel in the health care sector in sub-Saharan Africa, it is important to determine the impact of epidemics such as Human Immunodeficiency Virus (HIV) and tuberculosis (TB) have on the health workforce.

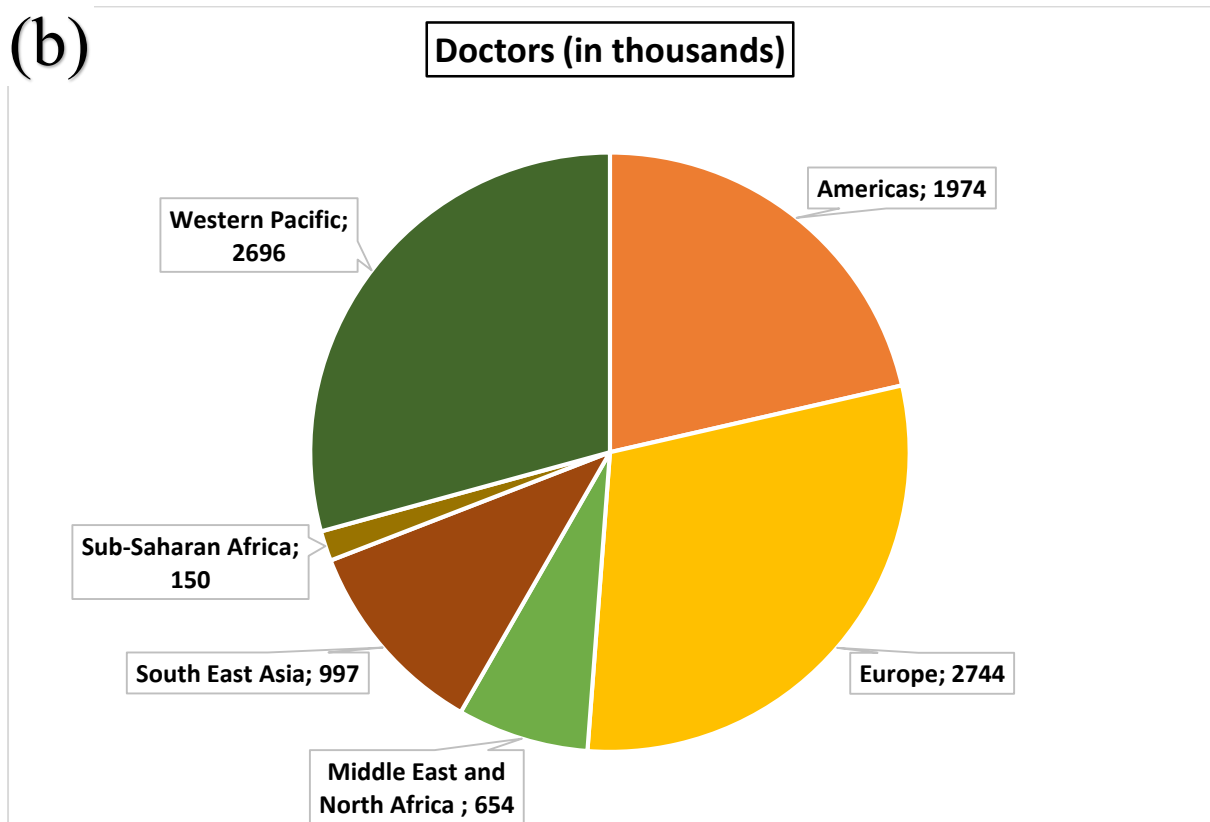
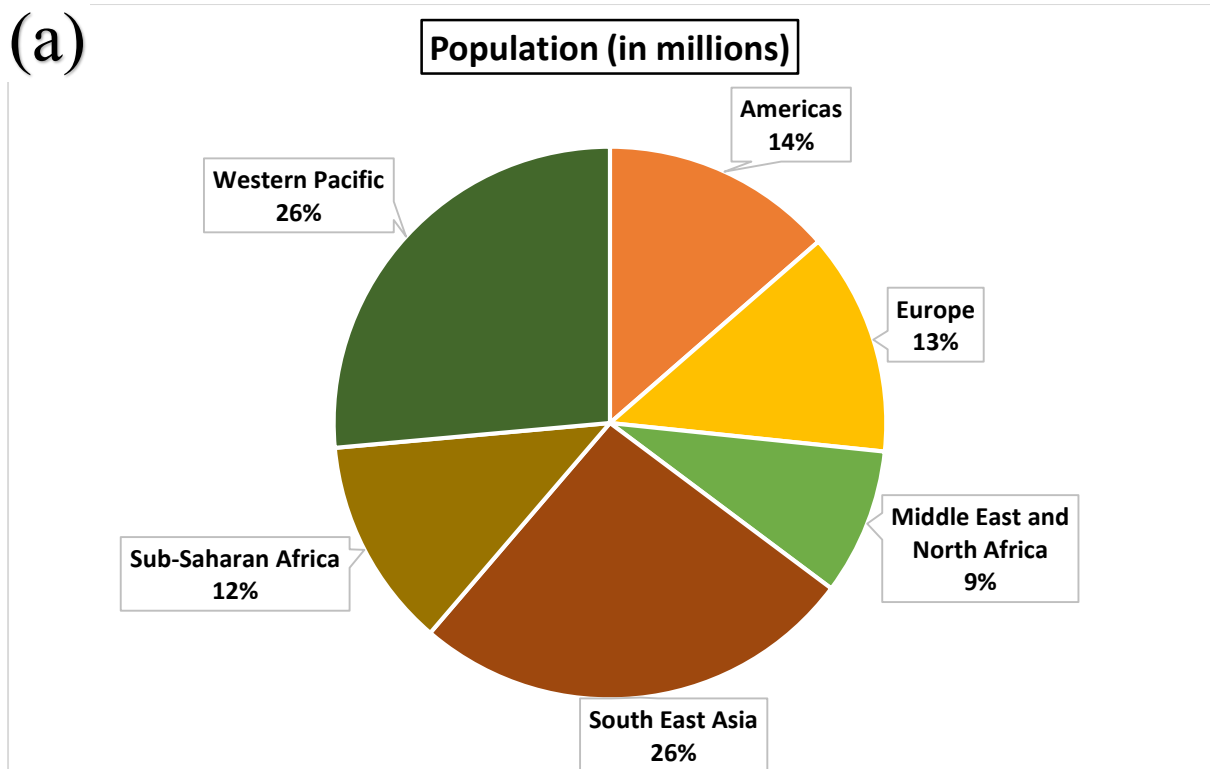


Figure 2.1: (a) Pie chart showing the distribution of the world's population per region in 2010; (b) Pie chart of the number of doctors in each of the regions in 2010. The data was obtained from References [8] and [9].

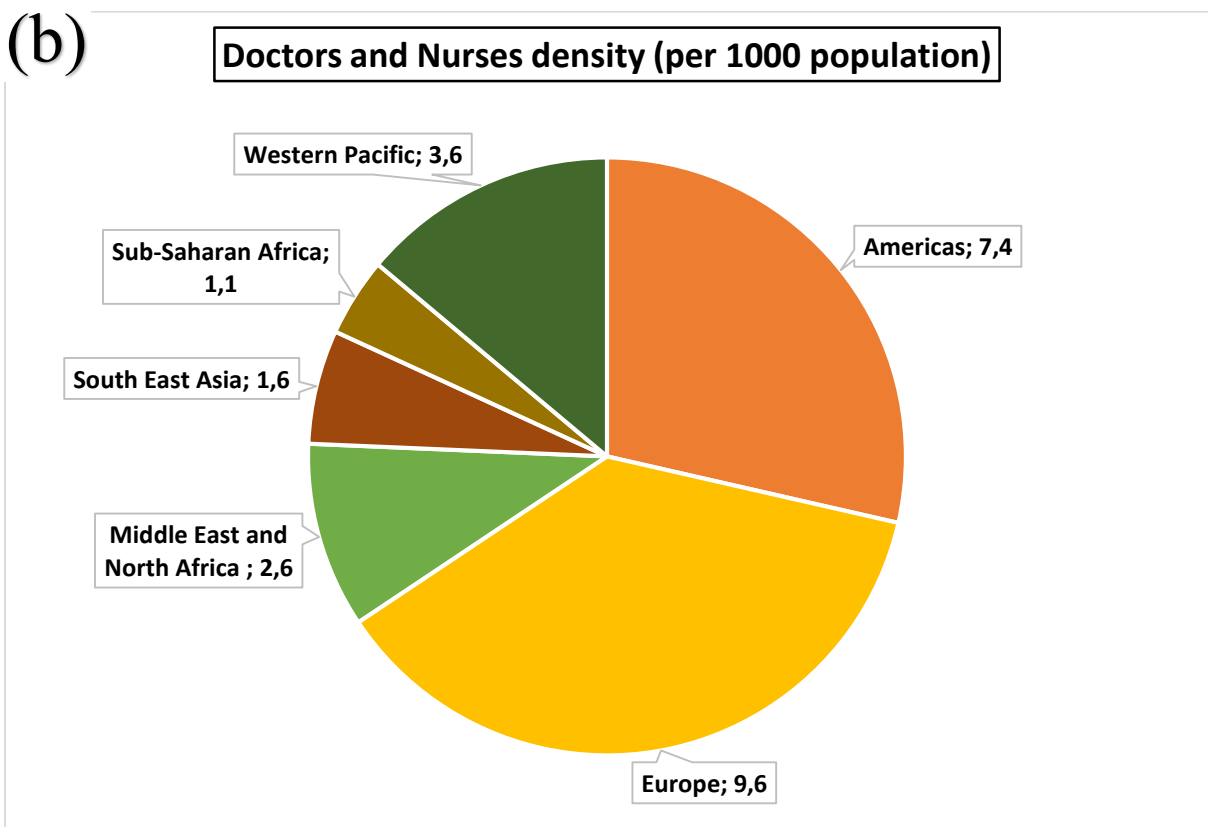
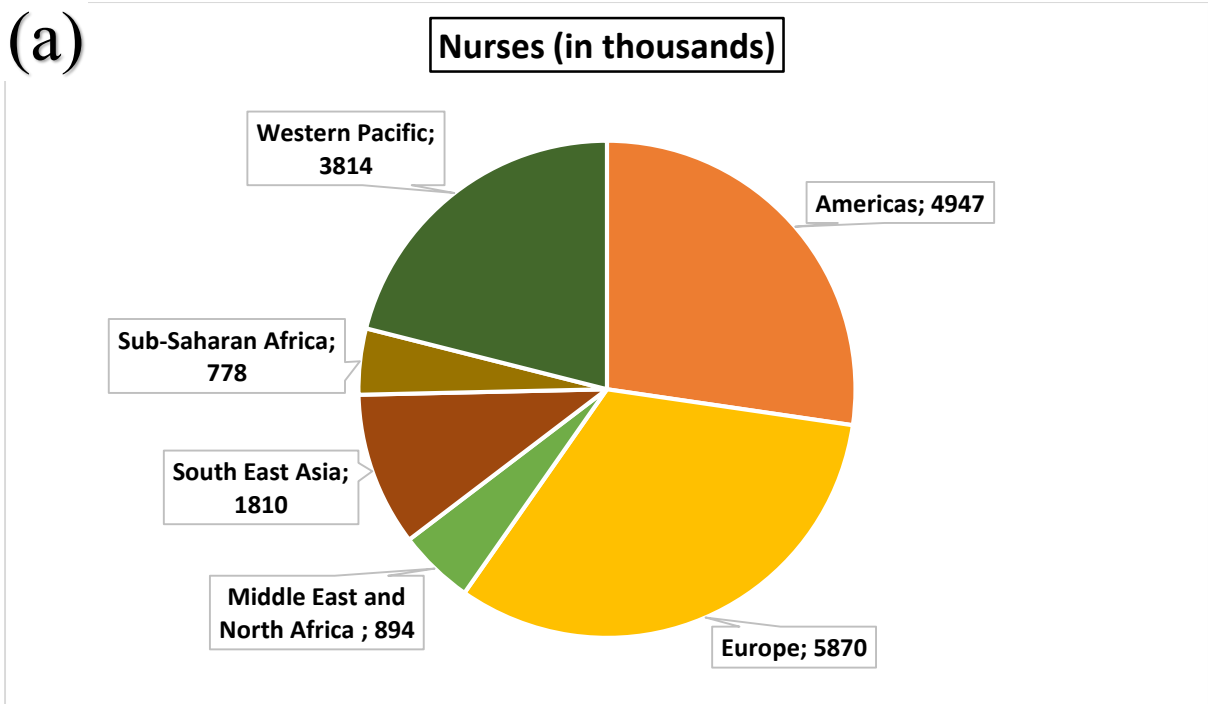


Figure 2.2: (a) Pie chart showing the distribution of the nurses in the world's population according to region in 2010; (b) Pie chart showing the doctors and nurse density in each of the regions in 2010. The data was obtained from References [8] and [9].

2.1.1 The Impact of HIV/AIDS, Tuberculosis on the Health Service Infrastructure and the Health Workforce in Sub-Saharan Africa.

In the same way the Human Immunodeficiency Virus (HIV) virus prior the stage of Acquired Immune Deficiency Syndrome (AIDS) subdues the human immune system, the HIV epidemic has severely overloaded the health service infrastructure in resource limited countries and threatens to systematically suppress the societies' capacity to cope with the killer diseases.

Before the emergence of the HIV/AIDS pandemic, health systems in sub-Saharan Africa were progressively improving the general health status of the populace [10]. The steady improvement of the health service delivery was accredited to the quality and increased access to various health services in an era with 'manageable' diseases. When HIV/AIDS arrived on the global scene, there was a substantial increase in the demand for health services in the populace. The worst hit regions were the low and middle income countries. In 2013, an estimated 35 million people were living with HIV worldwide [11]. Sub-Saharan Africa, which consists of most low and middle income countries, had approximately two thirds (24.7 million) of the people living with HIV [11, 12].

By bringing about the resurgence of previously well controlled diseases such as tuberculosis, malnutrition, diarrhoea and other opportunistic infections, their prevalence has increased due to HIV/AIDS which led to a shift in the status quo of human health, disease and health care delivery systems [10]. One of the resurgent diseases is tuberculosis (TB) and its most threatening strains, Multidrug Resistant Tuberculosis (MDR-TB) and Extensively Drug Resistant tuberculosis (XDR-TB), is being ranked as one of the deadliest communicable disease. In 2013, an estimated 9 million people developed TB worldwide and about a quarter of those where people in Africa [13]. TB remains the leading cause of death in people living with HIV, with an estimated 360 000 deaths in 2013 [13]. Most TB deaths are preventable (especially for health care givers who come into contact with these patients), however, the death tolls are still unacceptably high and efforts are being put into place to reduce it within the contexts of the Millennium Development Goals (MDGs).

The health workforce is at risk of many infections at the workplace through airborne, blood borne, faecal-oral transmission and direct contact [14]. The emergence of HIV on the global scene increased the attention of the high risks of exposure the health workforce face to blood borne pathogens. The two disease synergy, HIV and TB has led to the overcrowding of available health facilities and little is known about the impact these epidemics have had on the health care workers [15]. This synergy and other infections have also directly impacted on the health workforce. The co-existence of HIV (blood borne pathogen) and TB (airborne pathogen) poses a threat to the already under-equipped health care workforce as this synergy increased the risks of occupational exposure to either or both of the

diseases. Blood borne pathogens may be transmitted through percutaneous (contact with intact or non-intact skin) or mucocutaneous (contact with mucous membranes) and exposure to other body fluids [14]. Airborne pathogens can be transmitted through inhalation of pathogens that travel on dust particles or small respiratory droplets that become aerosolized when people sneeze, cough, laugh or exhale. One of the ways health workers get TB infections is through airborne transmission of aerosolized respiratory droplets created by TB patients when they cough and sneeze.

For successful implementation of health reforms such as prevention and treatment approaches, the human resource (health staff) need to compliment the health services. The increased disease burden in the low and middle income countries has a negative impact on the morale and job satisfaction of health workers [16], thus the balance between health care service delivery and the available health workforce has not been met.

Case studies evidently show that most HIV/AIDS and TB patients seek health care services in public hospitals at an advanced stage of illness resulting in the high inpatient death rates combined with the limited health care service deliverables such as diagnostic tools, medication, counselling has contributed to the increased professional demoralization, absenteeism and reduced productivity on the human resource [10, 16]. In many resource limited countries, the working conditions of the health workers has been characterized by poor salary and wage bills resulting in the migration of professionals to greener pastures further impacting negatively on the health care system [16]. For rural areas in these resource limited countries, they lack the access to the requisite technology and the necessary trained personnel to perform the diagnostic tests and carry out the subsequent diagnoses, especially where the situation is complicated for patients with multiple concomitant infection and malnutrition [17]. In South Africa, it is reported that health workers experience stress, fear, frustration and depression due to their contact with patients living with HIV/AIDS and some limitations of their work environments [18]. Care of dependents and funeral attendance amongst health workers attribute to the increased absenteeism. Reports suggest that an average person can be absent from work fifty (50) percent of their final year of life once they develop AIDS [10]. For example in the case of Botswana in 2003, if an average person was to use just sixty (60) days and six (6) months of sick leave in their last year, the public health sector could have lost around 23 000 and 42 500 work days respectively to AIDS amongst its health workforce [10]. This study showed the significance of the health workforce in the public health care sector.

Another example of the impact of HIV/AIDS, TB and other opportunistic diseases on the health workforce was in the year 2000, where an estimated 66 000 hepatitis B (HBV), 16 000 hepatitis C (HCV) and 1 000 HIV infections occurred worldwide amongst the health care workers due to occupational exposure to percutaneous injuries [14].

The global community has introduced improved health reforms that reduce the impact of HIV/AIDS, TB and other opportunistic infections on the health workforce [15]. There has been an increase in safer nursing and surgical techniques [16] and improvements in waste disposal, especially with needles and increased awareness of occupational post exposure prophylaxis (o-PEP) providing adequate barriers that help prevent the health workers from being infected at the workplace [14].

One suggestion to address the negative impact of the co-epidemics of HIV and TB on the health workforce is the improvisation of already existing diagnostic devices available on the market. An increased investment into new research and development of latest medical diagnostic devices can provide economically viable point-of-care diagnostics. A positive outcome of the successful implementation of these suggestions is the research and development of POC diagnostics that adequately protect the health workforce thus reducing occupational risks of exposure to infectious pathogens.

This credits a need to understand what point-of-care (POC) medical diagnostics is and how they address the impact of the co-epidemics of HIV and TB on the public health care sector and its workforce.

2.2 Current Point-of-Care Diagnostics for HIV/AIDS and TB.

In consideration of the following factors such as:

- i. Sub-Saharan Africa has the heaviest disease burden.
- ii. Sub-Saharan Africa has a critical shortage of health personnel.

Sub-Saharan Africa health care service delivery systems are poorly equipped to contend with emerging health care threats such as HIV, TB, Ebola and other opportunistic infections. Typical conditions in a mid-level health care centre in resource limited settings such as those found in sub-Saharan Africa are rather different from those in a developed-world mid-level clinical laboratory [19]. Sources of running water and electricity may or may not be available, with power being at best sporadic with wide fluctuations in voltage [19]. Dust, wind and contaminating pathogens are very common coupled by ambient temperatures that range from 10 °C to more than 40 °C [19]. Potentially high-risk human samples, containing biosafety level (BSL) -2 and BSL-3 pathogens are casually handled with few to none precautions taken except using gloves [19]. With such conditions in place, it is still possible to perform microscopy, most lateral flow assays, some blood chemistry, cytology and enzyme-linked immunosorbent assays (ELISAs) in these mid-level health care centres [19]. With stretched and scarce medical professionals, limited resources and heavy disease burden, low-cost point-of-care (POC) tests have transformed the management of several major infections such as HIV, TB and malaria [20]. Examples include, the HemoCue WBC system (HemoCue AB, Sweden); a POC

testing device used in hematology for obtaining white cell counts, Daktari CD4 system (Daktari Diagnostics Inc., USA); a POC device used for CD4 cell counting in HIV/AIDS management, Xpert MTB/RIF (Cepheid, USA); a POC device used to simultaneously detect mycobacterium tuberculosis (MTB) and rifampin (RIF) resistance by Polymerase Chain Reaction (PCR) amplification in TB diagnostic testing and the VIKIA® Malaria Ag Pf/Pan (BioMérieux/IMAccess, France); an immunochromatographic technology based POC test for malaria diagnostic testing.

Point-of-Care (POC) testing is the laboratory diagnostic testing performed outside the well-controlled environment of the traditional, physical facilities of the clinical laboratories near the clinical care delivery site [21]. The medical diagnostic tools and techniques used in such an environment are called POC diagnostics.

POC tests are designed in such a way that they are simple enough to use at the primary care level in remote and resource limited settings with no laboratory infrastructures. POC tests are often cost-effective for both developed and developing nations to complement their health care delivery systems [22].

2.2.1 HIV POC Diagnostics and the Need for Portable, Automated, Cost Effective, High Volume and Rapid Sample Processing Diagnostic Systems.

The HIV health care service delivery includes a spectrum of services such as diagnosis, treatment, monitoring and support. The HIV diagnosis sub-spectrum involves the HIV testing (for adults and children), early infant (younger than 18 months) diagnosis (EID), disease staging, and treatment, monitoring and drug resistance assay [6].

HIV initial tests include HIV antibody tests (measured in blood, saliva or urine), p24 antigen tests and polymerase chain reaction (PCR) tests [23]. Amongst these tests, HIV antibody tests are most commonly used for routine diagnosis and HIV rapid disposable tests which use blood or saliva are most commonly used for screening at point-of-care for patients older than 18 months of age [23]. For EID, PCR based tests are performed on HIV-infected and HIV-exposed infants and are most commonly used in programs that provide prevention of mother-to-child transmission (PMTCT) services. Confirmatory tests of the diagnosis, when patient tests positive for HIV are also performed using rapid disposable tests and this is the common practice in resource limited settings. In other settings the confirmatory tests include the use of an enzyme-linked immunosorbent assay (ELISA) at point-of-care or a Western Blot and Radio Immunoprecipitation Assay (RIPA) which are conducted in a laboratory.

Table 2.1, is a summary of the available HIV diagnostic tests being used by health systems. Most serological tests are POC and enzyme immunoassay-based methods thus most of the POC diagnostic tools that use these methods are immunochromatographic-lateral flow devices [6].

Immunochromatographic-lateral flow devices also commonly referred to as ‘sol particle immunoassay (SPIA)’ [24], ‘immunochromatographic strip (ICS)’ [25], ‘test strip’ or ‘immunocapillary tests’ are all lateral flow tests (LAT) tests that fall under the ‘Capillary’ microfluidic platform. In lateral flow tests, the liquids are driven by capillary forces where liquid movement is controlled by the wettability and feature size of the porous or microstructured substrate [26]. A basic necessity of these tests is that all the required chemicals for the reaction should be pre-stored within the strip beforehand, and once the test is performed, the readout is usually optically visible to the naked eye and this is often implemented as a colour change in the detection area [26]. A LAT device is comprised of an inlet port and a detection window. Within the device is the core made up of several pre-stored wettable materials that provide the biochemicals and capillary capacity to drive the sample through the core during the test. A sample is introduced into the device via the inlet port and onto a sample pad which holds back contaminations and dust [26]. Through capillary action, the sample is transported into the conjugate pad, where antibodies conjugated onto a signal-generating particle are rehydrated and bind to the antigens in the sample [26]. The binding reaction is repeated as the sample flows into the incubation and detection pad where on the first line (referred to as the control line) a second type of antibody catches the particles coated with antigens and in the event that there are particles that did not bind to an analyte in the first test line; these are caught by a third type of antibodies. Typically, for lateral flow devices, in the detection window, the first control line shows a successful processed test, while the second line (referred to as the test line) shows the presence or absence of a specific analyte [25, 26]. Examples of immunochromatographic-lateral flow devices are, the OraQuick *ADVANCE*® Rapid HIV-1/2 Antibody Test [27], Reveal G3 Rapid HIV-1 Antibody Test (Reveal G3) [28] and the Uni-Gold™ Recombigen HIV [29].

Typically, some of the advantages offered by serological POC diagnostic tools are:

- i. Rapid: - quick turnaround time to obtain results, usually within minutes.
- ii. Cost effective: - the tools make the test inexpensive and affordable.
- iii. High sensitivity: - they have a good sensitivity, for example, ELISA commercial kits have a sensitivity greater than 99.5 %, making them useful for screening a large number of blood samples [25].

Table 2.1: HIV-1 and HIV-2 Diagnostic Testing and Monitoring Landscape obtained from Reference [25]. For example, many POC serological tests and enzyme immunoassay-based methods use immunochromatographic-lateral flow devices even though specificity is a limitation on these tests. Most of the HIV-1 antibody screening assays have more patient approval because of their non-invasive nature.

TEST	Examples
HIV-1 Antibody Screening Assays	<ol style="list-style-type: none"> 1. ELISA 2. Rapid Latex Agglutination 3. Rapid Tests 4. Home Access 5. Dot Immunobinding 6. Urine 7. Oral Fluid
HIV-1 Viral Identification Assays	<ol style="list-style-type: none"> 1. Plasma HIV RNA Assays 2. Viral Culture 3. DNA PCR 4. p24 Antigen Assay
HIV-1 Confirmatory Antibody Assays	<ol style="list-style-type: none"> 1. Western Blot 2. Indirect immunofluorescence 3. Line Immunoassay 4. Radio immunoprecipitation Assay
HIV-2 Monitoring Tests	<ol style="list-style-type: none"> 1. Lymphocyte Analysis 2. Viral Identification Assays <ol style="list-style-type: none"> i. Reverse transcriptase Polymerase Chain Reaction (RT-PCR) ii. Branched DNA Assay (bDNA) iii. Nuclei Acid Sequence based assay (NASBA) 3. Drug Resistance Tests <ol style="list-style-type: none"> i. Genotyping ii. Phenotyping

One of the major limitations of serological POC diagnostic tools is specificity. There has been a consensus on the specificity of some of these tests. In cases of false positives, confirmatory testing is required, and when another serological test was used, there were flaws in the performance as highlighted by work done by [30]. According to a study performed in the Democratic Republic of Congo, the most probable causes of the false-positive results were serological cross-reactivity or non-specific immune reactivity [31].

For HIV POC diagnostics that include non-blood fluid samples such as saliva and urine, they offer the same advantages as serological tests and have more patient approval because of their non-invasive nature. HIV POC diagnostics show comparable accuracy to serological tests [32] and therefore one could apply the same serological tests limitations to such tests.

Another important HIV POC diagnostic tool is the use for CD4 counts. POC tools for CD4 counts include flow cytometric devices, cartridges with microfluidic adaptations to flow cytometry or immunochromatographic strips [6]. Some of the advantages of such CD4 count POCs are that they offer rapid results and absolute CD4 counts. Two major limitations of CD4 count POCs is that they are relatively expensive and offer limited throughput of results [33]. An improvement to newer CD4 count POC diagnostic tools by incorporating biochips eliminates the manual sample preparation process step, which was one of the limitations of these devices [6].

With the current available POC tools, there is still a need for simple and cost effective POC diagnostics for EID for viral load determination. The current diagnostic tools for EID and viral load testing are expensive and some require laboratory infrastructures for support and those that are not are not readily available in resource limited settings [33]. It is believed that anti-retroviral therapy (ART) programs in resource limited settings that do not have access to simple and cost effective HIV POC diagnostics lead to treatment failure thereby impacting the quality of clinical management [33]. If the need for HIV viral load POC diagnostics is met, there is an expected reduction in the cost of ART programs and a reduction of laboratory infrastructures required [23].

The requirement for an automated, compact and portable, user-friendly, accurate, highly sensitive, contained POC diagnostic tool that requires minimal human involvement (decrease exposure of infectious agents to health personnel) with a high turnaround time, high throughput of sample processing and that is accessible by the poorest and most vulnerable people in resource limited settings is still unmet.

2.2.2 TB POC Diagnostics and the Need for Portable, Automated, Cost Effective, High Volume and Rapid Sample Processing Diagnostic Systems.

Tuberculosis is still one of the world's deadliest communicable diseases. TB has an enormous global burden, with an estimated 9 million people worldwide developing TB in 2013 alone and TB diagnosis remains a problem [13]. The epidemic is most deadly in high burden countries with high HIV prevalence. An estimated 1.1 million (13%) of the 9 million people who developed TB globally in 2013 were HIV-positive and Africa was the region with most of the HIV-associated TB cases [13]. Conventional TB diagnosis mainly relies on sputum smear microscopy, culture, tuberculin skin test and chest radiography. These tests do provide the needed diagnosis and are often used in resource limited settings however they do have several limitations. Some of these diagnostic tests have shown to be insufficient to help the control of TB in HIV ravaged regions [34]. Figure 2.3 shows some of the available TB diagnostic platforms being used in the current health care system. Amongst the current available TB diagnostics, there are those that can be classified as POC and those that are immune based systems of which some involve serological tests. Focusing on some of these available diagnostics, we discuss their strengths and limitations.

Sputum smear microscopy offers the following advantages to some extent such as; its relatively inexpensive, rapid (i.e. offers same day results when direct Ziehl-Neelsen microscopy is used in conjunction with LED fluorescence microscopy) and its non-requirement of specialized equipment such as the microscope which also can be used for other scientific purposes such as the diagnosis of other infectious diseases such as malaria and urinary tract infections. However, this diagnostic test has its limitations which includes the requirement of laboratory infrastructure and well-trained technician on-site [33]. These factors alone make this platform less viable for the much required high throughput and accurate POC TB diagnostics in resource limited settings where there are health personnel and laboratory infrastructure shortages.

Culture based growth detection tests are one of the most traditional and common reliable tests in resource limited settings. Culture based tests have high sensitivity and allows identification of mycobacterium tuberculosis and the differentiation between drug-sensitive and drug-resistant strains [35]. This diagnostic test has many limitations such as the requirement of laboratory infrastructures (Biosafety level, BSL 2 or BLS 3) and trained personnel. It also has a turnaround time of 2-6 weeks which is not ideal for high disease burdened regions with stretched resources. Depending on the disease burden of the region and availability of laboratory structures, this test can be very expensive (consumables, safety equipment, transportation and storage of samples etc.), as large incubation spaces and trained personnel are required to process the large volumes of samples that need processing.

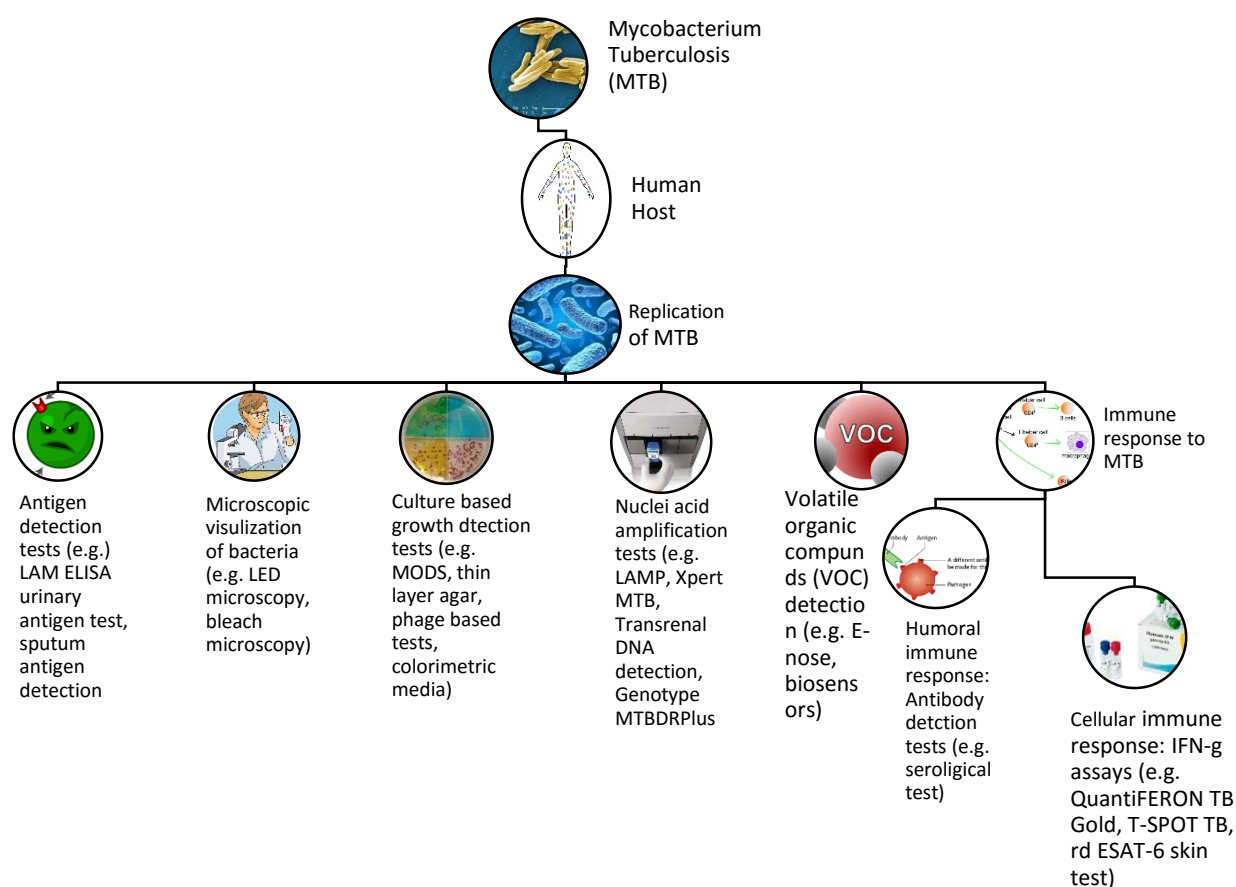


Figure 2.3: A schematic diagram showing various available TB diagnostic platforms. Amongst the current available TB diagnostics, there are those that can be classified as POC and those that are immune based systems of which some involve serological tests. For example; sputum smear microscopy offers the following advantages to some extent such as; its relatively inexpensive, rapid (i.e. offers same day results when direct Ziehl-Neelsen microscopy is used in conjunction with LED fluorescence microscopy) and its non-requirement of specialized equipment such as the microscope which also can be used for other scientific purposes such as the diagnosis of other infectious diseases such as malaria and urinary tract infections. Culture based growth detection tests are one of the most traditional and common reliable tests in resource limited settings. Culture based tests have high sensitivity and allows identification of mycobacterium tuberculosis and the differentiation between drug-sensitive and drug-resistant strains. Images obtained from References [36-46].

These limitations hamper the decentralisation of culture based tests in resource limited settings as governments are forced to build less laboratory infrastructures leading to overcrowding of already existing infrastructures ultimately leading to large volumes of unprocessed samples and increased turnaround times to get results to patients.

Most TB diagnostics used at POC are the humoral immune response tests (e.g. serological tests for antibody detection); cellular immune response tests (e.g. Interferon-Gamma Release Assays (IGRAs), tuberculin skin tests etc.) and antigen detection tests (e.g. urine LAM tests). These POC tests offer a rapid (same day results), are inexpensive and require minimal training for performing the tests. In spite of the inexpensiveness of these tests, they are known to be highly inaccurate, inconsistent and often associated with poor sensitivity. Due to these limitations, for example, antibody detection tests are not WHO recommended for clinical use [33].

Nucleic acid amplification tests (NAATs) have been evaluated for TB diagnosis and detection of drug resistance for nearly two decades [47]. NAAT tests offer many advantages such as high specificity, high accuracy, minimal training required for health personnel, rapid results (get results within 90 minutes). The most common NAAT is the Xpert MTB/RIF system which also provides MDR-TB screening. The Xpert MTB/RIF assay simultaneously detects mycobacterium tuberculosis (MTB) and rifampin (RIF) resistance by PCR amplification. The Xpert MTB/RIF offers accurate results and has the potential to be used for TB POC diagnostics as it requires minimally trained health personnel. However, the Xpert MTB/RIF fails to meet the important POC requirements on two important grounds: at current prices, it is expensive and unaffordable in many resource limited settings and it requires sophisticated equipment that cannot be deployed at the community level [33]. A further drawback of the Xpert MTB/RIF assay is that in developing countries, its pricing in the private sector is higher than that in the public sector further imposing barriers in its accessibility to patients.

With the current TB diagnostic tools available, it is evident that the most effective tools are still laboratory based and one of the potential POC tests, the Xpert MTB/RIF has a major economical drawback that comes with it. Most TB diagnostics still require trained health personnel and a lot of human involvement in the sample preparations.

With this in mind, one could say that a new TB POC diagnostic tool that is automated, compact and portable, user-friendly, accurate, highly sensitive, and requires minimal human involvement (decrease exposure of infectious agents to health personnel) with a high turnaround time and high throughput of sample processing is highly required. Most importantly, this POC must be accessible to the poorest and most vulnerable people to help TB control in resource limited settings.

2.3 Global Investment in HIV/AIDS and TB Management Programs and the Unmet Needs in HIV/AIDS and TB POC Diagnostics.

Based on the current available POCs platforms for HIV and TB diagnosis, an effective way to have these epidemics under control is the design, development and implementation of economical viable solutions to HIV and TB diagnosis in resource limited settings. It is estimated that diagnostics comprise about 3-5% of the health care spending only, yet it has an impact of about 70% on health care decisions, therefore relatively modest investment in diagnostic technology could potentially lead to drastic improvements on the overall health care service delivery system [48].

An estimated global expenditure of about US\$ 19.1 billion was available from all sources for the AIDS response in 2013 [11]. Global funding for TB prevention, diagnosis and treatment was estimated to be US\$ 6.3 billion in 2014 [13] and this excludes resources required for research and development for new TB diagnostics, drugs and vaccines. An estimated US\$ 2 billion a year is required for research and development for new TB diagnostics, drugs and vaccines. A major source of funding in the global fight against HIV and TB epidemics has been the US President's Emergency Plan for AIDS Relief (PEPFAR) [49]. PEPFAR has contributed about US\$ 46.5 billion through the United States government bilateral HIV/AIDS programs, about US\$ 1.9 billion to United States government bilateral TB programs and about US\$ 10.6 billion through the Global Fund, in total over US\$ 59 billion has been provided by PEPFAR from 2003 to 2014 to support HIV/AIDS and TB programs [50]. Many new diagnostic technologies are under development and some are steadily entering the market, even with the enormous global expenditure mentioned above, funding is still required to rapidly evaluate whether these tests are accurate and ready for implementation.

The unmet needs of HIV diagnosis in Sub-Saharan Africa and other resource limited settings are clearly substantiated by the lack of 'suitable' HIV POC diagnostic platforms for adult diagnosis, early infant diagnosis (EID) and for viral load measurements. The term 'suitable' here refers to simple, affordable, quick, accurate, equipment-free, automated, high sample processing throughput and user-friendly. Unmet needs in TB diagnosis can be seen by the lack of an affordable 'dipstick' type of molecular TB POC test that offers POC tests for all forms of active TB, regardless of HIV status or CD4 count, which is laboratory decentralized, affordable and self-contained (to provide safety for health personnel).

Despite the efforts and financial resources that have been invested, suitable HIV and TB POC diagnostics for resource limited settings are still unavailable. To reduce the global expenditure and required funding for HIV/AIDS and TB programs and simultaneously provide a support structure for some of the failing health care infrastructures in resource limited settings with the fight against

HIV/AIDS and TB epidemics, an ideal POC diagnostic platform that encompasses some of the following specifications ideal for POC delivery [51] is required:

- i. Readout and Medical decision: User-friendly platforms that require at most one day of training time for health technicians operating the POC diagnostic tool this and should also provide conclusive results that allow a medical decision to be made, e.g. if treatment initiation is required depending on the results.
- ii. Sensitivity and Specificity: When performing tests, it should have high sensitivity for a wide range of infection types regardless of HIV status or CD4 counts, age (adult or infant) compared to other testing methods.
- iii. Time to results: Patients must receive results the same day. A desirable timeframe would be 15 minutes to 3 hours depending on the test and number of tests required.
- iv. Throughput: Be able to do more than 20 tests per day by a single laboratory technician.
- v. Specimen type: Depending on age, for adults, desired specimens would be urine, oral swabs, breath, finger pricked blood, and if necessary sputum. For children/infants, desired specimens would be urine, oral swabs, finger/heel pricked blood.
- vi. Reagents: Small volume of reagents to help reduce test cost.
- vii. Instrumentation: A platform that is light, portable (increasing the access of health diagnostics by poorest and vulnerable people) with less maintenance cost and works in all POC field conditions (e.g. atmospheric conditions such as temperature and humidity conditions, and also environmental conditions such as high and low altitudes etc.).
- viii. Sample preparation: Automated to reduce human involvement.
- ix. Power Source: Preferably easily rechargeable battery power platforms.
- x. Waste disposal: Environmental acceptable disposal, and normal sharps disposal protocols (if sharps where required for the test), desirably sharps should not be required to reduce infectious agents exposure to health care technicians [14].
- xi. Cost: Desirably ZAR 100 or US\$10 per test after scale-up.

A scientific platform that offers commitment to the development of HIV and TB POC diagnostic devices in Microfluidic Large Scale Integration (MLSI). This leads to understanding the curiosity of what microfluidics really is and how it addresses the specifications of an ideal HIV and TB POC diagnostic tool for resource limited settings.

2.4 Microfluidics

2.4.1 Historical Background of the Development of Microfluidic Systems.

Microfluidics encompasses the science and technology of small volumes (10^{-9} to 10^{-18} litres) of fluid (liquids and gases) manipulation in channels having cross-sectional dimensions in the order of tens to hundreds of micrometre [2, 52]. The distant microfluidic origins lie in micro-analytical methods such as gas-phase chromatography, high pressure liquid chromatography and capillary electrophoresis and it does not come as a surprise that the first miniaturized microfluidic device was a gas chromatographic analyser fabricated on a silicon (Si) wafer that was developed at Stanford University in the 1970s [53]. The first high-pressure liquid chromatography (HPLC) column microfluidic device fabricated using Si-Pyrex technology was developed and then published in 1990 by Manz [54]. The combination of these micro-analytical methods that form the origins of microfluidics and the emergence of laser use in optical detection gave microfluidics the ability to use very small quantities of samples and reagents to perform separations and detections with high resolution and sensitivity [2].

Besides molecular analysis, microfluidic technology advancements can be attributed to other fields such as biodefense, molecular biology and microelectronics. The advent of chemical and biological weapons on the global forefront, provide an opportunistic time for microfluidic technologies to be further developed since these weapons posed major military and terrorist threats. To counter these threats, the Defence Advanced Research Projects Agency (DARPA) of the US Department of Defence supported a series of programmes aimed at developing field-deployable microfluidic systems designed to serve as chemical and biological threat agent detectors [2]. One such developed microfluidic device was the Autonomous Pathogen Detection System (APDS) [55]. Increase in the demand for improved microanalysis methods in molecular biology due to advancements in genomics in the 1980s especially the need for high-throughput DNA sequencing further stimulated the advancement of microfluidic technology.

The most contributing stimulant to advances in microfluidic devices was microelectronics. Processes such as photolithography and other techniques that had been successful in silicon microelectronics and in the microelectromechanical systems (MEMS) had a direct impact on microfluidics [2], especially on the fabrication processes needed to form micro-channels.

Since its birth, microfluidics has many platforms which vary in the way fluids are manipulated, method of micro-channel fabrication, materials used in the fabrication process and the intended

application of the microfluidic technology. This milestone stimulated the further development of microfluidic technology for molecular biology especially in genomics.

The ability to use very small quantities of samples and reagents, and when coupled with technological advancements; microfluidic devices can perform separations and detections with high resolution and sensitivity. For these reasons, the field of microfluidics is being used in molecular analysis, biodefense, molecular biology, microelectronics and medical diagnostics.

2.4.2 Basic Principles of Microfluidics.

There are three important parameters that help describe the basic principles of microfluidics, these are the Reynolds Number, Poiseuille's Law and Surface Area to Volume Ratio.

2.4.2.1 Reynolds Number.

At the microscale level it is fluid viscosity that dominates fluid behaviour rather than inertia. For this reason, microfluidic flow is laminar and not turbulent, thus enabling the observation of cellular behaviour under high magnification. The flow of fluid through a microfluidic channel can be characterized by the Reynolds number.

The Reynolds number is defined mathematically by equation (1) below,

$$Re = \frac{l \cdot V_{avg} \cdot \rho}{\mu} \dots\dots\dots (1)$$

Where, l is the most relevant length scale and is given by $l = 4 \frac{A}{P}$, A is the cross-sectional area of the channel, P is the wetted perimeter of the channel, μ is the viscosity, ρ is fluid density and V_{avg} is the average velocity of the flow.

The Reynolds number Re depends on material properties like density and viscosity. For laminar flow, $Re \ll 1$ and turbulent flow occurs at high Reynolds number, typically $Re > 10^3$ [56]. Due to the small dimensions of microchannels, the Re is usually less than 100, often less than 1 [57]. Reynolds numbers for common microfluidic devices can be estimated as follows. With water at 20 °C and 1 atmospheric pressure as the working fluid, typical fluid velocity is $V_{avg} = 1 \text{ cm/s}$, channel length scale as $l = 100 \text{ }\mu\text{m}$, fluid density as $\rho = 1.0 \text{ g/cm}^3$ and fluid viscosity as $\mu = 10^{-3} \text{ Pa}\cdot\text{s}$ [56, 58, 59]. With these numbers, $Re = [10^{-5} \text{ (m)} \times 10^{-2} \text{ (m/s)} \times 10^3 \text{ (kg/m}^3)]/[10^{-3} \text{ (kg m}^{-1}\text{s}^{-1})] = 0.1$. This low value of Re affirms that microfluidic flow is laminar. Low values of Re in microfluidic devices is due to the dominant viscous forces in microfluidic flow, which thus provide smooth fluid motion [60].

2.4.2.2 Poiseuille's Law.

Since microfluidic flow is laminar, laminar flow of viscous and incompressible fluid, the pressure drop and the flow rate as well as the effective resistance might be obtained by using the Poiseuille Equation [57], shown by equation (2) below,

$$\Delta p = \frac{8\mu L Q}{\pi r^4} \quad \underline{\text{And}} \quad R = \frac{8\eta \Delta x}{\pi r^4} \quad \dots\dots\dots (2)$$

Where Δp is the pressure drop, L is the length of the channel, r is the radius of the channel, R is the resistance to flow, η is the dynamic fluid viscosity, Q is the volumetric flow rate and x is the distance in the direction of flow.

2.4.2.3 Surface Area to Volume Ratio (SAV).

One other characteristic principle of microscale and nanoscale devices is the Surface Area to Volume ratio (SAV). Typically, for large SAVs, surface forces (such as surface tension) are made the dominant force while the influence of inertial and body forces is greatly reduced [61]. Digital microfluidic technology utilises a microfluidic architecture that takes advantage of the effect of having large SAVs. In this technology, the droplets of water or oil are created and transported in a controlled fashion to achieve functions such as storage, mixing, chemical reaction or analysis in a discrete manner [61]. These droplets are formed using the surface tension properties of liquid and hydrophobicity control of the substrate is done using electrical fields and material coating [61]. Having large SAVs is a beneficial for on-chip microfluidic Capillary Electrophoresis (CE) devices as it increases efficiency in the microchannels by removing excess heat more rapidly [62]. Small SAVs in CE devices leads to the unfavourable effect of nonlinear flow, excessive heat dissipation and faradaic reactions [61]. However, when transporting fluids using electrokinetic flow, the large SAVs allows macromolecules to quickly diffuse and adsorb to channel surfaces thereby reducing the efficiency of the pumping [62]. Although there has been much research to diminish this problem, microfluidics in not yet ideal to use when surface fouling is a concern [61].

2.4.3 Microfluidic Platforms and Channel Fabrication Processes.

2.4.3.1 Microfluidic Platforms.

Microfluidics research was pioneered by individuals from the traditional engineering and science disciplines. Because of this, microfluidics research has evolved into a multidisciplinary field with widespread applications available on various microfluidic platforms.

A microfluidic platform comprises of an easily combinable set of microfluidic unit operations that allows assay miniaturization within a consistent fabrication technology [26]. These platforms are mainly classified according to their fluid handling mechanisms. There are five major microfluidic platforms, and these are:

- I. Capillary
- II. Pressure driven
- III. Centrifugal
- IV. Electrokinetic
- V. Acoustic

I. Capillary Microfluidics

This platform utilizes capillary forces as the driving force of liquids. Liquid movement is controlled by the wettability and feature size of the porous or micro-structured substrate [26]. Lateral flow tests commonly referred to as test strips (e.g. pregnancy test strip kit) are a good example of a capillary based microfluidic platform. The use of colour change within the visible light region of the electromagnetic wave spectrum is used as a detection criterion.

II. Pressure Driven Microfluidics

This is one of the most common and diverse microfluidic platforms that encompassed technologies used in other subcategories such as Microfluidic Large Scale Integration (MSLI), segmented flow microfluidics, linear actuated microfluidic devices and pressure driven laminar flow microfluidic devices. In this platform, pressure is used for fluid handling by:

- i. Mechanical displacement of the fluid itself, for example using a plunger system.
- ii. Creating pressure gradients which lead to hydro-dynamically stable laminar flow profiles in the micro-channels using pumps, micropumps and pneumatic displacement of membranes [26].

- iii. Pneumatic displacement of membranes using microvalves.

N.B.: This project was performed in the Pressure Driven Microfluidics Platform, specifically Microfluidic Large Scale Integration (MLSI). A more detailed account of MLSI will be given in one of the following sections with “*Microfluidic Large Scale Integration*” as the title.

III. Centrifugal Microfluidics

In centrifugal microfluidics, all processes are controlled by the frequency protocol of a rotating microstructured substrate where the forces at play include the centrifugal force, Euler force, Coriolis force and the capillary force [26]. Assays are put into practise as a sequence of liquid operations arranged from radially inward positions to radially outward positions. Liquid transport is instigated by the centrifugal force directed outwards in the radial direction where the frequency of rotation makes it possible to scale the centrifugal force over a wide range of magnitudes [26]. Using a tunable flow resistance of the fluidic channels, small flow rates in the order on nL per second and high throughput continuous flows up to 1 mL per second can be generated [63]. This allows the successful scaling of flow rates over 6 orders of magnitude independent of chemical composition, ionic strength, conductivity and pH value of the liquid and because of this attribute, it opens a wide field of possible applications [26]. Depending on the channel geometry and wetting properties of the liquid, liquid transport at rest is realized by capillary forces. Liquid valves in centrifugal microfluidics are generally classified as passive valves [26]. These include valves like the geometric capillary valve [64], hydrophobic valve [65], centrifugo-pneumatic valve [66] and hydrophilic siphon valve [67]. Centrifugal microfluidics has the potential to be used in POC settings as shown by work done by S. Hugo et al. [68] and S. Smith et al. [69].

IV. Electrokinetic Microfluidics

In electrokinetic microfluidics, the unit operations are controlled by electric fields acting on electric charges or electric field gradients acting on electric dipoles [26, 57]. Depending on buffers and the sample, several electrokinetic effects such as electroosmosis, electrophoresis, dielectrophoresis and polarization superimpose each other [26]. Of the above mentioned effects, electroosmosis can be used to transport the whole liquid bulk while the other mentioned effects can be used to separate different types of molecules or particles within the bulk liquid. In this platform, the microfluidic channel has a charged solid surface that induces an opposite net charge in the adjacent liquid layer [26]. When an electric potential is applied along the channel, the positively charged liquid molecules are attracted by electrostatic forces and thus move towards a corresponding electrode. Basically, fluid motion in electrokinetic microfluidics is superimposed by the movement of ions and charged molecules, which are either attracted or repelled by the electrodes depending on their charge and the velocity of these molecules depends on the charge and hydrodynamic radius [26]. The molecule's charge and hydrodynamic radius provides a distinction between molecular entities and it is this distinction that is used in electrophoresis to separate charged molecules.

V. Acoustic Microfluidics

The microfluidic unit operations in this platform are mainly controlled by surface acoustic shock waves. The shock waves are generated by well-arranged surrounding sonotrodes which define the droplet manipulation area [26]. The droplets reside on a hydrophobic surface that is in a gaseous environment.

2.4.3.2 Microfluidic Channel Fabrication Processes.

The manufacturing of microfluidic channels depends upon the material capabilities cost, intended microfluidic platform and ultimately the application area. Commonly used materials are Corning 0211 borosilicate glass fused silica, quartz silicon, polymethylmethacrylate (PMMA), polydimethylsiloxane (PDMS), SU-8, steel, aluminium and copper [70]. Table 2.2 below shows some of the different manufacturing/fabrication processes and the associated materials used.

As an example, we described the fabrication processes performed in this project in the section titled “*Microfluidic Large Scale Integration*”.

Table 2.2: Microfluidic Channel Fabrication Processes or Methods. The manufacturing of microfluidic channels depends upon the material capabilities cost, intended microfluidic platform and ultimately the application area. Information obtained from References [70-74].

Fabrication Process	Materials	Principle of the fabrication Process
Lithography	PDMS, PMMA, SU-8, Corning 0211 borosilicate glass fused silica	Using UV light and a series of chemical reactions to produce microfluidic channels and features.
Microinjection Molding	Amorphous Metallic Alloy (“metallic glass”), Cyclic Olefin Polymers and Cyclic Olefin Copolymers	Transferal of micron or submicron features of metallic moulds to a polymeric product.
Laser Ablation	Copper, Steel	Bond-Breakage by pulsed UV source
Micromachining	Steel, Copper, Aluminium	Cutting of materials with tool
Etching	Silicon, Silicon dioxide, silicon nitride	Chemically removal of layers (wet silicon etching) and/ or plasma assisted removal of the layers (dry silicone etching)

2.4.4 Fluid Control Systems.

Various microfluidic devices have different channel networks depending on the fabrication process used like those mentioned earlier in the previous section. Typically, the cross-sectional shapes of the microchannels are either rectangular, square or circular. One of the most important components in microfluidic systems is the fluid manipulation methods. To perform fluid manipulation in fluidic systems, devices such as actuators, valves, pumps and mixers are used. However, in microfluidics, microvalves, micropumps and micromixers are used within the microfluidic devices.

2.4.4.1 Microvalves

The ability to manipulate fluid flow using valves is an essential principle of microfluidics. A compiled classification of the available microvalves in microfluidics is shown in Figure 2.4.

Valves can either be active or passive. Active valves require energy whereas passive valves do not require energy for operation. The type of valve used in a device depends on the amount and type of control needed for the application.

Most active valves often use external macroscale devices that control the actuation and provide the energy [62], these include electromagnetically actuated microvalves [75] and pneumatically driven pressure valves [3].

Passive valves can be used to limit flow in one direction, to remove air or to provide a temporary flow stop and the most common way of constructing passive valves involves the use of porous hydrophobic materials or surface treatments to create selective vents or flow stops [62]. In such a system which uses porous hydrophobic materials, vents control the fluid movement by allowing air to pass, but not the liquid being moved.

The work described in this project makes use of the following valves:

- i. External active microvalves that are actuated by the aid of external pneumatic means. This is highlighted in Figure 2.4, i.e. ‘in-line’ pneumatic microvalves. The full description of this microvalve will be given in the ‘Microfluidic Large Scale Integration’ section.
- ii. External active microvalves that are micro-electrically actuated. This is highlighted in Figure 2.4, i.e. ‘rotary’ modular microvalves. A modular rotary microvalve valve, has origins of the multi-directional switching valve with a rotary mechanism developed by Hasegawa [76]. This microvalve requires continuous power to be applied to keep the valve actuation in operation. More details of this valve will be provided in the ‘Methodology’ chapter.

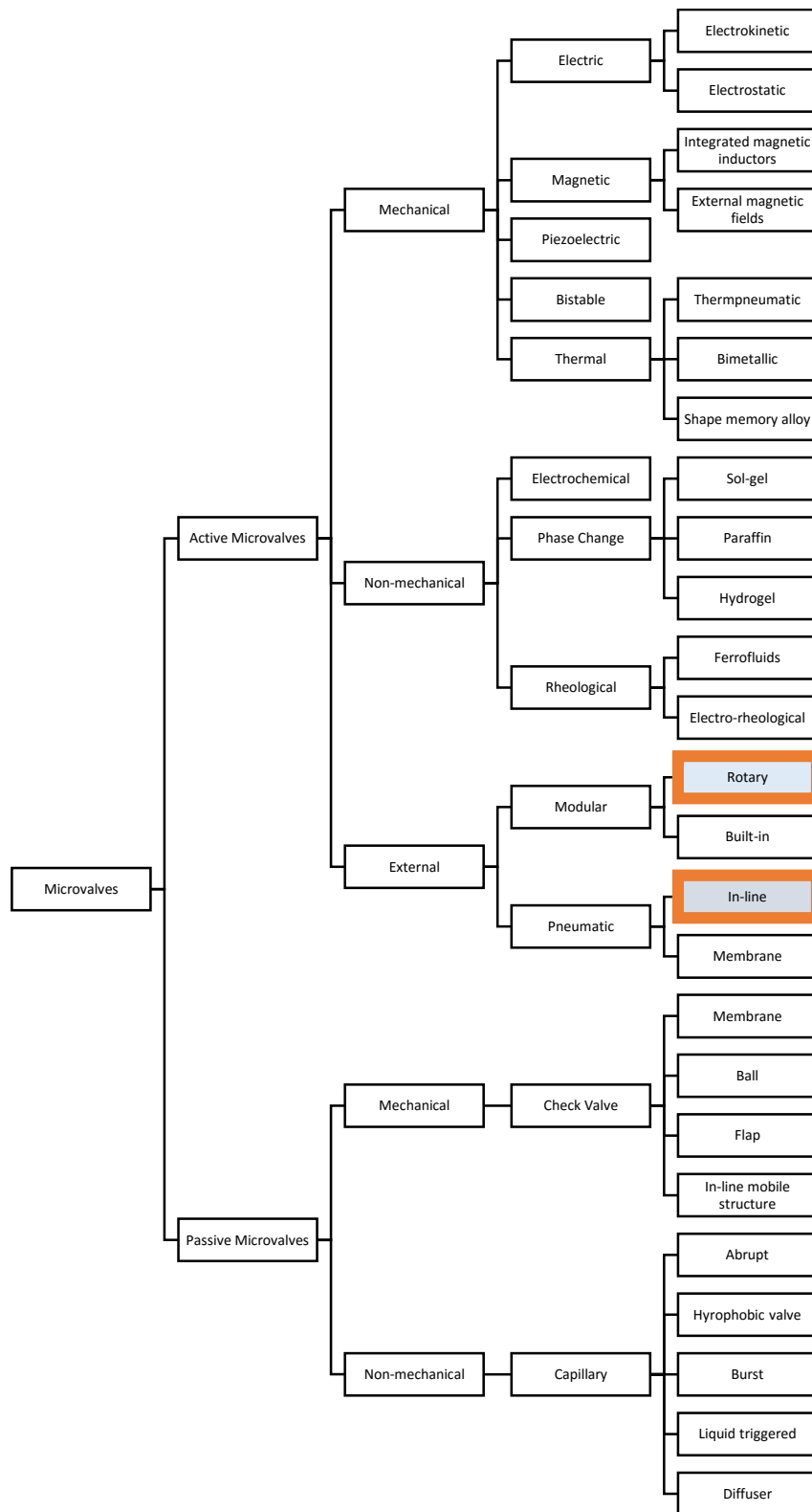


Figure 2.4: The different types of microvalves. Valves can either be active or passive. Active valves require energy whereas passive valves do not require energy for operation. The type of valve used in a device depends on the amount and type of control needed for the application. The work described in this project makes use of the highlighted valves. This classification of microvalves was gathered from References [77-79].

2.4.4.2 Micropumps.

One of the first micropumps was developed by Smits in the late 1980s [80]. Since then, there has been advancements in the fabrication and development of micropumps and earlier classifications by Krutzch and Cooper [81] made it possible to identify a micropump suitable for each of the emerging microfluidic platforms. Figure 2.5, shows a compiled classification of the available micropumps in microfluidics.

Depending on their construction, pumps are usually classified into two main categories:

- i. Displacement pumps - which exert pressure forces on the working fluid through one or more moving boundaries [82], also referred to as mechanical pumps, because there is movement of parts.
- ii. Dynamic pumps – which continuously add energy to the working fluid in a manner that increases either its momentum or its pressure directly [82], also referred to as non-mechanical pumps, because of the absence of moving parts.

Many displacement pumps operate in a periodic manner, incorporating some means of rectifying periodic fluid motion to produce net flow, and often such pumps are subcategorized into the reciprocating displacement pumps and peristaltic pumps in which the moving surface is a diaphragm [79].

Dynamic pumps include centrifugal pumps, electrohydrodynamic pumps, magnetohydrodynamic pumps, electroosmotic and acoustic-wave micropumps. Most dynamic pumps are ineffective at low Reynolds number (e.g. centrifugal pump) and thus have been miniaturized to a limited extent [82].

Due to the limited extent of miniaturization of dynamic micropumps as mentioned above, the micropump of choice in this project was the pneumatic micropump classified as a reciprocating diaphragm pump, and it is highlighted as such in the Figure 2.5. More details of the functionality of this pump will be presented in the ‘Microfluidic Large Scale Integration’ section.

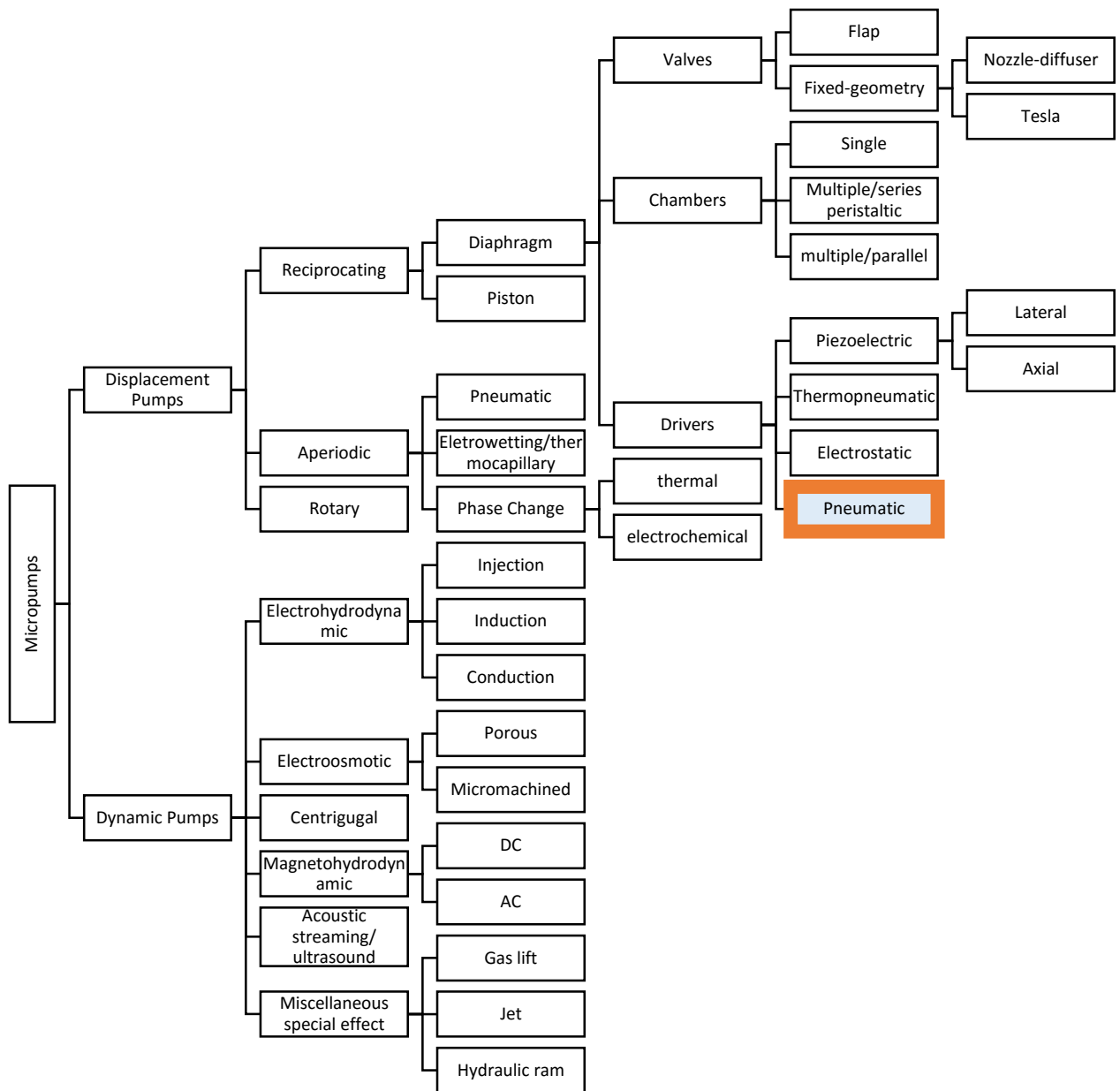


Figure 2.5: The different types of pumps and micropumps. Depending on their construction, pumps are usually classified into two main categories, displacement and dynamic. Displacement pumps exert pressure forces on the working fluid through one or more moving boundaries and dynamic pumps continuously add energy to the working fluid in a manner that increases either its momentum or its pressure directly. The micropump of choice in this project is highlighted above. This classification of pumps and micropumps was gathered from References [79, 81, 82].

2.4.4.3 Micromixers

Besides the microvalve and the micropump, the micromixers are often the important and indispensable components in microfluidic platforms as the mixing of fluids is a basic process required for biological applications. At microscale level where laminar flow is prevalent, mixing occurs by diffusion. However, for some microfluidic-based assays, particularly those that require relatively large particles (i.e. cells) to mix, the diffusion process is slow [62]. There are two ways of mixing in microfluidics, using active micromixers and passive micromixers. A list of micromixers and their respective classification is given in Figure 2.6.

Passive micromixers use channel geometry to fold fluid streams to increase the area over which diffusion occurs [62]. Y/T-type flow, recirculation flow and Droplet micromixers are all examples of passive micromixers.

Active micromixers are those that use external sources to increase the interfacial area between fluid streams [62]. Electrokinetically-driven, acoustically-driven and magnetodynamic-driven micromixers are examples of active micromixers. Another crucial active micromixer is a combination micromixer which has integrated microvalves and micropumps.

The type of mixer preferred generally depends on the type of reagents that need mixing and the fluid regime operation (i.e. Re number) [62]. In this project, the preferred choice of micromixer that is consistent with the microfluidic platform used is the active micromixer which has integrated microvalves and micropumps. The details of how this pump functions will be explained in the 'Microfluidic Large Scale Integration' section.

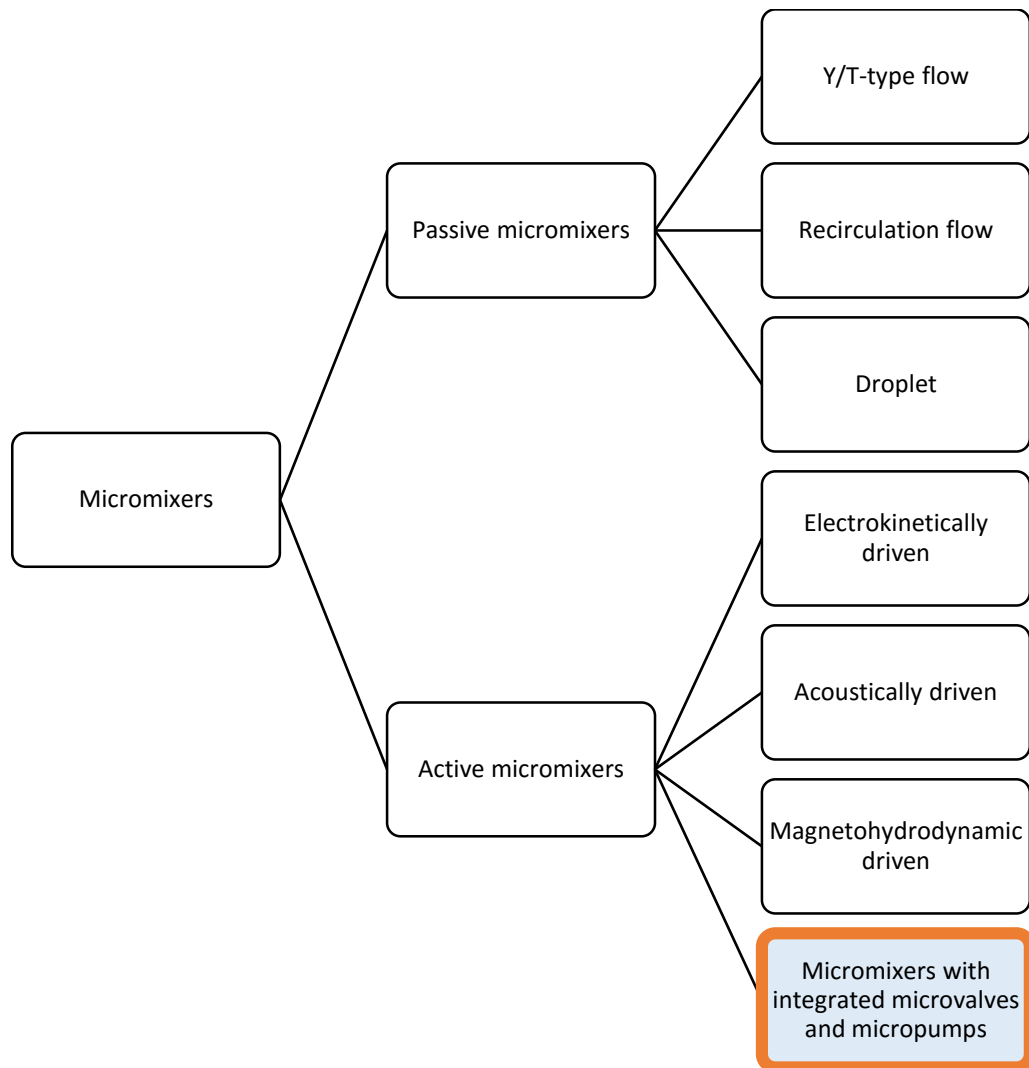


Figure 2.6: The different types of micromixers. There are two ways of mixing in microfluidics, using active micromixers and passive micromixers. Passive micromixers use channel geometry to fold fluid streams to increase the area over which diffusion occurs. Active micromixers are those that use external sources to increase the interfacial area between fluid streams. The type of mixer preferred generally depends on the type of reagents that need mixing and the fluid regime operation (i.e. Re number). In this project, the preferred choice of micromixer that is consistent with the microfluidic platform used is the active micromixer which has integrated microvalves and micropumps, this is highlighted above. This classification of micromixers was gathered from References [62, 79].

2.5 Microfluidic Large Scale Integration (MLSI)

2.5.1 Background.

Microfluidic Large Scale Integration (MLSI) is a microfluidic platform that refers to a microfluidic channel circuitry with chip-integrated microvalves based on flexible membranes between a liquid-guiding layer and a pneumatic control channel layer [26].

Microfluidic large scale integration platform emerged in the 1990s as evidenced in the early work published by Abbott, Singhvi and Kumar and many others in the Whitesides research group [83-85]. A few years later, after success in the lithographic molding of structures with sub-micrometer dimensions [86], a novel fabrication technology for microfluidic channel development called soft lithography arrived on the global scene [87]. This technology is mainly based on the use of elastomeric stamps, master molds, conformable photomasks which are then later used to fabricate and replicate microstructures. This technology was a major success using the rubber like elastomer, polydimethylsiloxane (PDMS) which had the needed optical transparency, biocompatibility (with aqueous solutions), gas permeability, inertness and non-toxicity to perform biochemical/biological experimentation and microscopic observations.

The technology was improved and expanded by Stephen Quake's research group who reported a series of microfluidic systems which used a multilayer soft-lithography (MSL) process [3]. This allowed several layers of PDMS to be bonded on top of each other to produce a monolithic, multi-layered PDMS structure. This was the birth of a new type of microvalve in microfluidics and is now commonly being referred to as the Quake valve. The Quake valve is classified as a pneumatically actuated in-line microvalve and it is now the core microvalve and fabrication process in the MLSI platform based microfluidic systems.

The two functional states of the microvalve, the open and closed state, are dependent upon the applied pneumatic pressure on the control channel layer. The development of a microfluidic chip that has thousands of microvalves and the manner in which microvalves are configured and laid out leads to the formation of fluidic control units such as micropumps, micromixers, multiplexers etc. all in a single microfluidic chip. This Quake developed technology and its novel microvalve functionality is being made commercially available to the scientific community by the company, Fluidigm Corp., CA, USA, co-founded by Stephen Quake.

2.5.2 Device Fabrication.

Microfabrication has its foundations in microelectronics. Microfabrication is a process used to construct physical objects with dimensions in the micrometer to millimeter range using some of the already established fabrication processes used to make integrated circuits [88]. Microelectromechanical systems (MEMS), lab-on-a-chip (LOC) and micro-total analysis systems (μ -TAS) are all microfabricated devices and have been a success in the commercial and scientific research industries. Microfabrication offers more uniform, accurate and reproducible flow chamber geometries that can be precisely constructed as compared to conventional machining (e.g. injection moulding). Most microfluidic devices are fabricated using photolithography, soft-lithography and popular multi-layer soft-lithography. We now present the principle of these fabrication processes.

2.5.2.1 Photolithography and Soft-Lithography.

Photolithography is the microfabrication process of transferring geometric patterns envisioned by a designer onto a physical surface of compatible material, usually a silicon wafer. Photolithography is the most successful microfabrication technology since its invention in 1959 and since most of the integrated circuits are made using this technology, it has been applauded as the workhorse of the semiconductor industry [87].

The photolithographic technique currently used for manufacturing microelectromechanical structures is based on a projection printing step in which the image of the geometric pattern is reduced and projected onto a thin film of photoresist that has been spun-coated onto the surface of a either a silicon, glass or plastic wafer through a high numerical aperture lens system [87, 88]. For microfluidic devices, an improved method was developed, which allowed the replication of the pattern and this is called soft-lithography.

Soft-lithography has the same pattern transferal principles as photolithography, however, in this process; the pattern replicating is done using elastomeric polymers. Therefore, soft-lithography is referred to as a non-photolithographic method for replicating a pattern [52]. The microfabrication process of soft-lithography follows a sequence of process steps (a process flow) that can be categorized into three major collective processes, namely, **concept developing**, **rapid prototyping** and **replica molding**. Figure 2.7 shows the general process flow of soft-lithography microfabrication.

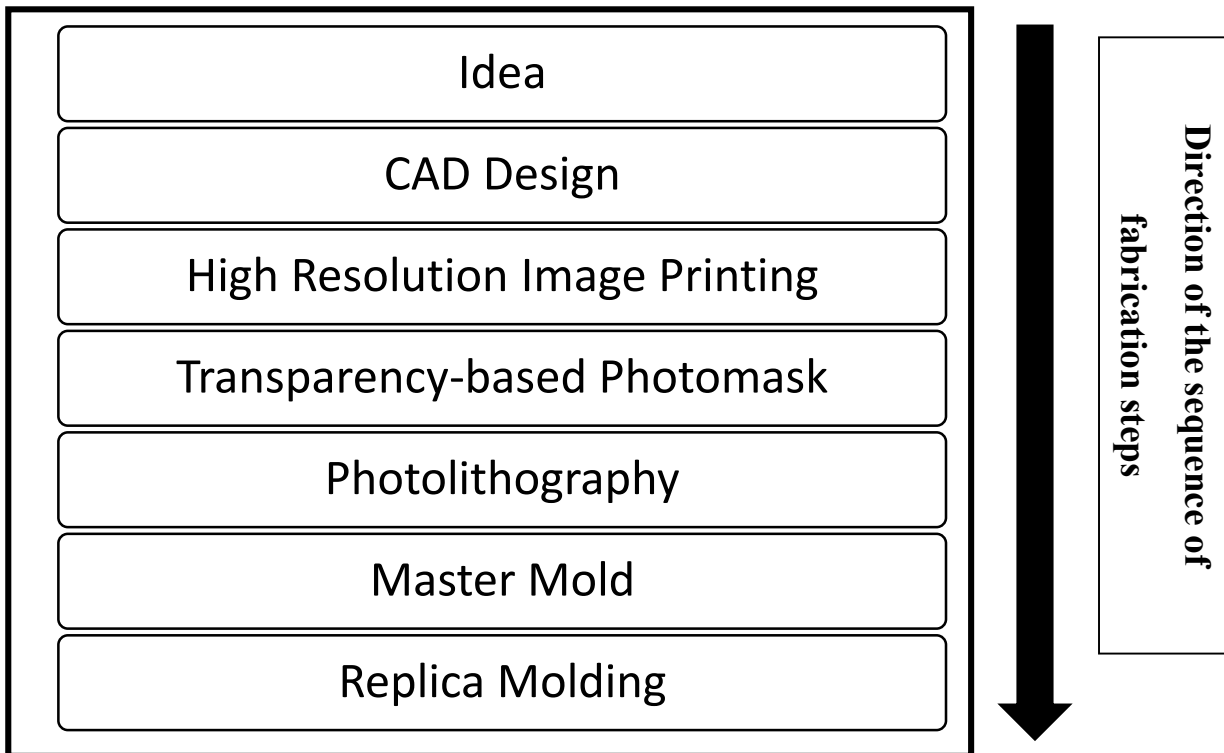


Figure 2.7: Schematic of microfluidic device fabrication using soft-lithography. Soft-lithography has the same pattern transferal principles as photolithography, however, in this process; the pattern replicating is done using elastomeric polymers. The microfabrication process of soft-lithography follows a sequence of process steps (a process flow) that can be categorized into three major collective processes, namely, concept developing, rapid prototyping and replica molding. In concept developing, device designing is done using a computer-aided design (CAD) program to make a photomask. In rapid prototyping, the photomask is then used to perform photolithography. The replica molding process involves the casting of a transparent, silicone-based liquid pre-polymer, against the master mold using an elastomeric material (e.g. PDMS).

In concept developing, the first step will be the device designing. Device designing is usually done in a computer-aided design (CAD) program (e.g. AutoCAD[®] software). In this step, the designer needs to consider the size of the channels, shape of the channel (i.e. straight or curved) and also the nature of the angled features within the minimal feature sizes attainable in respect to photolithography. High resolution printing would be the next step, in which a high resolution commercial image setter is used to print the pattern on a transparency film. High resolution printing allows one to obtain design features with sizes up to about 8 microns (8 μ m) [89]. The printed transparency will serve as the photomask for the next step in the process. The photomask can be printed as clear-field (for positive photoresist) or dark-field (for negative photoresist) dependant on the photoresist to be used.

In rapid prototyping, the photomask is then used to perform photolithography. Positive or negative photoresist is spin coated on a clean silicon wafer at specified thicknesses as required for each designed features and then exposed to UV light. UV light passes only through the clear regions in the mask onto the photoresist spun silicon wafer to selectively crosslink the features represented by photomask. Once the photoresist is exposed, it is developed with photoresist-specific solvents that remove un-cross-linked polymers. The final result after developing is the ‘master mold’, whose features precisely represent the desired device structures. Figure 2.8, shows the rapid prototyping step in soft-lithography when using either positive or negative photoresists and the resultant master mold features that are obtained after developing while Figure 2.9 (a) shows a diagrammatic illustration of obtaining the master mold.

The replica molding process involves the casting of a transparent, silicone-based liquid pre-polymer, against the master mold using an elastomeric material (e.g. PDMS) to generate a negative monolayer (or monolithic layer) replica of the master [57]. The pre-polymer is poured onto the master wafer and heat-cured in place to form a rubbery silicone solid. The replica molding process using an elastomeric material is the backbone of soft-lithography and the process is illustrated using Figure 2.9 (b). The silicone that has heat-cured on the master mold is then peeled off to reveal the inverted pattern topology represented on the mold. Access ports, i.e. the inlet and outlet ports are punctured using a cylindrical punch. It is then attached to a coverslip surface and heat-cured again. After this step the replica molding step has been completed and the microfluidic device would be ready for use.

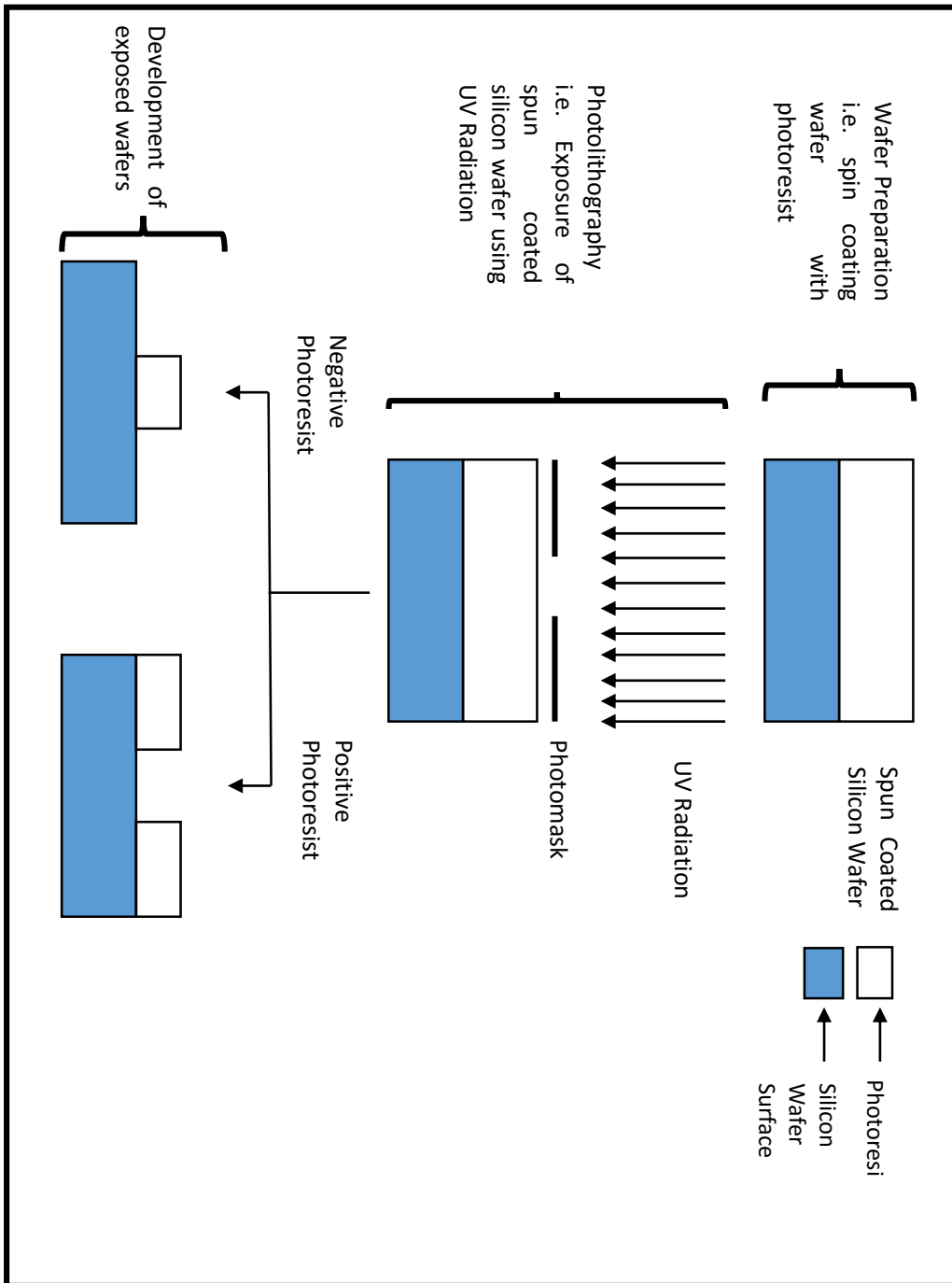


Figure 2.8: The photolithography and soft-lithography process. Positive or negative photoresist is spin coated on a clean silicon wafer at specified thicknesses as required for each designed features and then exposed to UV light. UV light passes only through the clear regions in the mask onto the photoresist spun silicon wafer to selectively crosslink the features represented by photomask. Once the photoresist is exposed, it is developed with photoresist-specific solvents that remove un-cross-linked polymers. The final result after developing is the ‘master mold’,

whose features precisely represent the desired device structures. The steps in this process were obtained from References [90, 91].

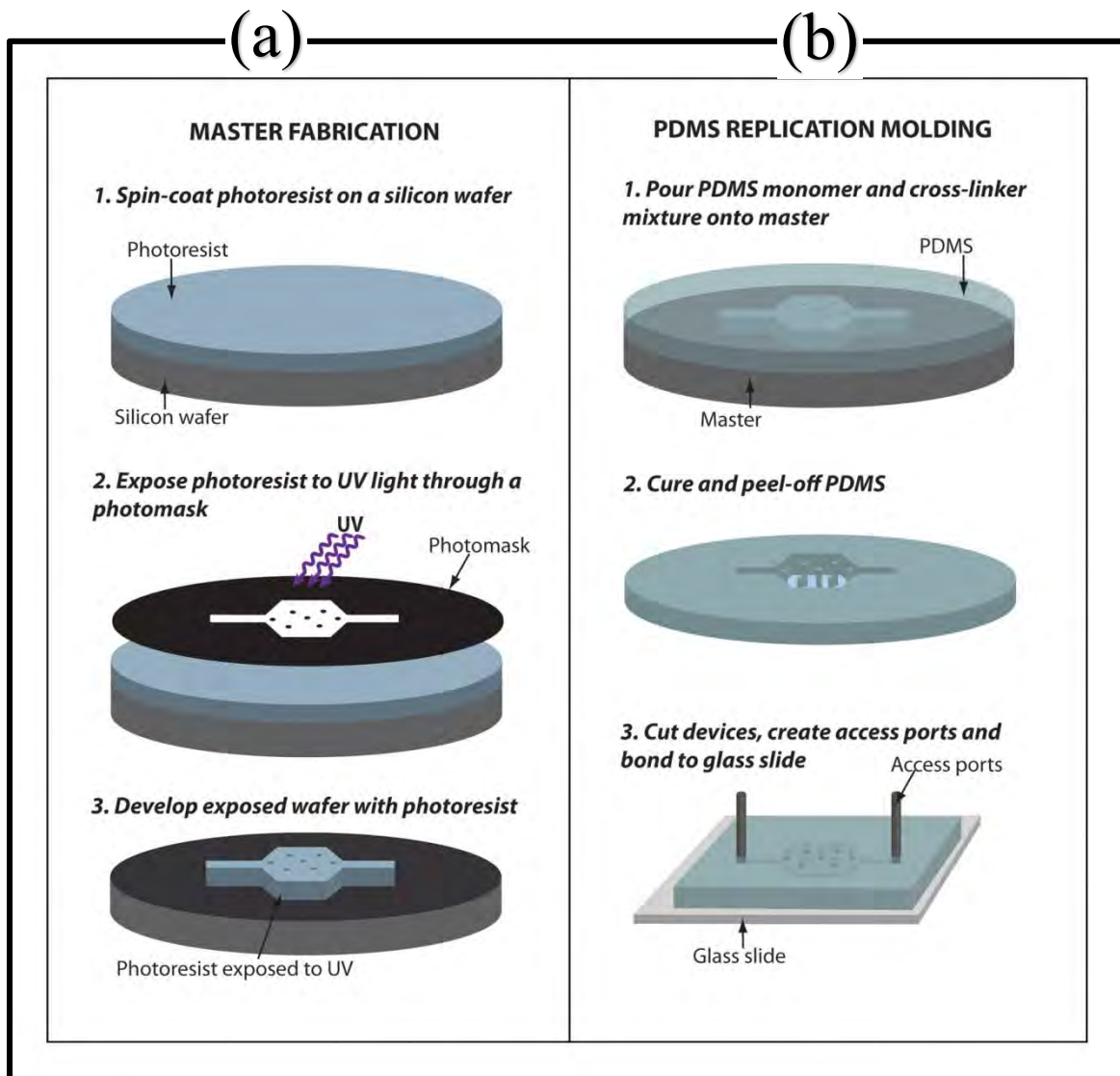


Figure 2.9: (a) The master mold fabrication and (b) the replica molding processes in soft-lithography. The image was obtained from Reference [92].

2.5.2.2 Multilayer Soft-Lithography.

Multilayer Soft-Lithography (MSL) developed by the Quake research group is an extension of the soft-lithography technique developed by the Whitesides research group. MSL provides the capability to bond multiple monolithic layers of elastomeric material created during the replica molding processes [3]. The process is similar to the soft-lithography process.

In the concept developing step, after the entire design/pattern architecture of the microfluidic device has been completed, the design is separated into multiple layers where all features of a given height are placed on a single layer and then printed in high resolution to produce a photomask. The photomasks are printed according to the channel architecture where some layers will be printed on a positive (clear-field) photomask and some on a negative (dark-field) photomask.

Rapid prototyping is then performed using the photomasks. Both negative and positive photoresists are used and often the positive photoresist is used to produce rounded channels. Square channels become rounded because a reflow occurs when the positive photoresist spun silicon wafer is baked at high temperatures [3]. Similar developing techniques and reagents are used, and each layer will have its respective master mold.

The extension of this technique to the already existing replica molding process is that, each layer of elastomeric material is cast separately and then later bonded together [3]. In this case, the elastomeric material that is used is PDMS, thus this process can be referred to as a PDMS replica molding process [93]. After the bonding process, the resultant microfluidic device is a monolithic three-dimensionally patterned structure composed entirely of elastomeric material [3]. MSL makes it possible to create multiple layered fluidic devices. A unique concept that was brought about by MSL was the establishment of an active, external, pneumatically actuated in-line microvalve and a pneumatically driven series multi-chamber reciprocating displacement micropump. Depending on the arrangement and geometry of the microvalves, there are two forms of the micropump, a linear pneumatic peristaltic and rotary pneumatic peristaltic micropump [3]. The device can also have a unique micromixer, which is the integration of the active, external, pneumatically actuated in-line microvalve and the pneumatic peristaltic rotary micropump [3].

2.5.3 General Principle: Microvalve, Micropump and Micromixer.

The basic principle behind functionality of the Quake valve is that the pneumatic channel can be deformed under pressure to pinch off the flow of fluids in an in-line microchannel. Two monolayers (e.g. control channel and flow channel) casted separately via the PDMS replica molding process are bonded together, on top of each other with the control channel and flow channel intersecting orthogonally [3, 94]. The resultant bonded PDMS structure is then sealed on top of a glass substrate as shown in Figure 2.10.

A microfluidic device can be configured in two architectural designs: ‘push-down’, in which the flow channels are located below the control channels as shown in Figure 2.10 (a), and ‘push-up’ in which the flow channels are bonded on top of the control channels as shown in Figure 2.10 (b), or an architectural design with both push-up and push down valves as shown in Figure 2.10 (c), [1].

When pressure is applied to the control channel during actuation, the flexible membrane at the intersection of the channels is deflected, thereby closing the channel. This is illustrated by Figure 2.11. Typical channel sizes are 100 microns wide and 10 microns high, making the active area of the valve 100 microns by 100 microns and the membrane is usually made to be 30 microns thick [3]. The nature of the membrane, i.e. the width, height and thickness determines the valve actuation pressure level [1]. Push-down designed devices allow channels to be in direct contact with a substrate, assisting applications which require custom-functionalized surfaces [95]. Push-down designed devices generally require high pressures to actuate since the control layer is the thicker layer and also because of this, push down designed devices have limited heights for the flow channel [1]. Push-up designed devices allow the use of taller flow channels, and since the control channel is the thinner channel, it requires low pressures for actuation.

There should be a rounded profile in the flow channel and a rectangular profile in the control channel if the valve has to close completely during actuation or else the rectangular flow channel and rectangular control channel will produce a ‘sieve’ valve, and these are also illustrated in Figure 2.11 [3]. Sieve valves can be used in applications where the manipulation of an assortment of different sized cells, beads, droplets and other large objects is required, because the valve opening can be precisely controlled by varying the pressure applied to the control line [3].

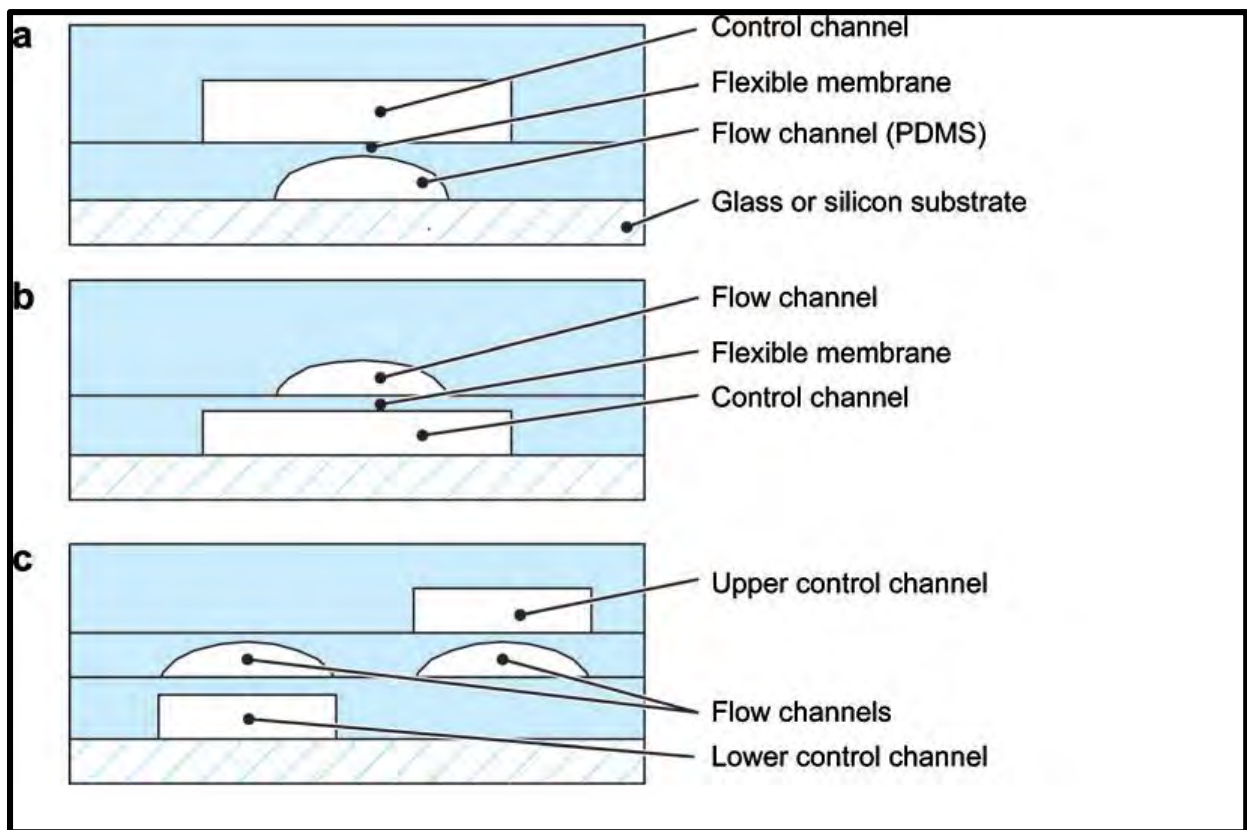


Figure 2.10: A microfluidic device can be configured in two architectural designs: ‘push-down’, in which the flow channels are located below the control channels as shown in (a), and ‘push-up’ in which the flow channels are bonded on top of the control channels as shown in (b), or an architectural design with both push-up and push down valves as shown in (c). The image was obtained from Reference [1].

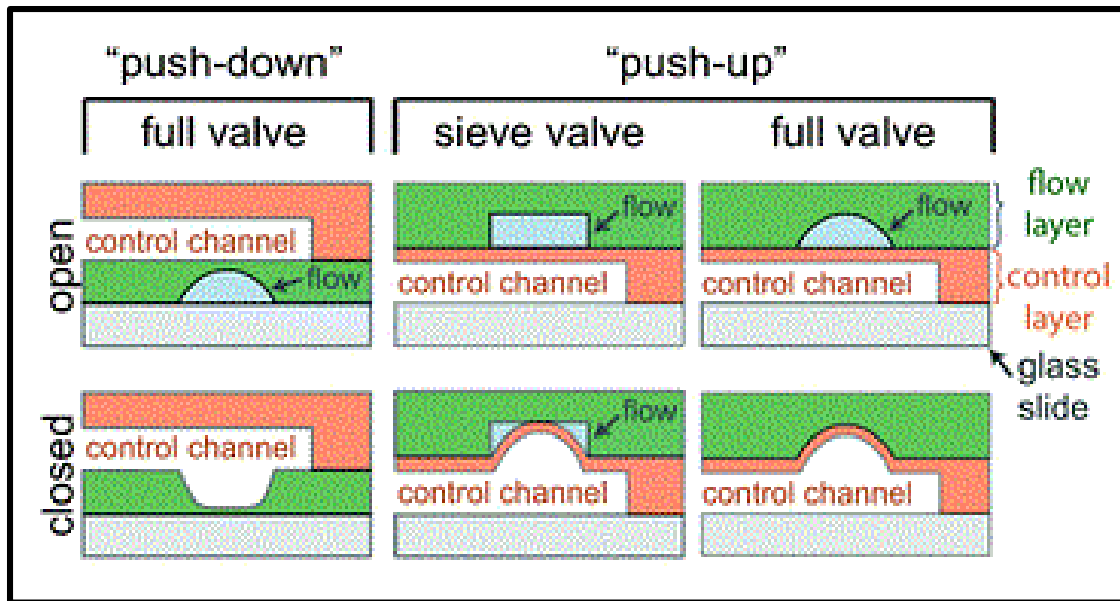


Figure 2.11: Side view illustrating the functionality of the two-layer PDMS push-down and two-layer PDMS push-up valves. When pressure is applied to the control channel during actuation, the flexible membrane at the intersection of the channels is deflected, thereby closing the channel. Push-down designed devices generally require high pressures to actuate since the control layer is the thicker layer and also because of this, push down designed devices have limited heights for the flow channel. Push-up designed devices allow the use of taller flow channels, and since the control channel is the thinner channel, it requires low pressures for actuation. There should be a rounded profile in the flow channel and a rectangular profile in the control channel if the valve has to close completely during actuation or else the rectangular flow channel and rectangular control channel will produce a ‘sieve’ valve. Sieve valves can be used in applications where the manipulation of an assortment of different sized cells, beads, droplets and other large objects is required, because the valve opening can be precisely controlled by varying the pressure applied to the control line. The image was obtained from Reference [95].

When 3 of these microvalves are linearly arranged, with specific spacing, on top or below a flow channel, a linear pneumatic peristaltic micropump is created and when the design architecture has rotary geometry in the flow channel and 3 microvalves arranged on top or below the flow channel, a pneumatic peristaltic rotary micropump is created as shown in Figure 2.12 and Figure 2.13 respectively [3]. A peristaltic pumping function occurs when the 3 microvalves are actuated in the pattern 101, 100, 110, 010, 011, 001, where 0 and 1 represent valve open and valve closed states respectively [3]. An open valve is when there is no pressure applied in the control channel and valve closed state is when there is applied pressure in the control line thereby deflecting the membrane. There is no need for precision regulating external pressure sources for pumping because on-chip peristaltic pumping provides the required level of fluid flow [1].

The fluidic manipulation required in most biological experimentations is efficient fluid mixing. The versatility of MLS is that the pneumatic peristaltic rotary micropump can be used as an on-chip continuous-flow micromixer. Continuous-flow mixing is the dynamic mixing which takes place when two solutions are flowing down the channel continuously [79]. For the micromixer, two fluids rotate in the same flow channel loop/ring, and when the peristaltic pump is activated, the centre of each fluid flows faster than the edge. Therefore, the interface between the solutions keeps stretching and eventually there is a shorter diffusion distance allowed for mixing and drastically reduce the mixing times when compared to normal passive diffusion [1]. This micromixer is classified as an active micromixer which is an integration of microvalves and micropumps [79]. This micromixer can also be used for on-chip fixed-volume mixing, which is mixing of two different solutions (e.g. sample and reagent) of fixed volumes completely before the next stage of the process is performed [79].

In summation the Quake valve provides a precise control over fluid flow within microfluidic devices and is versatile in that it can be combined to form a variety of complex structures such as micropumps, micromixers and multiplexers while simplifying channel routing.

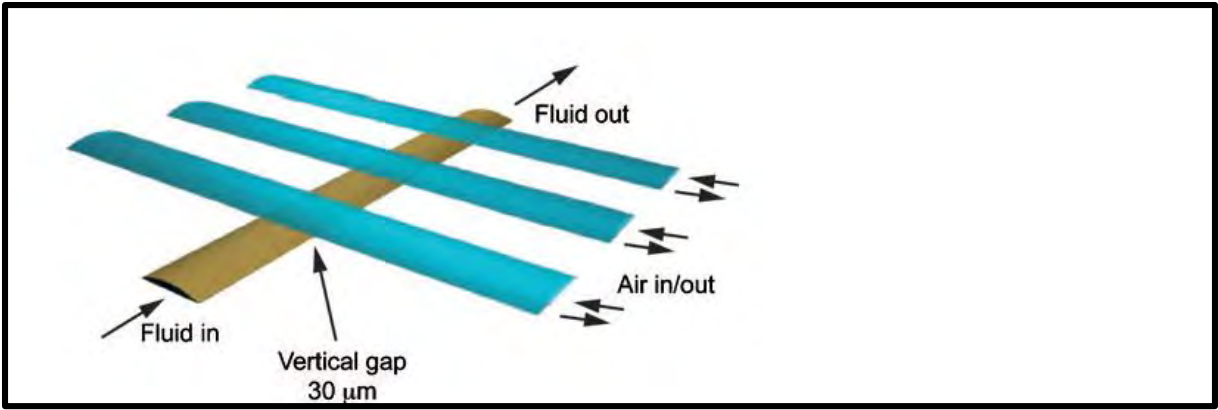


Figure 2.12: Linear pneumatic peristaltic micropump. When 3 of these microvalves are linearly arranged, with specific spacing, on top or below a flow channel, a linear pneumatic peristaltic micropump is created. A peristaltic pumping function occurs when the 3 microvalves are actuated in the pattern 101, 100, 110, 010, 011, 001, where 0 and 1 represent valve open and valve closed states respectively. The image was obtained from Reference [3].

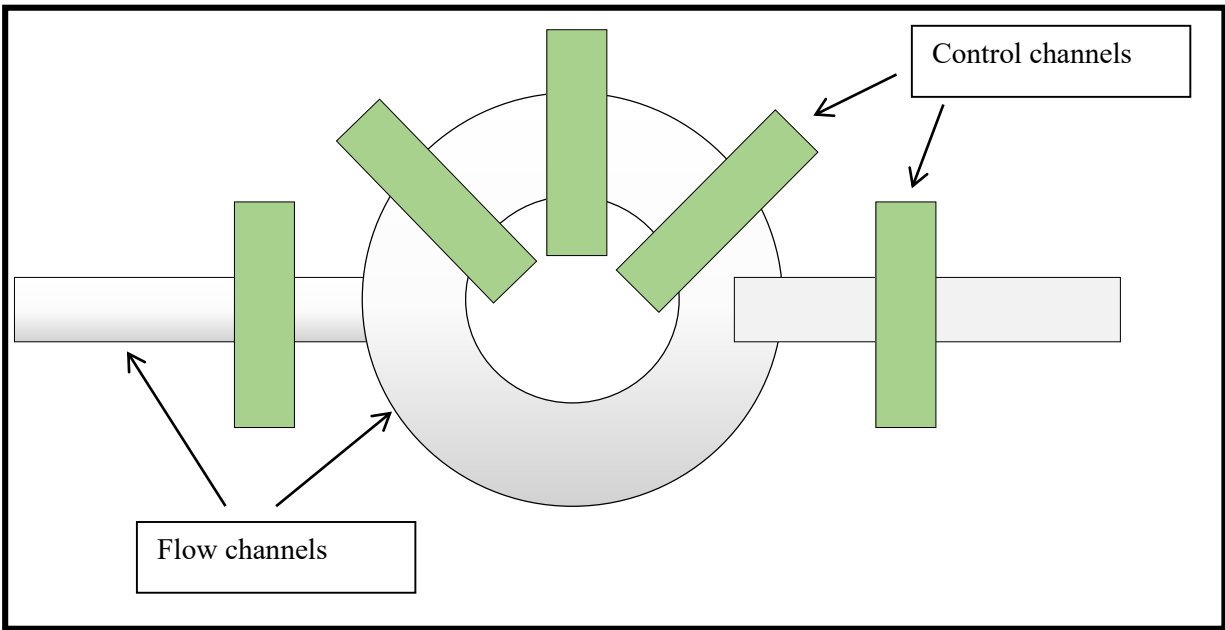


Figure 2.13: When the design architecture has rotary geometry in the flow channel and 3 microvalves arranged on top or below the flow channel, a rotary pneumatic peristaltic micropump is created. A Rotary pneumatic peristaltic micropump is also used as the continuous-flow micromixer in Microfluidic Large Scale Integration systems.

2.6 Point-Of-Care (POC) Testing Using Microfluidic Large Scale Integration

2.6.1 Barriers to adoption POC technologies in Resource Limited Countries.

In the global health community, there is an increasing demand for new ways to simplify and improve the efficiency and cost of diagnostics in the fight against infectious diseases. The new ways are expected to significantly increase the access level to robust, high-quality diagnostics especially in resource limited settings where the early detection and treatment of infectious pathogens is of paramount importance.

The goal in sub-Saharan Africa is to test and treat at large scale for multiple patients at point-of-care, facilitates the decentralization of laboratory based diagnostic services. In the townships and villages of resource limited settings of sub-Saharan Africa, power running water and refrigeration are often intermittent or absent, therefore whatever assays that are to be performed have to be self-contained [19]. It is not the technology that defines a POC test, but it is the intent to use technology that defines a diagnostic process as POC testing [96]. In research and development of diagnostic tools, it is necessary to develop POC diagnostic technology that suits the available POC settings. In general, POC testing can be thought of as a spectrum of technologies ranging from simplest to sophisticated, that can be operated by users who range from laypersons to highly trained persons, and the present POC technologies can be sub-categorized into target product profiles (TPP) in association with the POC testing setting as follows: homes (TPP1), communities (TPP2), clinics (TPP3), peripheral laboratories (TPP4) and hospitals (TPP5) [96]. Figure 2.14, shows the present spectrum of POC testing according to [96].

For each TPP, there is a desired purpose. For home based POC testing, TPP1, the test can be performed by the untrained person, i.e. any lay person by following the instructions on the over the counter POC diagnostic technology packaging. The purpose of TTP1 testing is for self-assessment and if need be, referral to other TTP's such as TPP2, TPP3 and TPP4. At community settings, TPP2, POC testing can be performed minimally trained health workers and the aim would be for referral to TPP3 and TPP4. Clinics, TPP3, which is one of the most common POC testing setting in resource limited settings offers rapid diagnostic testing (RDT) performed by trained health care providers. At TPP3, there is diagnosis and treatment offered as well as voluntary counselling. TPP3 is infrastructure based, thus does not provide a high level of access to the offered services especially in remote places of the resource limited countries. Because there is diagnosis and treatment at TPP3, there is no need for referral to TPP4 and TPP5 unless the circumstances require so. TPP4 and TPP5, offer diagnosis,

treatment and monitoring of patients and all this is managed by trained health care personnel or laboratory technicians. These services are infrastructure based, and do not provide the decentralization of the much needed high quality diagnostic testing. Though TPP4 and TPP5 offer POC testing capabilities, these POC testing settings are impractical in resource limited countries where the ‘test and treat’ goal is required to be mobile and reach out to the people rather than the people coming to the test site.

The widespread adoption of POC technologies has its challenges. Examples of these challenges that affect the adoption process is also highlighted by Pai [96], and these include:

- i. Awareness: A lack of awareness by the health care service providers of the potentially available POC technologies that can be used instead of resorting to referrals to laboratories.
- ii. Training: Untrained and informal health care service providers who lack the knowledge and training needed to implement and perform POC testing such that the error prone results decreases the health system’s faith in POC technology.
- iii. Support infrastructure: Most clinics and primary care centres lack support infrastructures such as, constant power supply, refrigerators, storage space, and waste disposal units.
- iv. Infection risk: The health workforce, who primarily perform POC testing are unwilling to do tests that may expose them to the risk of infections.
- v. Economic: POC testing using certain POC technologies may be too expensive and unaffordable in many resource limited countries.
- vi. Singularity POC technology: Some available POC tests are often applicable for single diseases and there is worry that most infections are missed this way. There is need for a more diversified POC technology that reduces the chances of missing infections when one test is performed.
- vii. Cultural/societal: Perceived lack of confidentiality and stigma may reduce acceptance of POC testing in the communities.

There is need for therapeutic systems and POC technologies for clinical diagnostics to change the diagnostic platforms in resource limited countries and overcome the challenges responsible for the lack of widespread adoption of these systems and technologies. One such POC technology that promises to address the needs of resource limited countries is POC microfluidic large scale integration systems.

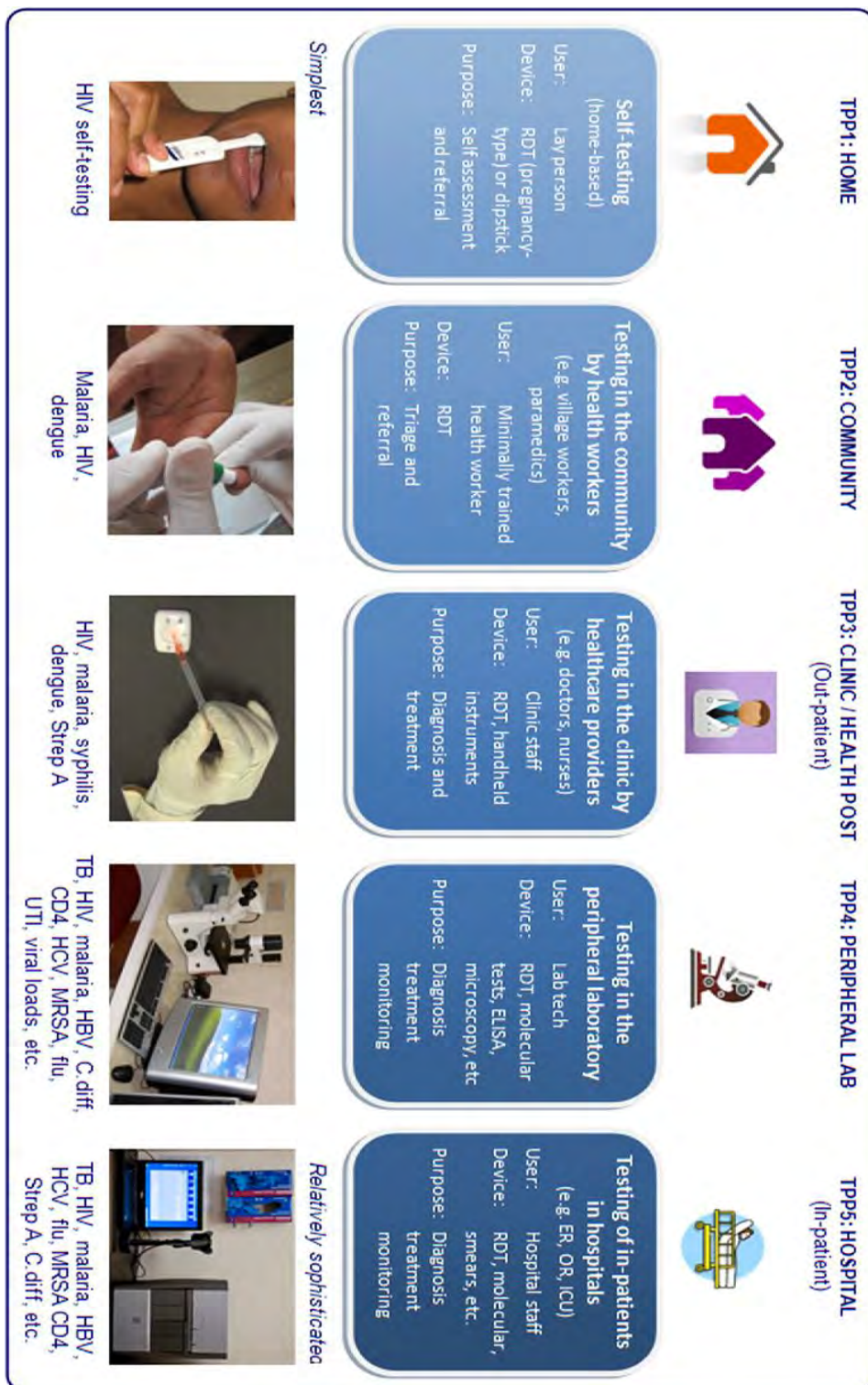


Figure 2.14: In general, POC testing can be thought of as a spectrum of technologies ranging from simplest to sophisticated, that can be operated by users who range from laypersons to highly trained persons, and the present POC technologies can be sub-categorized into target product profiles (TPP) in association with the POC testing setting as follows: homes (TPP1), communities (TPP2), clinics (TPP3), peripheral laboratories (TPP4) and hospitals (TPP5). The image was obtained from Reference [96].

2.6.2 The Promise of Using Microfluidic Large Scale Integration systems in POC clinical diagnostic Testing.

For some infectious agents, tests are needed to better distinguish past from current infections while for some, improved POC methods are needed to return same-day test results so that patients can receive appropriate therapy while they are still at the clinic [19]. Unfortunately, a common aspect in resource limited settings is that they often lack modern laboratories, fully automated instruments that provide highly reproducible, quantitative and hence sensitive and accurate diagnostic results [17]. There are three approaches to diagnostic technologies as mentioned by Yager et al. [19] and these are:

1. Permanent integrated instruments: These are mainly comprised of instruments found in centralized laboratories in developed countries. These systems are infrastructure dependent and are best suited for high throughput work.
2. Pure disposables: These mainly comprise of immunochromatographic-lateral flow devices. They provide POC diagnosis in areas without access to well-staffed, well-trained personnel and well-equipped clinical laboratories. Basically, this technological approach is for regions that do not offer permanent integrated instruments. Pure disposables rely on relatively inexpensive, off-the-shelf components and reagents making them relatively affordable.
3. Disposables with a reader: This technological approach is a compromise that allows high performance with low per-test cost, but with added complexity (such as using a reader) while at the same time using single-use only disposables. Calibrants would be stored on the disposable and during the diagnostic test, the sample and waste would be retained within the disposables such that the reader does not need to be cleaned between sample loadings.

Microfluidic large scale integration platform based systems can be thought of as a technological approach best suited in the ‘disposables with a reader’. The microfluidic large scale integration platform based systems have the potential to become the most adaptable platform in clinical diagnostics especially for high-throughput POC testing. Its fabrication process, which involves PDMS, is comparably cheap and strong for biological experiments, thus also enabling MLSI systems to have disposable units. MLSI thus provides low-cost device fabrication and cost-efficient POC diagnostic testing. MLSI platform based systems also offer biological automation found in a ‘permanent integrated instruments’ technological approach such that the diagnostic testing minimizes human involvement thereby increasing the confidence level in POC testing technologies.

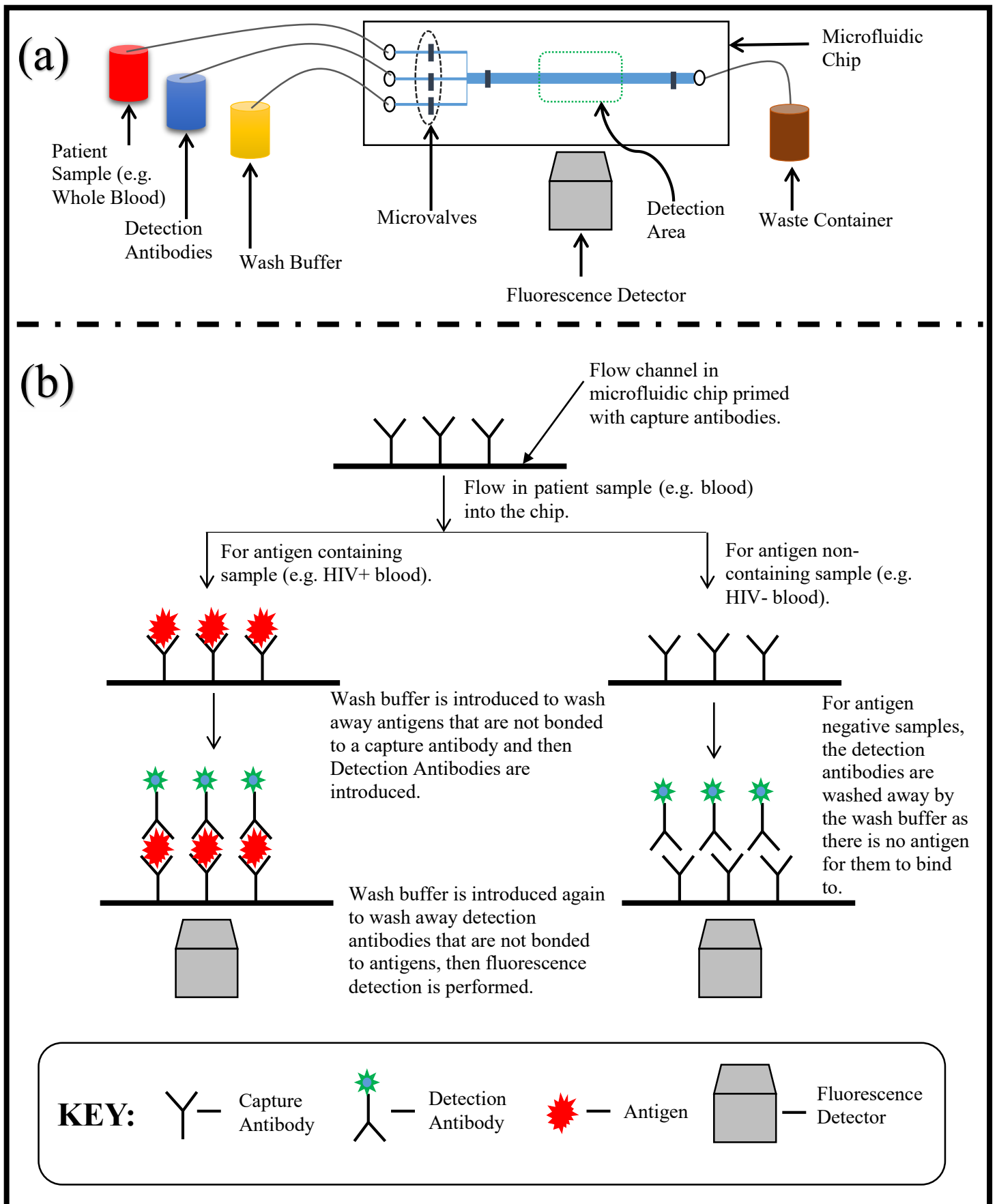


Figure 2.15: Hypothetical sketch showing a MLSI based system performing an ELISA. (a) A MLSI diagnostic set-up to perform an ELISA. (b) Generic ELISA system amenable to MLSI systems.

Figure 2.15 shows a hypothetical sketch of how an MLSI based system could perform a capture and quantification test such as an enzyme-linked immunosorbent assay (ELISA). Figure 2.15 (a) shows a general experimental set-up at POC to perform an ELISA test. Figure 2.15 (b) shows a generic principle of an ELISA test and how it would be performed using an MLSI system. Patient samples, detection antibodies, and the wash buffer will be introduced into the microfluidic chip via an automated system with minimal human involvement. Direction and order of flow of the patient samples and reagents to the main flow channel in the detection area will be actuated by the on-chip microvalve action. The main flow line in the detection area will have capture antibodies already primed onto the surface of the channel beforehand. The patient sample (e.g. whole blood) will be flowed into the main flow channel. Assuming that these capture antibodies only bind to a specific antigen, if the sample is antigen containing (e.g. HIV +) the antigen (e.g. HIV virus) will bind to the capture antibodies and if it is antigen non-containing, nothing will bind to the capture antibodies. A wash buffer will then be flowed into the main flow channel to wash away all the antigens that are not bonded to the capture antibodies. Detection antibodies (e.g. with fluorescence markers) are then flowed into the main flow channel and these will bind to the antibody-antigen complex. During this step, if the sample is antigen non-containing, again, these will bind to nothing and will be washed away when the wash buffer is reflowed into the main flow channel. After the wash buffer washes away the 'loose' detection antibodies, i.e. those not binding to anything, the automated system will trigger the fluorescence detector to commence the detection procedure. Speculating, from patient sample introduction, such a system is expected have a time to results of 10-15 minutes. The results will then be available via a printout interpretable by a technician or clinician. MLSI promises to perform such a diagnostic test at a large scale where thousands of samples are tested on a single chip simultaneously. This would make MLSI systems fast and high throughput diagnostic devices most suitable for resource limited settings.

An example of a microfluidic device though not an MLSI based system, that was used for POC testing is the mobile microfluidic chip, referred to as the 'mChip', developed by the Sia group [97], specifically designed for diagnosis in resource limited settings. The mChip, which demonstrated how new manufacturing, fluid handling and signal detection procedure can be leveraged to overcome the challenges faced in real world applications [48], was successfully tested in Rwanda on hundreds of locally collected human samples [97]. The mChip, was introduced as an easy to use POC assay that replicated all steps of an ELISA at low material cost (about US \$0.10) [97]. The mChip provided an antenatal-care diagnostic test of HIV and syphilis. The device simultaneously detected antibodies against HIV and *Treponema pallidum* (the causative agent of syphilis) from a needle-prick sample volume of blood [97]. The test sensitivities, for detection of HIV-specific antibodies and treponemal-specific antibodies, respectively, were 100% (with 95% confidence interval of 98.6 - 100.0) and 95% (85.4 - 100.0), with specificities of 100% (99.2 - 100.0) and 81% (64.2 - 97.7) [97]. As reported by

C.D. Chin et al., the assays had a turnaround time of about 15 minutes and the sensitivities and specificities were comparable to commercial ELISA kits [97].

The mChip showed that it was possible for microfluidic technology to be used as a miniaturized ELISA in resource limited settings to perform what are usually lab-based immunoassays. Microfluidic materials are selected such that they minimize surface adsorption of analytes while at the same time allowing the analytes to move to the detection zones in the disposables [19]. MLSI systems offer such characteristics, the PDMS allows certain analytes to move to detection zones (except those that have small and hydrophobic molecules) and is excellent for fabricating low-fluorescence devices.

However, MLSI based systems like most ground-breaking technologies, suffers some drawbacks in its widespread use. MLSI based systems might have a large initial start-up expense but because they have disposable components in the test e.g. the microfluidic chip, the overall cost per-test is expected to be relatively cost friendly when compared to commercially available laboratory tests. MLSI based systems need to be made more accessible to research in order to have the technology being used in an even wider range of biological and biochemical applications [1]. MLSI systems still need more redefined designs that involve high-level design architecture with many fluidic control modules and also to give it the much needed portability (i.e. a hand held or portable device with disposable cartridges) if it is to succeed in the POC testing environment. Examples of commercially available MLSI systems that can be categorized as ‘disposables with a reader’ are Fluidigm systems, such as the BioMark™ technology for molecular biology, the TOPAZ™ system for protein crystallography and the Fluidigm® EP1 system for genetic analysis developed by Fluidigm Corp.(CA, USA. However the Fluidigm systems are yet to be refined to be useable for POC testing. To just mention a few, the POC tests that would be most amenable to refined MLSI systems would be tests like the ELISA based tests for quantifying agents (e.g. HIV antibodies), complete blood count, Polymerase Chain Reaction (PCR) based drug susceptibility testing, MTB drug susceptibility testing [98].

In summation, MLSI platform based microdevices, have the potential for creative designs that allows the development of a POC diagnostic toolbox containing a POC device or that has POC devices which perform a spectrum of clinical diagnostic testing ranging from HIV testing and monitoring (including CD4 cell count, viral loading measurement, DNA PCR etc.) to TB diagnosis and other opportunistic infections. The success of such a creation that is capable of simultaneously testing for HIV, TB and other infections would dramatically improve care health care service delivery.

CHAPTER 3: RESEARCH AIMS AND OBJECTIVES

3.1 Problem Identification

Microfluidic Large Scale Integration technology is expected to revolutionize laboratory procedures involving clinical diagnostics. Advances in the technology has offered exciting possibilities but many of the possibilities suffer from a variety of technological drawbacks that limit its widespread practical application in hospitals and patient settings especially the immediate point-of-care diagnosis of disease. For example, Fluidigm systems, such as the BioMark™ technology for molecular biology, the TOPAZ™ system for protein crystallography and the Fluidigm® EP1 system for genetic analysis developed by Fluidigm Corp.(CA, USA) are attempts of ‘plug and play’ automated chip control. However, they do not give the user dynamic control over the valves. These systems are limited to the commercial applications they present with no custom manoeuvrability i.e. they do not allow user to design their own microfluidic chip, for example, the Fluidigm PCR microfluidic chip has a hard-wired control system with no user dynamic manipulation. We believe that the system we aim to develop will allow dynamic real-time chip based manipulation of automation designs.

The current microfluidic systems utilize a manual set-up process for off-chip to on-chip fluid transport. The off-chip to on-chip fluid transport is an essential process because it involves the functionalization of microfluidic chip control channels. The functionalization of the microfluidic chip control channels occurs when the control channels are filled with fluid and connected to a pressure source. The pressure source is actuated such that pressure is applied to the fluid in the control channels to close microvalves and no pressure is applied to the fluid in the control channels to open microvalves.

For this reason, most microfluidic large scale integration systems are laboratory infrastructure dependent, where expensive support equipment and the meticulous attention of highly trained personnel are required. These systems becomes incompatible for field work deployment to point-of-care testing sites in resource limited settings and very impractical to work with if the operation of the device requires the user to be thoroughly pre-trained in advance. It becomes even more impractical to use the current microfluidic systems on microfluidic chips with complex multi-layer architecture and have a high number of valves and fluidic inputs. Therefore, there is need to develop a microfluidic system that brings the practicality back such that these microfluidic systems can be used for point-of-care medical diagnostics and research with regards to the concerns of the impracticalities mentioned above.

3.2 Research Aims and Objectives

This research project partly relies on two clean room only processes, photolithography and soft-lithography. This research will utilize this special laboratory to perform a multi-layered soft-lithographic micro-fabrication process. Tiny hair-sized water channels and chambers typically 100 micro-meters (μm) wide and 10 μm high will be sculpted onto a prepared silicon wafer (i.e. photoresist spun coated) via a UV Mask Aligner. These channels are then to be cast onto a transparent cubic inch multi-layered polydimethylsiloxane (PDMS) chip and placed onto a glass substrate. The designed and fabricated microfluidic chips should have the capacity to perform complex multifunctional laboratory functions under the automated control of a multi-tasking computer with minimal human involvement for as many as one thousand patients on a single microfluidic chip the size of a postage stamp.

Basically, this research project aims to design and develop a user friendly off-chip to on-chip fluid transport system that will interface micromechanical valves used in MSLI and macro-mechanical valves used in High Pressure Liquid Chromatography (HPLC) such that a microfluidic system can be operated by one individual. The goal is to project MSLI towards achieving low cost, portable point-of-care medical diagnostic solutions for the growing crisis caused by HIV/AIDS and TB epidemics.

3.3 Specific Aims

The specific objectives of this study are to develop a microfluidic large scale integration system that achieves the following:

1. Time conservation: - to reduce the set-up time to less than thirty (30) minutes.
2. Standardized system: - to have a standard set-up and fluidic manipulation system to allow access and use of more complex platforms that use hundreds of micro-valves.
3. User-friendliness: - to enable unskilled personnel to flawlessly set-up and run a microfluidic system.
4. Portability: - to enable the mobility and implementation of microfluidic large scale integration platforms that perform medical diagnostics as practical health care solutions in resource limited settings.

3.4 Conceptual Framework

To achieve the aims of this research project, we will investigate several approaches to solve existing challenges on the current microfluidic systems.

A key reason for the long duration of chip set-up is the need to manually fill each control line with water independently using material shown in Figure 3.1 (a) and a dispensing syringe and then placing the control pins into the chip individually during the chip preparation. After the insertion of pins, the system will represent that shown in Figure 3.1 (b). A connection of each of the control channels to its respective pressurized line is to be made by connecting each control channel to its individual port on the pressure manifold as shown in Figure 3.2. This process coupled with the insertion of pins is prohibitively laborious as a lot of time is required for the set-up (6 hours to an entire day) and this requires the meticulous attention of highly trained personnel.

The first step of our new approach will be to investigate and develop ‘microfluidic plugs’ to incorporate multiple control pins into the chip simultaneously as shown in Figure 3.3.

The second step of our new approach will be to investigate the possibility of moving MSLI systems from a manual loading process during chip preparation to an automated loading process. Basically, the second step seeks to automate the off-chip to on-chip fluid transport.

The third step will be to investigate the possibility of miniaturization of the pressure and valve control module shown in Figure 3.4 that harbours the pressure manifolds (shown in Figure 3.2) into a portable device that is of low-cost maintenance.

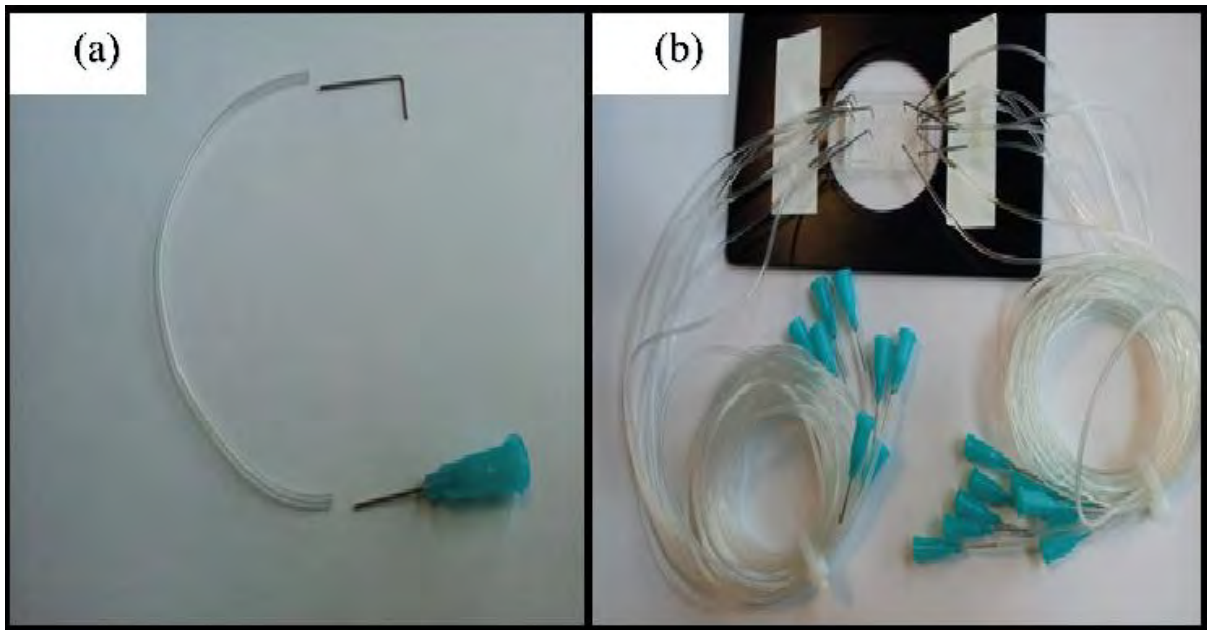


Figure 3.1: (a) Picture showing a microfluidic stainless steel stub (top), tygon tube (middle) and luer stub adaptor (bottom). Both the stub and the adaptor have a 23 gauge blunt-end stainless steel tube. (b) Picture showing a microfluidic chip connected to luer-tygon-tube connections.



Figure 3.2: Picture showing 8 luer stubs attached to an 8-port pneumatic pressure manifold.

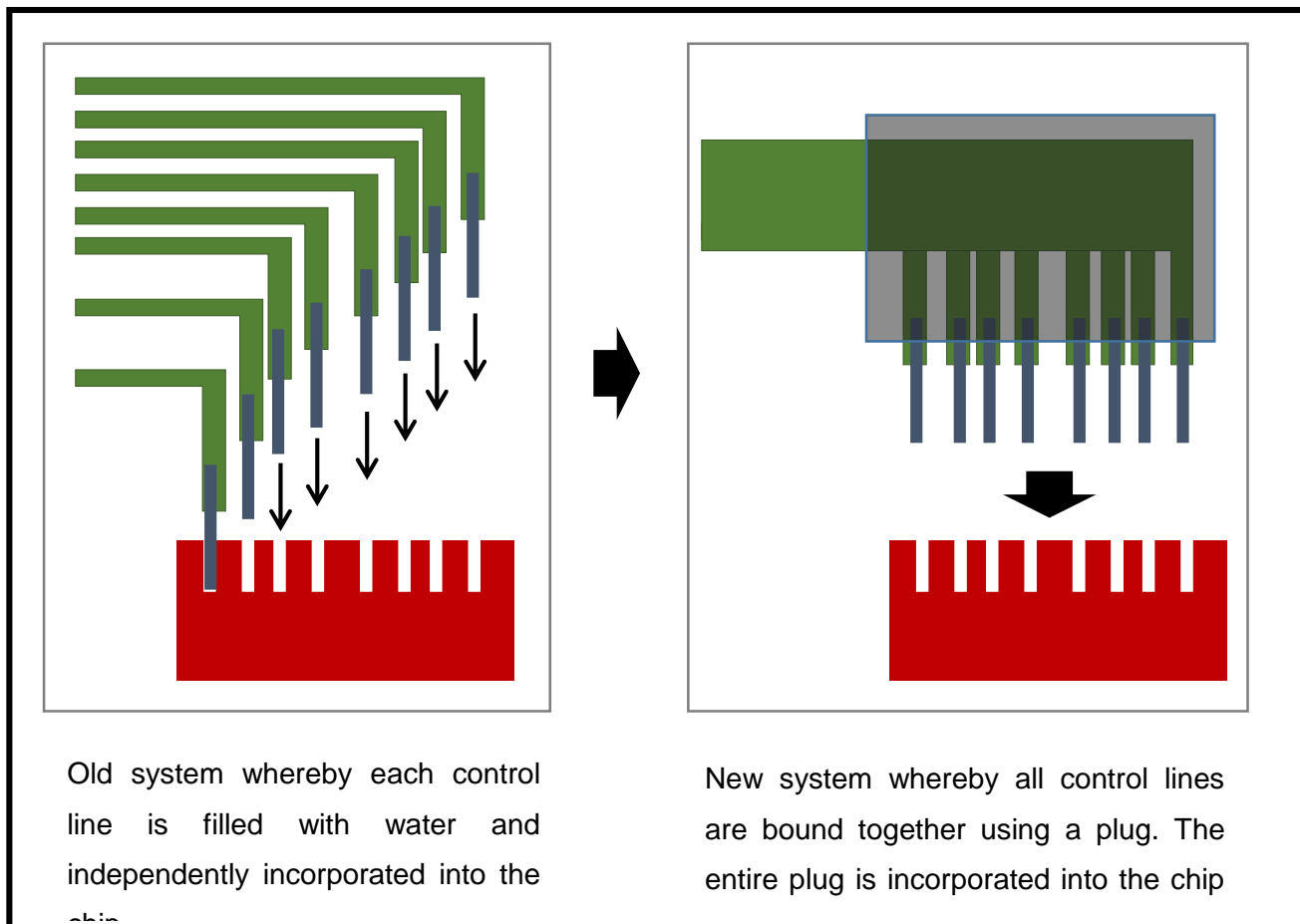


Figure 3.3: Diagram showing the new approach of using microfluidic plugs.

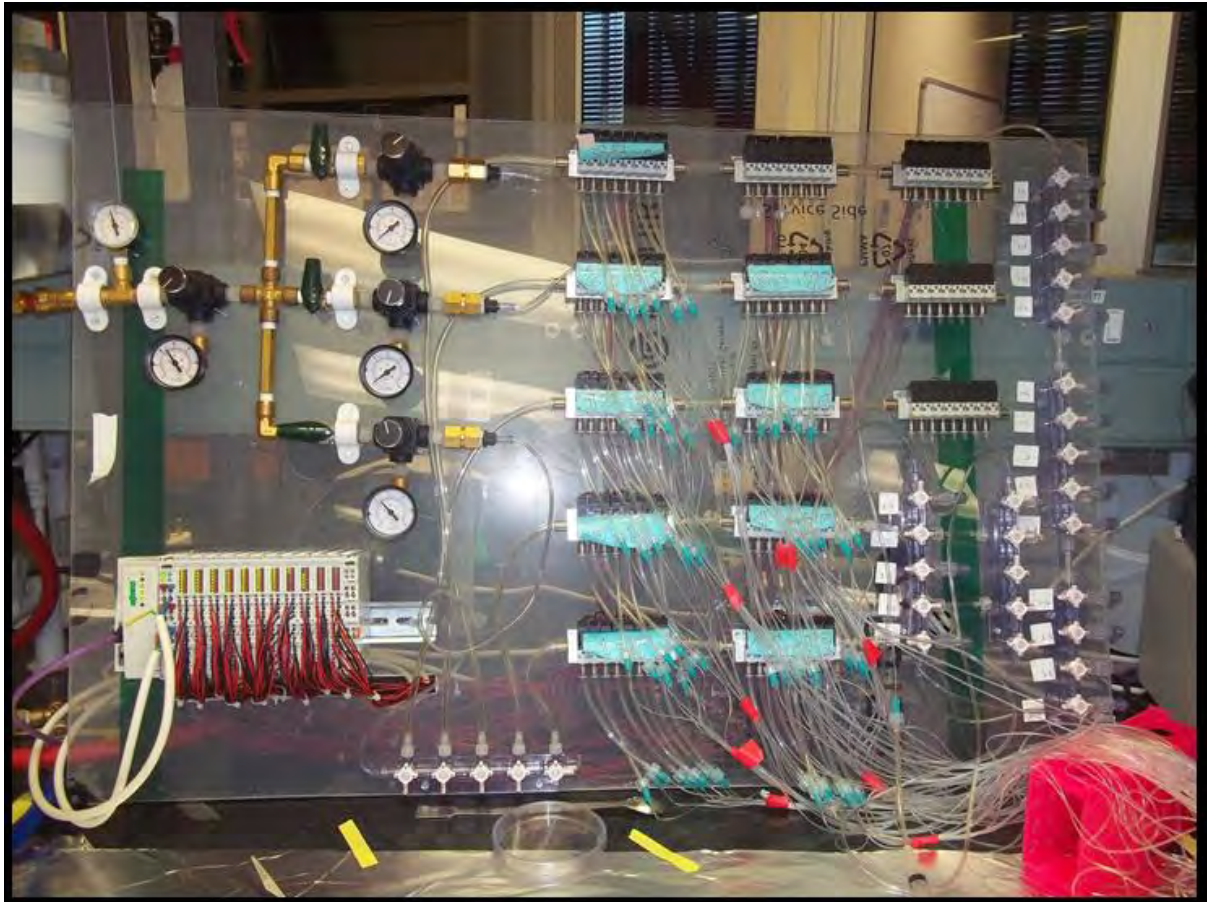


Figure 3.4: The pressure and valve control module. It is connected to the computer via an ethernet communication cable. This module comprises of a series of 8-port pneumatic pressure manifolds connected to pneumatic pressure regulators and a pneumatic pressure source (air compressor).

CHAPTER 4: METHODOLOGY

4.1 Materials

4.1.1 Microscopy.

The microfluidic system developed in this project consisted of an Olympus CKX41 inverted trinocular head microscope. The imaging was done using the Olympus UPlanFL N 4X/0.13PhP and Olympus CAch N 10X/0.25PhP objectives. Images captured and movies recorded were performed using the Olympus SC 30 and Olympus SC 100 colour digital cameras. The Olympus SC 30 camera is most suitable for live inspection and movie recording (It has a full resolution mode that offers 10 images per second at 3.2 megapixel resolution) while the Olympus SC 100 is most suitable for documentation (It is capable of capturing 10.6 megapixels with each single snapshots for unprecedented resolution at low magnification) [99]. The imaging was performed using Analysis getIT v 5.1, imaging software developed by Olympus Soft Imaging solutions GmbH.

4.1.2 Multilayer Soft-Lithography.

Multilayer Soft-lithography (MSL) offers a low cost technique of fabricating polydimethylsiloxane (PDMS) microfluidic devices with on-chip microvalves for automated and precise control of fluid flow [95]. The device described in this project was fabricated using the multilayer soft-lithography developed by the Quake research group, this was explained in detail in a previous chapter. The same 3 step microfabrication process of soft-lithography described in a previous chapter, was used.

For the concept development step, device designing was done with a computer-aided design (CAD) program (AutoCAD[®] software in particular). For the rapid prototyping step, the photomask was used to perform photolithography. Positive or negative photoresist was spun coated on a clean silicon wafer at specified thicknesses as required for each of the designed features and exposed to UV light. For the replica molding step, the process involved the casting of a transparent, silicone-based liquid pre-polymer, against the master mold using an elastomeric material (PDMS in particular) to generate a negative monolayer (or monolithic layer) replica of the master.

4.1.2.1 Multi-layered Soft-lithography Device fabrication protocol/method.

In the first step of device fabrication, the device was designed using Autodesk AutoCAD® 2014 software and the completed design was then sent to fabricating services such as The Stanford microfluidics foundry at Stanford University, USA [100] or printing services such CAD/Art Services Inc. in the USA. After this step, PDMS master molds and PDMS microfluidic device fabrication processes were performed. The procedures are presented in this sub-section. These processes were performed in the laboratory's clean room facility. A clean room is a specially designed laboratory where the size and the number of airborne particulates are highly controlled, together with the temperature, air pressure, humidity, vibration and lighting (yellow to avoid photoresist activation) [4].

PDMS Master Mold Fabrication Procedure

For the work described in this dissertation, the actual process parameters used in the fabrication of the microfluidic device master molds is presented in Appendix A.

Materials and Equipment

- 4” Silicon wafers
- Wafer tweezers
- Negative photoresist - SU-8 2010 from Microchem Corp., USA
- Negative photoresist developer - SU-8 developer from Microchem Corp., USA
- Positive photoresist - MAP 1275 from Microchem Corp., USA
- Positive photoresist (MAP 1275) developer - ma-D 531 from Microchem Corp., USA
- Isopropyl alcohol
- Deionized water
- Silanizing agent - hexamethyldisilazane (HMDS) and trichloromethylsilane (TCMS) from Sigma-Aldrich® Corp., USA
- Cleaning Solution – Micro-90 solution
- Transparency mask – clear glass plate
- Photomasks - CAD/Art Services Inc. (USA) printed masks on emulsion film.
- 3 or 4 hot plates
- Laboratory oven
- Sample shaker or rocker –
- Vacuum pump and desiccator – Wirsam Scientific & Precision Equipment (South Africa) desiccator.
- Spin coater - Laurell Technologies Corp.® WS-650Hz-23 Spin coater, equipment used to create a layer of specific height of un-cross-linked photoresist on a silicon wafer by spinning the substrate
- Mask aligner - SUSS MicroTec MJB4, equipment used to cross-link the photoresist by exposing the photoresist through the aligned photomask to UV light.
- Profilometer – KLA-Tencor D-120 profilometer, equipment used to measure widths and heights of photoresist features on silicon wafers.

Method Overview

1. Cleaning transparency mask: - The transparency mask (clear glass plate) is inspected for scratches and if scratches are absent, it is then cleaned with a cleaning solution (Micro -90 or isopropyl alcohol) to remove any surface particulates and rinsed off with clean water. It is then dried using an air gun. When clean, the photomask of a single layer is attached to the transparency mask and installed on the Mask Aligner in preparation for exposure stage.
N.B.: Each pattern of the photomask should be attached to its own clean transparency mask.
2. Cleaning silicon wafers: - Prior to starting the master mold fabrication process, it is important to ensure the silicon wafers are clean. This can be done by placing wafers in a bubbling piranha solution (1:3 sulphuric acid and hydrogen peroxide) for 10 minutes [92]. Afterwards, wafers should be rinsed with deionized water and dried using nitrogen gas. The cleaned wafers should then be placed on a hotplate for 15 minutes at 200 °C to evaporate any residual humidity [92]. After the heating process, let the wafer cool at room temperature before proceeding to the next step.
3. Spin coating photoresist: - According to desired height and feature profile (i.e. rectangular or rounded geometric profile) of the device, spin coat the silicon wafer with photoresist (negative photoresist for rectangular geometric profiles and positive photoresist for rounded geometric profiles). Spin time, speed and acceleration should be taken into account when using the spin coater to achieve the desired layer coat thickness. Layer thickness is inversely proportional to spin time, speed and acceleration [4].
4. Soft-bake or Prebake: - Bake the spin-coated wafer on a hot plate at 65 °C and 95 °C for the amount of time specific with manufacturer's instructions for coatings of your desired thickness. Times can be as short as a couple of minutes (layers < 5 µm thick) or as long as hours (layers > 200 µm thick) [4]. After the bake, let the soft-baked wafer cool at room temperature before the next step.
5. Exposure: - According to the light intensity provided by the mask aligner and the thickness of your coating, certain exposure energy is required as specified by manufacturer's instruction. In practice, the light intensity of the mask aligner is usually fixed and the exposure energy can be varied by changing the exposure time [4].
6. Post exposure bake: - After exposure, depending of the nature of the wafer (i.e. negative photoresist spin-coated wafer or positive photoresist spin-coated wafer), bake the wafer on a

hot plate at 65 °C and 95 °C for the amount of time specific with manufacturer's instructions for coatings of your desired thickness. Positive photoresist spin-coated wafers do not require a post exposure bake step. After the bake, let the wafer cool at room temperature before the next step.

7. Development: - Immerse the wafer into a container with photoresist developer and gently move or agitate the container around to mix the solution. Development times range from a few minutes (for layers thinner than 10 μm) to hours (for layers more than 400 μm thick) and the movement/agitation is usually done manually or using a shaker at an agitation rate of 60 Hz [4]. After development, thoroughly dry the wafer using an air gun and inspect the wafer on a microscope to determine if all desired features are visually observable and to determine if the master mold is useable for the PDMS device fabrication process or replica molding step.
8. Profiling: - Using a profilometer device, a measurement of the widths and heights of photoresist features on silicon wafers is performed to verify if the desired dimensions and channel profile (rectangular or rounded profile) on the master molds have been obtained.
9. Mold reflow: Only applies to positive photoresist spin-coated wafers. After the profiling step, bake the wafer on a hot plate at 65 °C and 95 °C for the amount of time specific with manufacturer's instructions for coatings of your desired thickness. After the bake, let the wafer cool at room temperature before profiling it again to check if the channel geometry is rounded.
10. Hard-Bake: This is one of the last steps that removes any casting solvent residue such as photoresists and development solvents. Bake the wafer in an oven. Hard baking temperatures frequently range from 120 °C to 150 °C and baking times are usually longer than those used in the soft-bake step. After the bake, let the wafer cool at room temperature before proceeding to the final step.
11. Silanization: - This is the last step, place the wafer and an open glass vial with small amount of silanizing agent in a desiccator and apply vacuum for a few minutes and turn it off and leave under vacuum for several hours or overnight in desiccator .

PDMS Microfluidic Device Fabrication Procedure

For the work described in this dissertation, the actual process parameters used in the fabrication of the PDMS microfluidic device is presented in Appendix A (push-up valve configuration) and Appendix B (push down valve configuration).

Materials and Equipment

- Master mold (finished product of the PDMS master mold fabrication process that contain the photoresist features)
- Vacuum pump and desiccator – Wirsam Scientific & Precision Equipment (South Africa) desiccator.
- Spin coater - Laurell Technologies Corp.[®] WS-650Hz-23 Spin coater, equipment used to create a layer of specific height of un-cross-linked photoresist on a silicon wafer by spinning the substrate
- Balance
- Stopwatch
- Laboratory oven
- Scalpel and razor blades
- Scotch tape
- Plastic petri dishes
- Glass slides or cover slips
- Microscope
- Wafer tweezers
- Planetary centrifugal mixer - Thinky Corp., USA, ARE-250CE planetary centrifugal mixer model.
- Silanizing agent - hexamethyldisilazane (HMDS) and trichloromethylsilane (TCMS) from Sigma-Aldrich[®] Corp., USA
- PDMS – Momentive RTV615 044-PLBX Kit obtained from RS Hughes[™], Sunnyvale, USA.
- Punch - Accu-Punch MP 10-UNV from Syneo, Texas, USA.

Method Overview

1. Cleaning master mold wafer: - To ensure easy PDMS release, all master molds are to be silanized by exposing them to a silanizing agent in an air tight container for a few minutes.
2. PDMS mixing: - Weigh the desired amount of PDMS pre-polymer in a disposable or reusable plastic cup. Pour in the appropriate amount of the cross-linker according to the desired final elastomer stiffness (e.g. 10:1 elastomer base to cross-linker base of the PDMS kit). Mix the PDMS using a planetary centrifugal mixer which has been adjusted according to manufacturer's instructions for the desired mixture properties.
3. Flow layer PDMS casting: - Each flow layer master mold (placed in an aluminium foiled covered petri dish) is then coated with an appropriate amount of PDMS mixture to obtain the desired layer thickness.
4. Control layer PDMS casting and glass slide/ cover slip coating: - According to desired height and feature profile of the device, spin coat the control layer master mold with an appropriately mixed PDMS mixture (usually 20:1 elastomer base to cross-linker base). Spin time, speed and acceleration should be taken into account when using the spin coater to achieve the desired layer coat thickness.
5. De-gassing/ de-bubbling: - PDMS on the flow layer master molds is then degassed in a desiccator under vacuum for 60 minutes or until all bubbles have disappeared.
6. Soft-bake: - PDMS coated glass slides or cover slips and both flow layer and control layer molds are then placed in an oven for baking. The soft-bake is done at 80 °C. Baking times can be shorter (up to 40 minutes) for thinner layers and longer (up to 60 minutes) for thicker layers.
7. Alignment: - Following baking, PDMS flow layers are peeled from the molds and cut to size using a razor blade or scalpel. Flow channel access ports are then created using a punch press. The punched flow layers are then aligned onto the PDMS spin-coated and soft-baked control layer master molds.

8. PDMS bonding: - Following alignment, the aligned devices are soft-baked for about an hour at 80 °C in an oven. After the soft-bake, the bonded device is then cut and peeled off the control layer mold and access ports to the control layer are created using a punch press.

9. Substrate bonding: - The multi-layered bonded device is then placed on a cured PDMS coated glass slide or cover slip and placed in an oven at 80 °C for several hours (usually 9 – 12 hours) to allow the PDMS structures control layer to bond to the substrate.

4.2 Chip Designs

The device designing was done using Autodesk AutoCAD® 2014 software. When designing the chip, several design specifics were taken into account, such as sizes of channels (i.e. height and width), type of channels (i.e. rectangular or rounded), feature architecture (i.e. push up or push down valves) and finally the function of the device (i.e. requirements of micropumps, micromixers or rotary channels). The completed design was then sent off to CAD/Art Services Inc. in the USA for high-resolution printing, 40 000 dots per inch (dpi) on transparency and the resultant transparency were the photomasks used for fabricating the device using the fabrication protocol explained above in section 4.1.2.1.

Three microfluidic devices/chips were fabricated and used in the work described in this dissertation, and these are:

A. Dual Port Microfluidic Chip.

This microfluidic device shown in Figure 4.1, is comprised of two PDMS layers bonded to a glass microscope slide. The device has normal microvalves with push-up functionality throughout the entire device and it has no sieve valves. The flow layer (comprising of flow channels used for biological assay transport) is bonded on top of the control layer (comprising of control channels which control the opening and closing of the microvalves for on-chip fluid manipulation) which in turn is bonded to a glass microscope slide with a thin PDMS layer to separate the two layers. These two layers are presented in Figure 4.2.

In the microfluidic device, the control layer contains channels that are 10 μm high and 50 μm wide with rectangular geometry. The flow layer contains channels that are 10 μm high and 100 μm wide with rounded geometry. The microfluidic device has two inter-connected access ports per control line, one on opposite ends of the chip (i.e. left hand side port connected to respective right hand side port) as shown in Figure 4.2 (a). The control line access ports are arranged in a ‘zigzag’ pattern. Because of this architectural layout, the chip derives its name, “dual port” microfluidic device. The microfluidic device has a rotary flow channel (also referred to as a reactor channel/ reactor ring) which is to be used where continuous flow mixing is required and this is shown in Figure 4.2 (b). There are six flow access ports for every reactor channel as shown also in Figure 4.2 (b).

The device’s design features also includes a rotary and linear pneumatic peristaltic micropumps shown in Figure 4.3 (a) and Figure 4.3 (b) respectively. The overall geometry of the combination of the two micropumps in the design is shown in Figure 4.4, this kind of geometry is useful for

biological experimentation that requires pumping of fluids (using a linear peristaltic pump) into a rotary channel where rotary peristaltic pump will act as a continuous-flow micromixer.

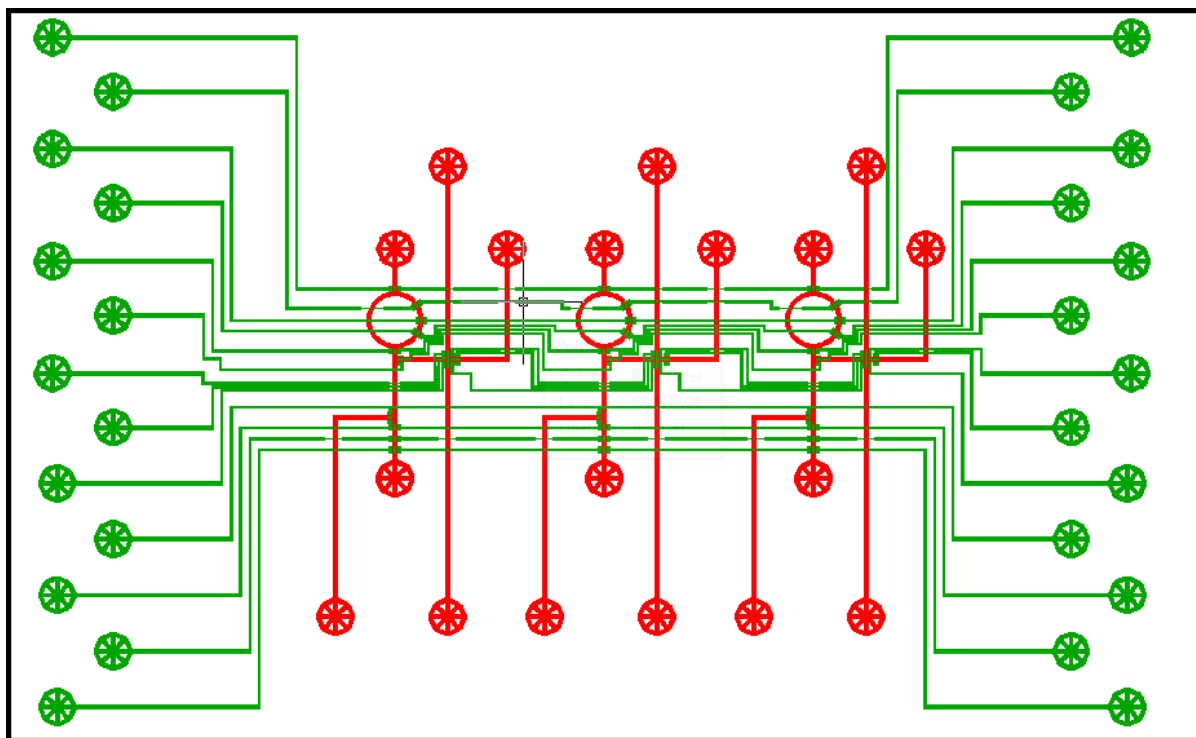
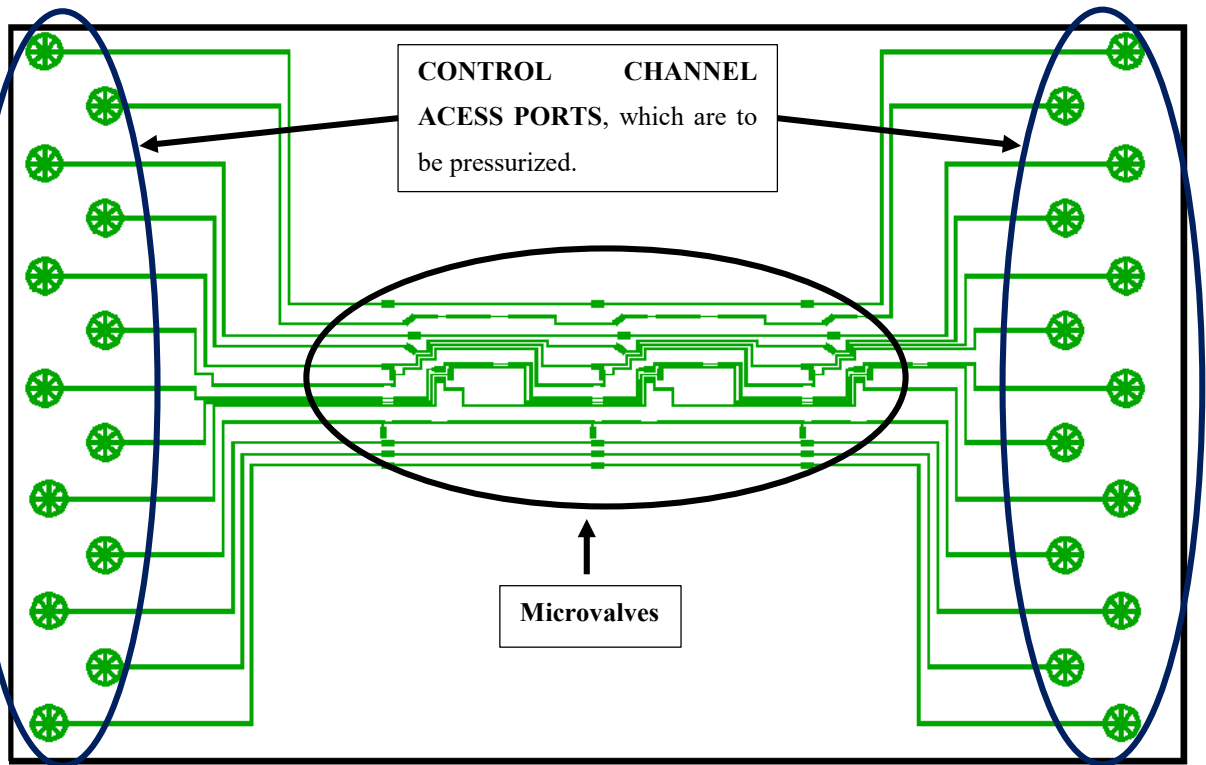


Figure 4.1: Dual port microfluidic device geometry.

(a)



(b)

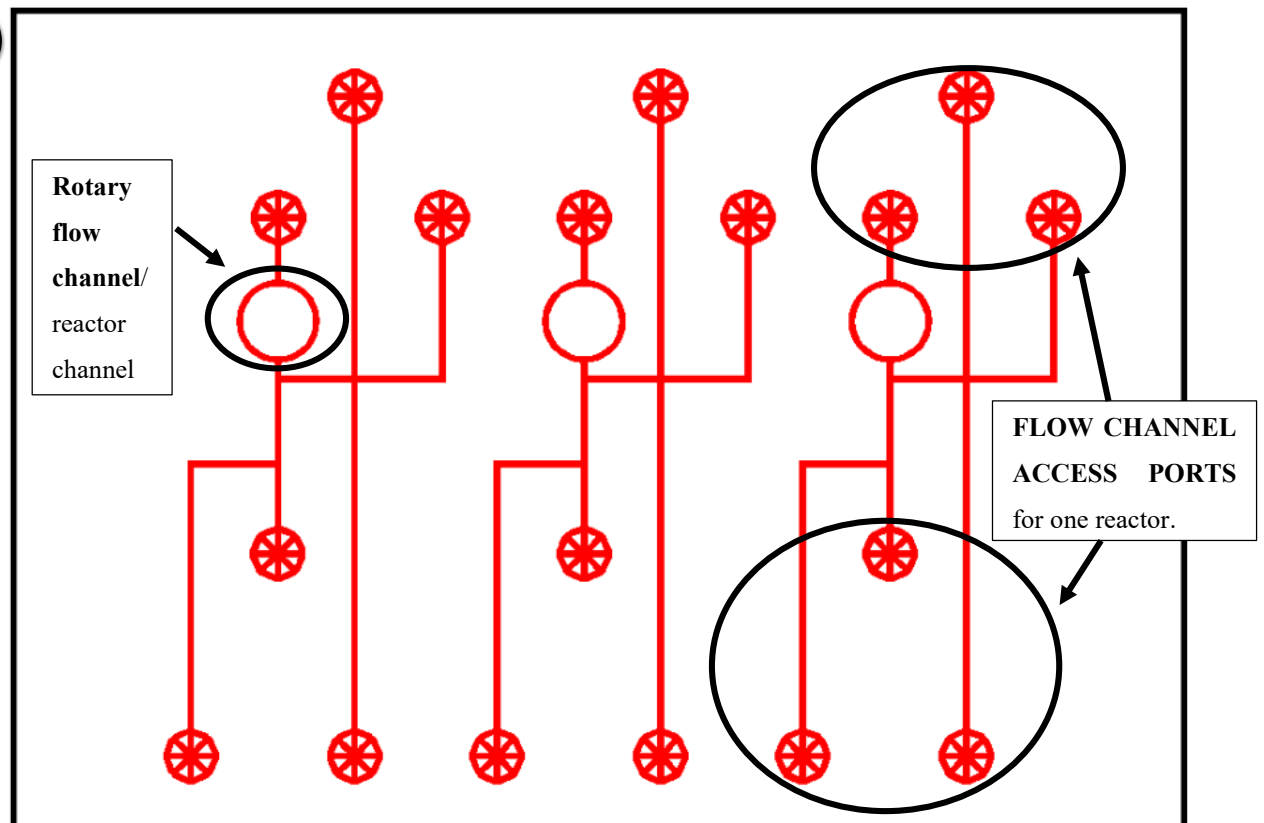


Figure 4.2: The individual layers of the dual port microfluidic chip: (a) shows the bottom PDMS layer, the control channels presented in the green colour; (b) shows the top PDMS layer, the flow channels presented in the red colour. It's a push-up valve configuration design.

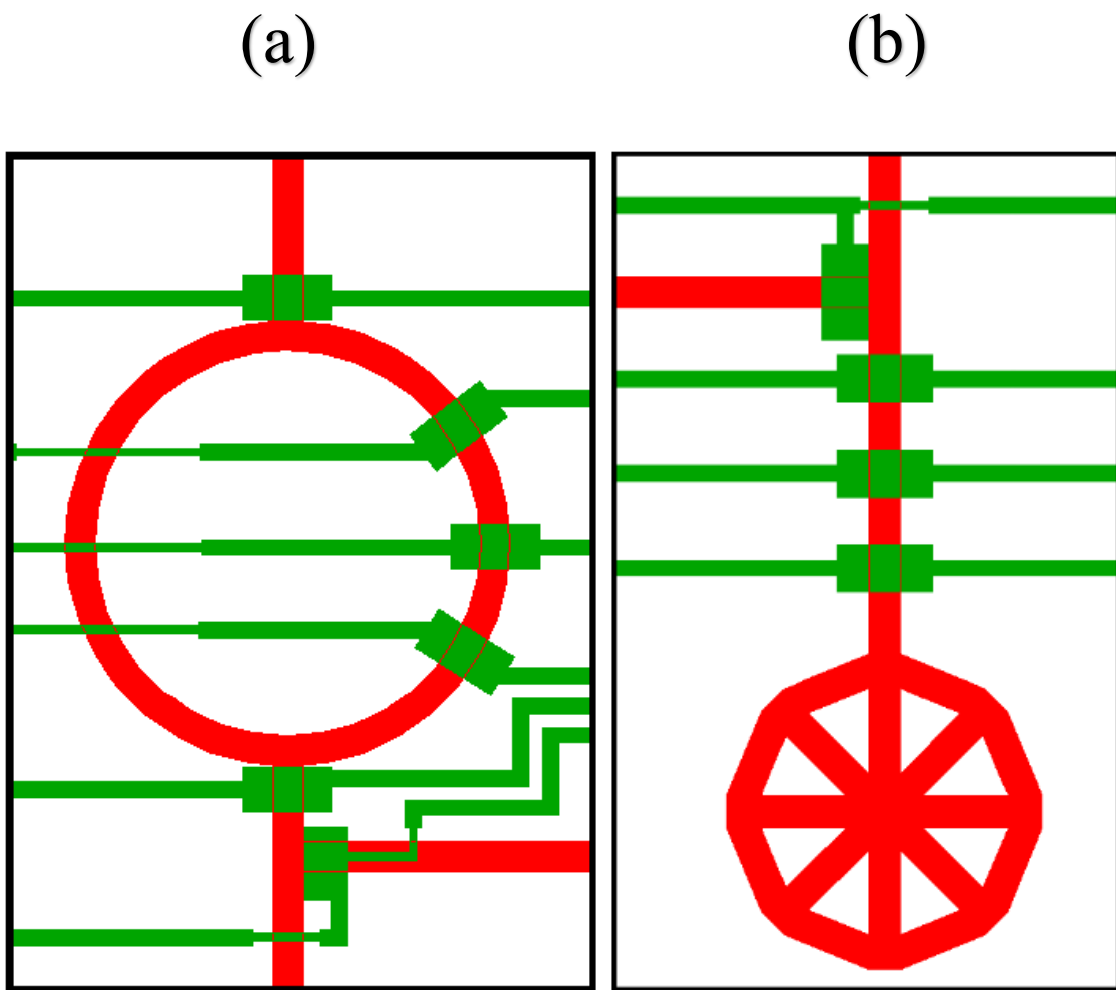


Figure 4.3: (a) - Rotary pneumatic peristaltic micropump, also considered to be micromixer in microfluidic large scale integration; (b) – Linear peristaltic micropump.

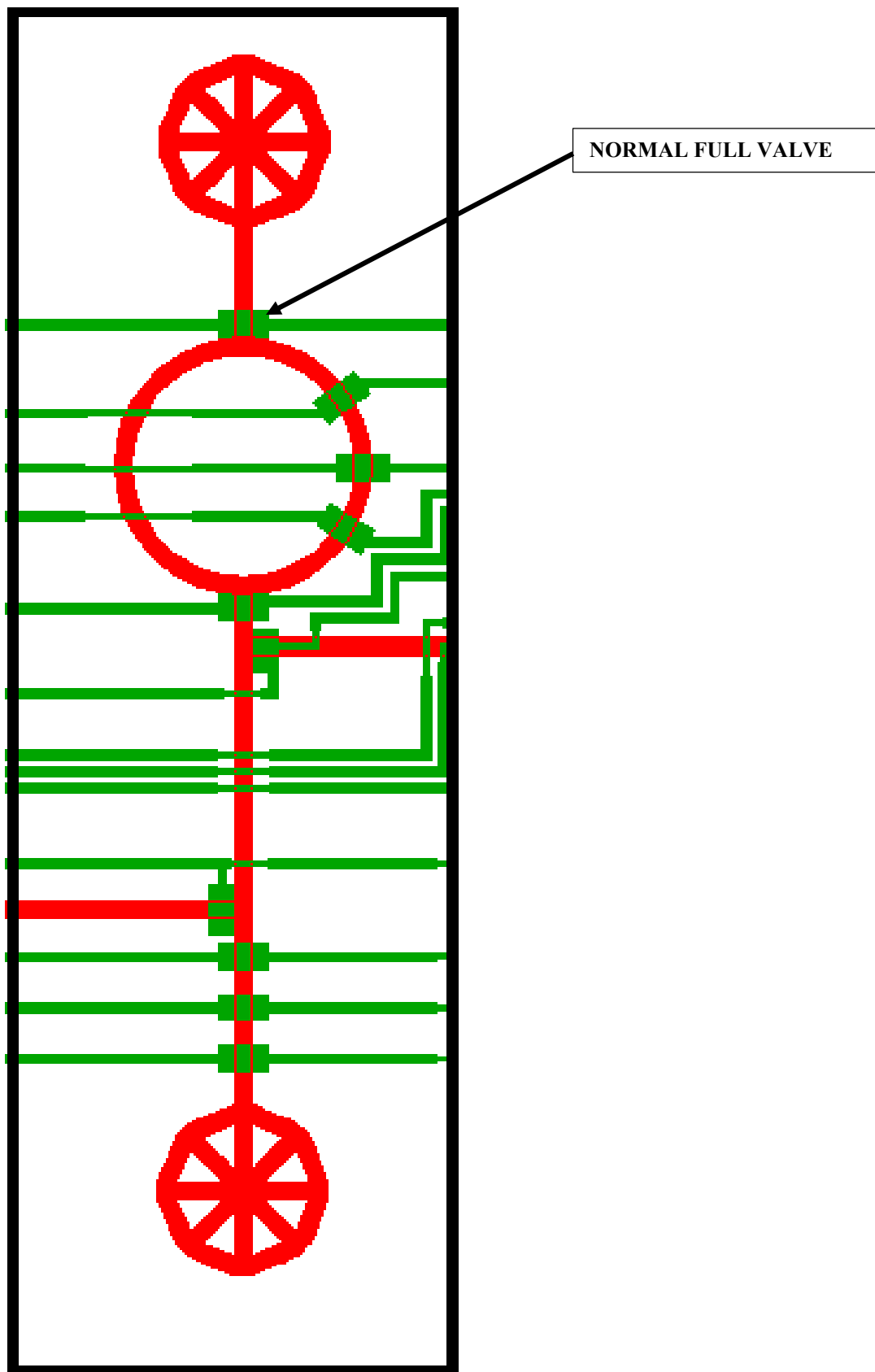


Figure 4.4: The microfluidic chip geometry showing the designed combination of the linear and rotary peristaltic micropump.

B. Single Port Microfluidic Chip.

This microfluidic device shown in Figure 4.5, is comprised of two PDMS layers bonded to a glass microscope slide. The device has normal microvalves with push-up functionality throughout the entire device and it has no sieve valves. The device architecture and features are exactly the same as that of the dual port microfluidic chip. The two layers of this microfluidic device are shown in Figure 4.6. The device is called a ‘single’ port microfluidic chip because it has one port per control line. This is the only difference between the dual port and single port microfluidic chip.

The device’s design features also includes a rotary and linear pneumatic peristaltic micropumps shown in Figure 4.3 (a) and Figure 4.3 (b) respectively. The overall geometry of the combination of the two micropumps in the design is shown in Figure 4.4.

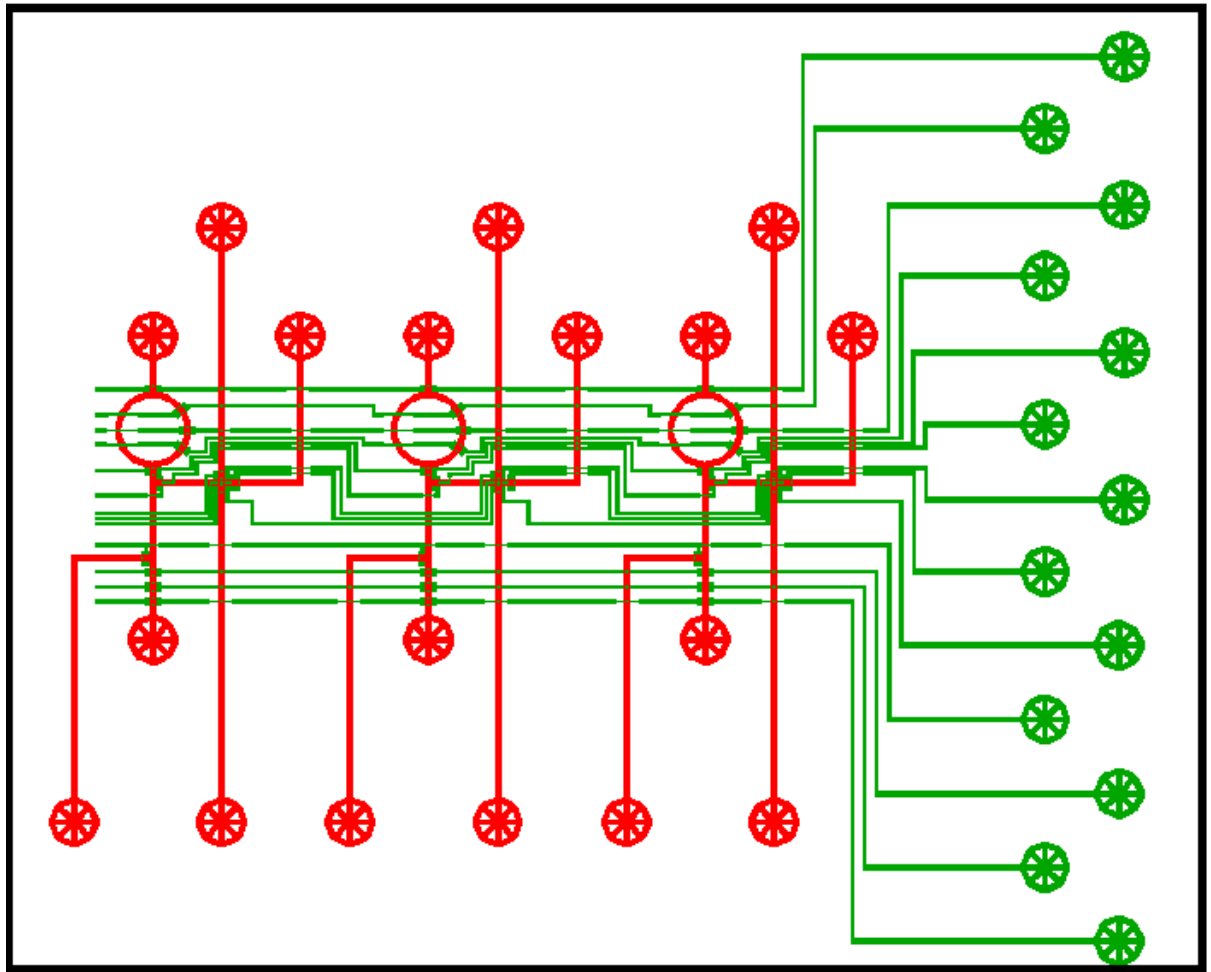
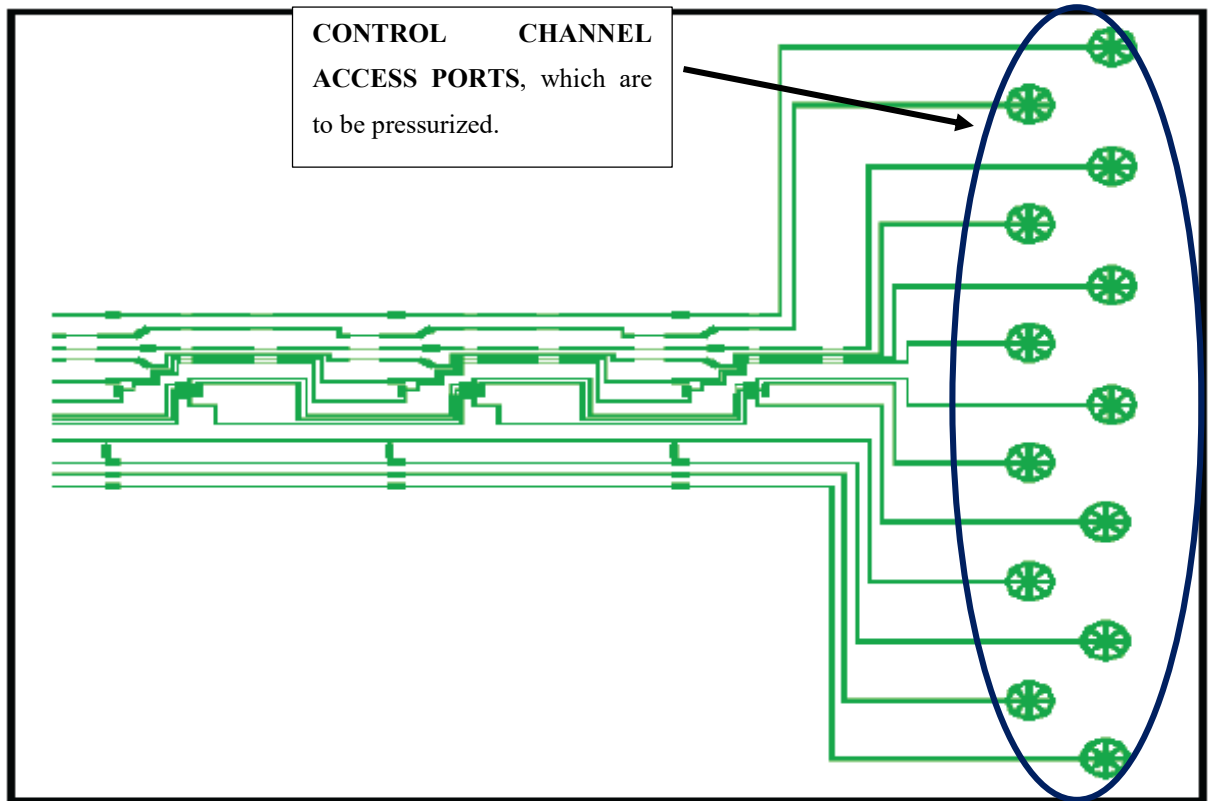


Figure 4.5: Single port microfluidic device geometry.

(a)



(b)

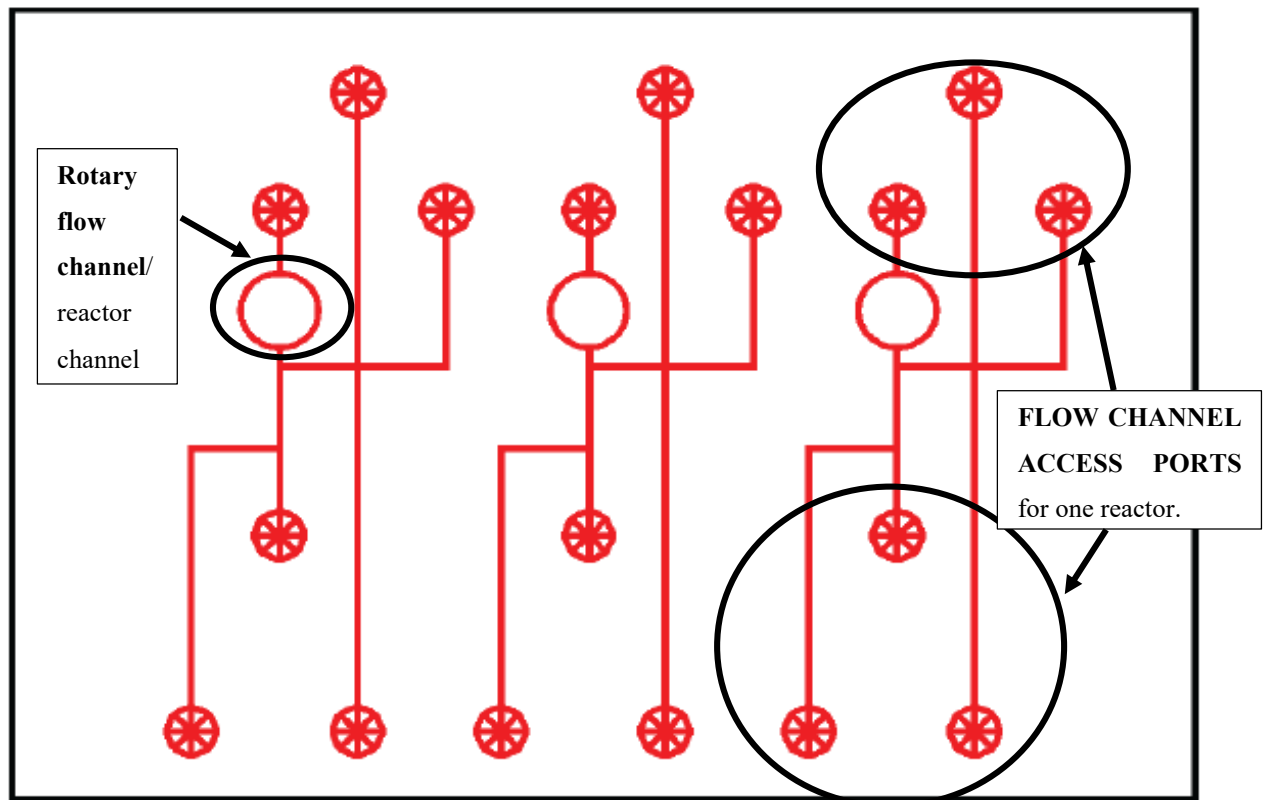


Figure 4.6: The individual layers of the single port microfluidic chip: (a) the control channels presented in the green colour; (b) shows the flow channels presented in the red colour. It's a push-up valve configuration design.

C. Hybrid Dual Port Microfluidic Chip.

This microfluidic device shown in Figure 4.7, is comprised of two PDMS layers bonded to a glass microscope slide. The device has normal microvalves with push-down functionality throughout the entire device and it has no sieve valves. The control layer (comprising of control channel which control the opening and closing of the microvalves for on-chip fluid manipulation) is bonded on top of the flow layer (comprising of flow channels used for biological assay transport) which in turn is bonded to a glass microscope slide with a thin PDMS layer to separate the two layers. These two layers are presented in Figure 4.8.

In the microfluidic device, the control layer contains channels that are 10 μm high and 50 μm wide with rectangular geometry. The microfluidic device has two inter-connected ports per control line on the same side of the device i.e. on the left hand side. These ports are also aligned in a 'straight' pattern as shown in Figure 4.8 (a) different to the 'zigzag' pattern used on the dual and single port microfluidic devices. This device has a control line access port architectural layout that maintains a dual port functionality. The dual port functionality is maintained in the sense that the two ports are interconnected by a 10 μm high and 100 μm wide bridging channel. Because of these modifications, the microfluidic device is called the 'hybrid' dual port microfluidic device.

The flow layer contains channels that are 10 μm high and 100 μm wide with rounded geometry. The device maintains the six flow channel access port per reactor channel like the two previously discussed devices. These access ports are also aligned in a 'straight' pattern on the opposite end of the control line access ports, different from the flow channel access port layout found in the dual and single port devices.

The device's design features also includes the rotary and linear pneumatic peristaltic micropumps shown in Figure 4.3 (a) and Figure 4.3 (b) respectively. The overall geometry of the combination of the two micropumps in the design is shown in Figure 4.4.

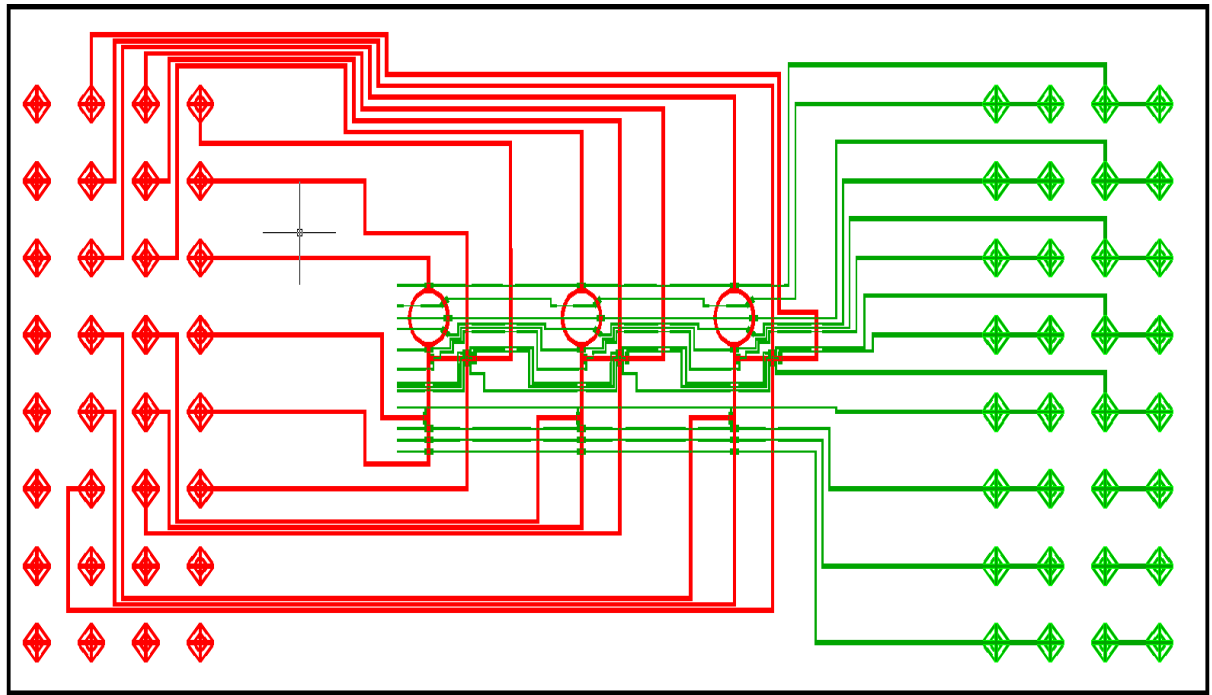


Figure 4.7: Hybrid dual port microfluidic device geometry.

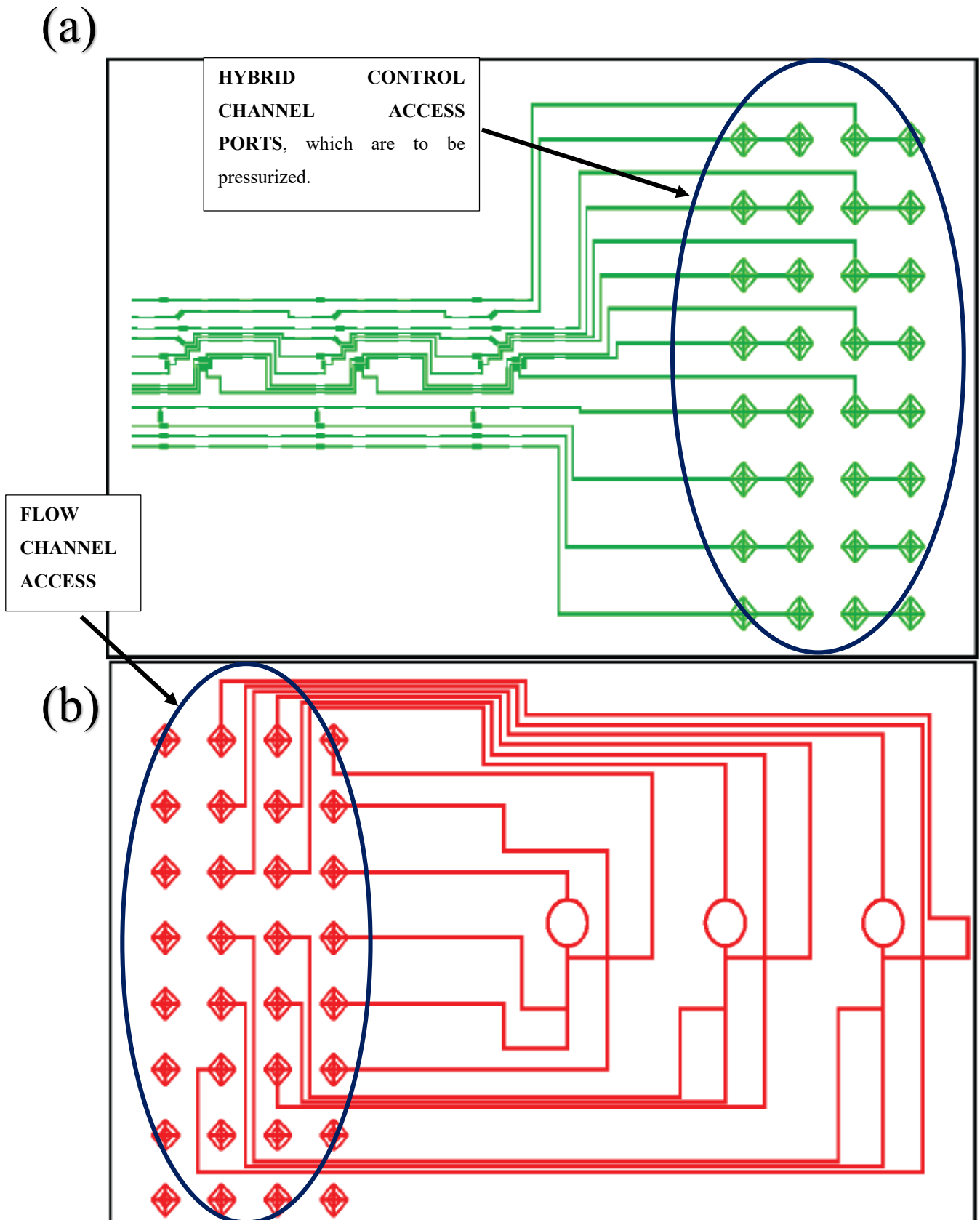


Figure 4.8: The individual layers of the hybrid dual port microfluidic chip: (a) shows the top PDMS layer, the control channels presented in the green colour; (b) shows the bottom PDMS layer, the flow channels presented in the red colour. It's a push-down valve configuration design.

4.3 Plug Designs

A key reason for the long duration of a microfluidic device set-up work flow is the need to manually fill each control line with water independently using a dispensing syringe and placing the control pins into the microfluidic device one at a time. After the insertion of pins, a connection of each of the control channel to its respective pressurized line is made by connecting each control channel to its individual port on the pressure manifold. This process coupled with the insertion of pins is prohibitively laborious as a lot of time is required to set-up (6 hours to an entire day) and requires the meticulous attention of a highly trained personnel.

The first step of the new approach will be to investigate and develop ‘microfluidic plugs’ to incorporate multiple control pins into the chip simultaneously as shown in Figure 4.9. In the work described in this dissertation, two different microfluidic plugs were designed and developed to be compatible with the commonly used tubing (0.02” OD X 0.06” ID, acquired from Cole Parmer, UK) for microfluidic applications.

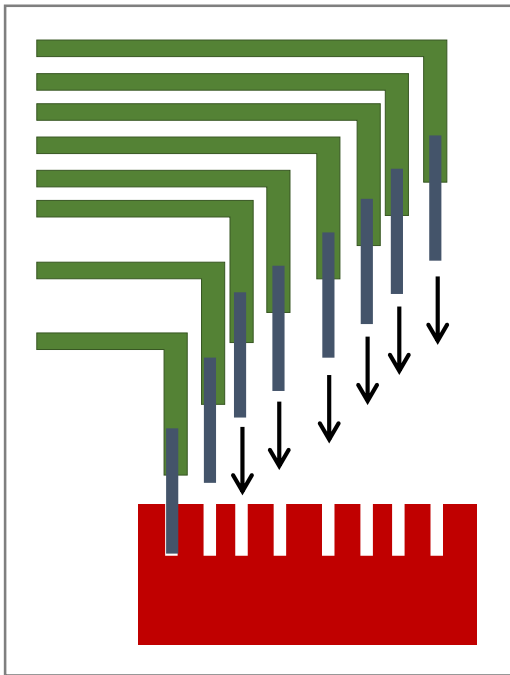
The two developed plugs are:

1. Polymethyldisiloxane (PDMS) Microfluidic Plug

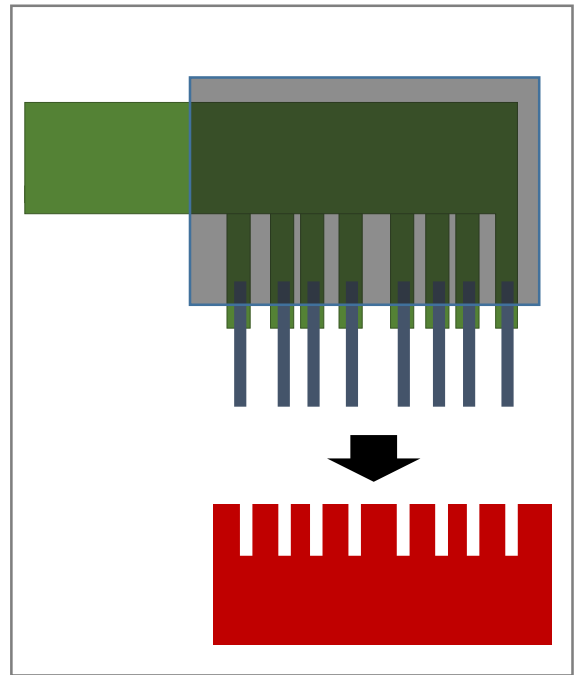
This microfluidic plug was made using the same material used to make the microfluidic device, polymethyldisiloxane (PDMS). The microfluidic plug is a PDMS monolayer fabricated using the control layer master mold in the same manner the microfluidic device’s control layer was made. Using a razor blade or scalpel, the PDMS control layer was trimmed or cut around the control line access ports; the cut area on the PDMS control layer is highlighted in Figure 4.10. The cut pieces (left hand side and right hand side rectangular pieces) were then punched in alignment to the access port pattern appearing on the surface to enable the plug to be easily matched on the microfluidic device when inserting the plug. 1” steel pins (0.025” OD X 0.013” ID X 1” long steel pins, acquired from New England Small Tube Corporation, UK) were then inserted through the punch ports. To hold the pins in place, a small layer of epoxy adhesive (Loctite M-31CL Hygol Medical Device Epoxy Adhesive) was plastered on plug surface and left to dry for 24 hours.

2. Epoxy Adhesive Microfluidic Plug

The microfluidic plug was made using an epoxy adhesive (Loctite M-31CL Hygol Medical Device Epoxy Adhesive) and 1” steel pins (0.025” OD X 0.013” ID X 1” long steel pins, acquired from New England Small Tube Corporation, UK). The epoxy microfluidic plug was made by using a microfluidic device and a PDMS monolayer of the control layer. The PDMS monolayer was cut around the control line access ports as highlighted in Figure 4.10, and the PDMS monolayer was left with hollow sections. It was then placed and aligned on top of the microfluidic device which has the 1” steel pins protruding from it. Once aligned, epoxy adhesive was carefully poured into the hollow sections and left to dry for 24 hours. After the epoxy was dried, the PDMS monolayer was peeled off the cured epoxy leaving the epoxy microfluidic plug shown in Figure 4.11.



The old system whereby each control line is filled with water and independently incorporated into the device.



The new system whereby all control lines are bound together using a plug. The entire plug is incorporated into the device.

Figure 4.9: Diagram showing the main difference between the old system of inserting pins and the proposed new system of using microfluidic plugs to insert pins into the microfluidic device.

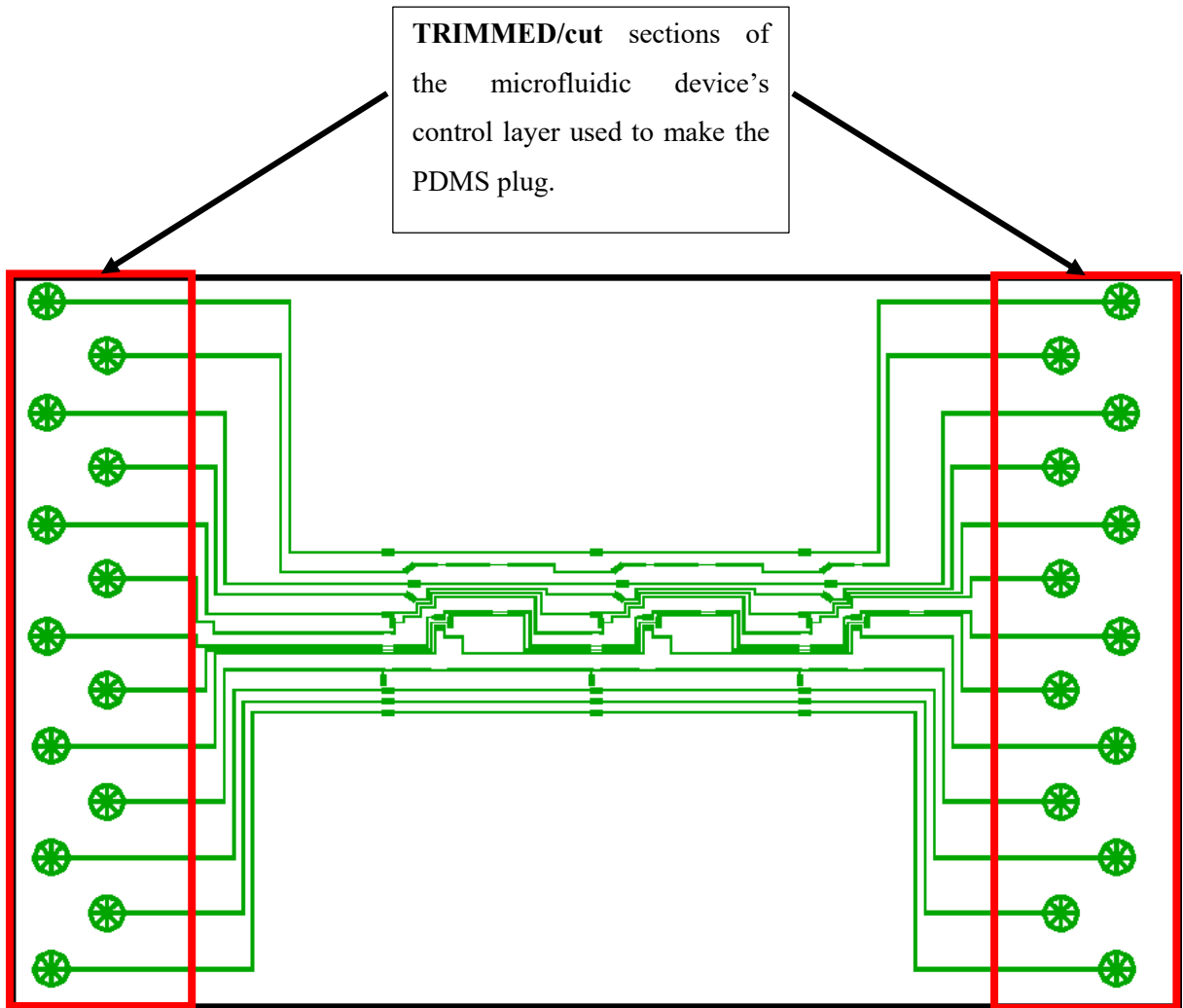


Figure 4.10: Diagram showing the trimmed sections of the PDMS microfluidic device's control layer used to make PDMS plugs.

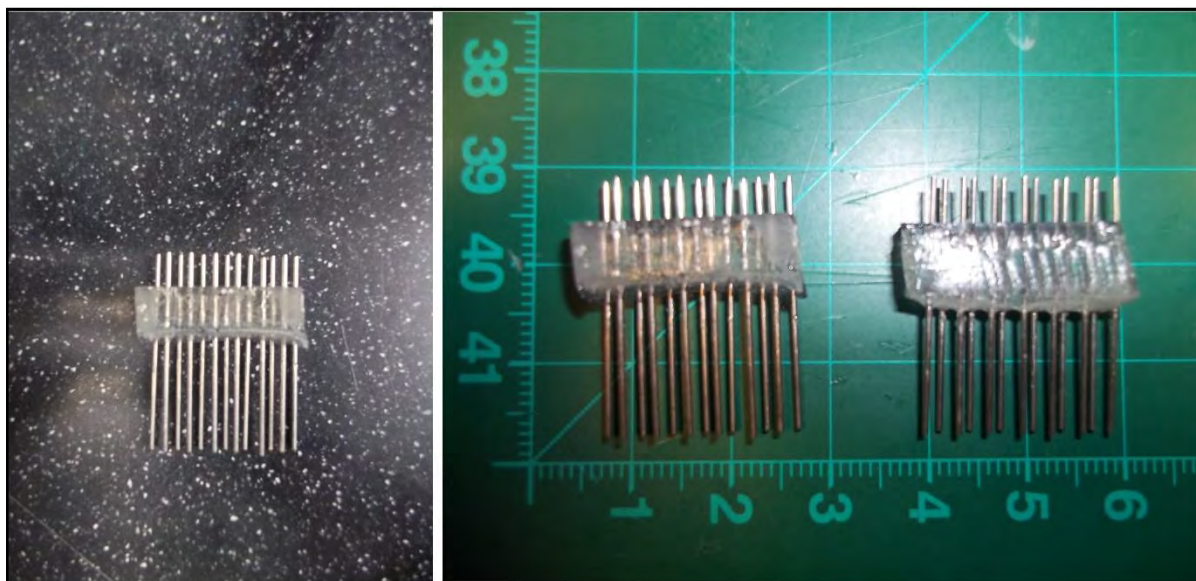


Figure 4.11: Epoxy adhesive microfluidic plugs.

4.4 Auto-loading System

4.4.1 Background and Significance.

One of the first commercially available laboratory automation platforms was developed by Skeggs and published in 1957 and made commercially available by Technicon Corporation [101]. The first machines, the Autoanalyzer utilized continuous flow analysis in which a continuous stream of fluid was divided into segments by air bubbles. The air bubbles were introduced into the stream to maintain separation between samples [101]. These first machines were successful and gave satisfactory analytical results of blood urea or glucose at the rate of up to 40 samples per hour [101]. While these systems were a significant advancement in laboratory automation, the serial processing and analysis design limited throughput.

The 1950s brought about the emergence and common use of microtiter plates which eventually made a significant impact on the standardization of laboratory automation. Microtiter plates enable parallel processing of clinical samples for high throughput analysis in molecular diagnostics assays such as enzyme-linked immunosorbent assay (ELISA) and those used in polymerase chain reactions (PCR) and the most common automated molecular diagnostics tests often utilize robotic sample handling systems compatible with 96-well plates [102]. These robotic arms can be programmed to dispense or withdraw reagent, control temperature, mix solutions by shaking and transport microtiter plates between locations [102].

Since the introduction of the multilayer soft-lithography (MSL) as one of the most convenient ways of fabricating complex microfluidic devices consisting of a vast network of channels, valves, mixers and pumps in the early 2000s, great advances have been witnessed in the microfluidics field especially in the Microfluidic Large Scale Integration (MLSI) platform. To date, selected automated microfluidic devices have been developed, and a variety of microfluidic instruments used for nuclei acid and protein electrophoresis analysis are now commercially available [103]. However, these instruments are currently constrained from being popularized in common laboratories due to their high cost of purchase and maintenance.

Most MLSI based microfluidic devices still require the traditional manual preparation procedure making it impractical for microfluidic devices with a high on-chip operation complexity to be used for either scientific research or point-of-care diagnostics. When the fluid transport during the microfluidic device preparation step is automated, fast and precise fluid operation can be anticipated and some of the existing biased malfunction problems existing in the manual set-up can also be eliminated. An automated fluid transport system for device preparation and sample handling coupled with the

microfluidic devices can provide an efficient, low-cost maintenance and portable solution to impracticality of using microfluidic devices in a point-of-care environment.

4.4.2 Automation (Auto-loading) Characterization.

Microvalves and micropumps on the microfluidic device/chip automate the transport of samples and reagents to various locations on a device for processing and analysis. The multi-layered soft-lithography fabricated microvalves, Quake valve [3], use a fluid, usually de-ionized water in the control channels. Pressure is applied in the control channels to close a valve and no pressure is applied to open a valve. This is how an off-chip pressure source opens and closes valves.

The on-chip fluid handling has been successfully developed and being deployed in many applications. However, there is a technological gap between off-chip fluid handling/transport and on-chip fluid handling, and for this reason most MLSI based microfluidics system are impractical to use in POC setting. The main issue is that there is need to form a physical connection (i.e. off-chip to on-chip interface) to deliver fluid into the control channels in a quick, safe and efficient way. This is important if we are to have a fully automated MLSI system that offers an automated handling of control channel fluid in the device preparation step with minimal human involvement. When this system is extended to the flow channels, it will also provide an automated biological auto-sampling system for off-chip to on-chip sample transport.

The off-chip to on-chip fluid transport is automated by making use of electrically actuated valves. We used a multi-position, dead-ended flow path, universal electrical actuated, high torque valve (EUTA-2CSD16MWE) which can be simply referred to as the SD valve and a multi-position, flow-through flow path, universal electrical actuated, high torque valve (EUTA-2CSF16MWE) which also can be simply referred to as the SF valve were procured from VALCO Instruments Company Inc. a company based in Switzerland.

The SD valve selects one of the 16 flow path streams. A stream refers to a flow path. The selected stream flows from the outlet to either another sampling valve, pressure sensor, liquid detector or microfluidic device etc. The same flow path can be used to direct one stream to a number of outlets. The schematic of this valve is shown in Figure 4.12. While the SD valve selects and isolates one of the 16 streams, with the remainder dead-ended, the SF valve works in a similar way but with a minor difference. The distinction between the SD and SF valves is that, for the SF valve, the non-selected streams allow flow through individual outlets. This is shown in the schematic in Figure 4.13.

The control of the electrically actuated valves was done using a computer. The connection to the computer was established using an RS-232 interface. The RS-232 input commands were transmitted to the device via a custom built graphical user interface software. We also had VALCO Instruments company Inc. custom make 2.3 mm diameter hose-barb SD and SF adapters for use with 3/32" (ID) X 5/32" (OD) aqua translucent, polyurethane tubing procured from Cole Parmer, UK.

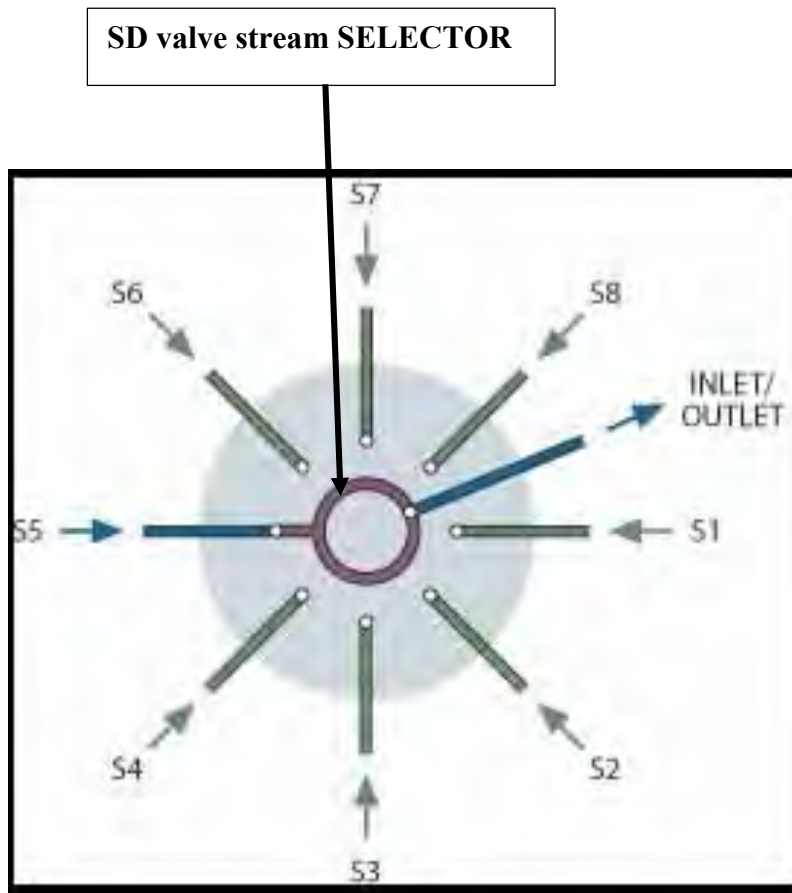


Figure 4.12: 8 position dead-ended flow path – SD configuration valve schematic. S1 – S8 denote the stream/port number. A stream/port refers to a flow path. If the stream (green flow paths) are not connected to a selector (red ring), those streams are dead-ended. When a stream is dead-ended, it implies that fluid cannot flow in/out of that stream because there is no bridging connection. In this schematic, the non-selected streams (except S5) are all dead-ended while stream S5 is open because it is connected to the selector thus allowing flow of fluid to either another sampling valve, pressure sensor, liquid detector or microfluidic device via the selector’s inlet/outlet port. The image was obtained from Reference [104].

SF valve stream SELECTOR

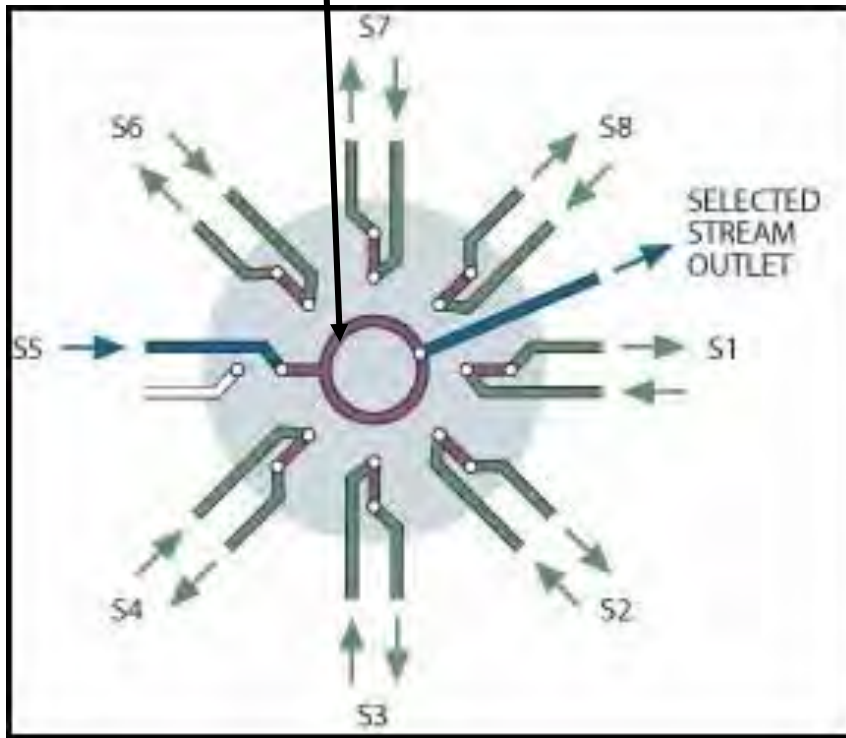


Figure 4.13: 8 position flow-through flow path – SF configuration valve schematic. S1 – S8 denote the stream/port number. A stream/port refers to a flow path. If the streams (green flow paths) are not connected to a selector (red ring), those streams allow flow of fluid to their individual outlets. In this schematic, the non-selected streams (except S5) are all allowing flow through of fluid to their individual outlets. The selected stream, stream S5 in this case is connected to the selector (thereby breaking the connection to its individual outlet), is allowing flow of fluid from the stream intake port to either another sampling valve, pressure sensor, liquid detector or microfluidic device via the selector's stream outlet port. The image was obtained from Reference [104].

4.5 Graphical User Interface Software

To maximize the automation platform consistency and modularity, each of the two automated platforms is controlled by a common, distributed application suite that was developed in LabVIEW. LabVIEW, which stands for **L**aboratory **V**irtual **I**nstrumentation **E**ngineering **W**orkbench is a graphical programming language first released in 1986 by National Instruments Corporation (USA). LabVIEW implements a dataflow paradigm in which the code is not written like in most traditionally programming languages, but rather drawn or represented graphically similar to a flow chart diagram [105]. Program execution follows connector wires linking processing nodes together [105]. Each function or routine is stored as a virtual instrument (VI) having three main components: the front panel which is essentially a form containing inputs and controls and can be displayed at run time, a block diagram where the code is edited and represented graphically and a connector pane which serves as an interface to the VI when imbedded as a sub-VI [105]. LabVIEW compiles the code as it is created thereby providing immediate syntactic and semantic feedback and reduces the time required for development and testing. For this reason, it is an appropriate programming platform for integrated automation systems for benchtop applications and even larger automation integrated system for rapid prototype development. One of many advantages LabVIEW has over other programming languages is that memory allocation/deallocation is automatically managed by LabVIEW [105].

The main graphical user program that is used in this work for microfluidic device microvalve automated control was developed using LabVIEW. The main VI program has been named ‘MagicElf’ and the front panel is shown in Figure 4.14. The automation of the loading valves for the microfluidic device described in this work was done by a sub-VI we created and incorporated into the main VI program and this is shown in Figure 4.15.

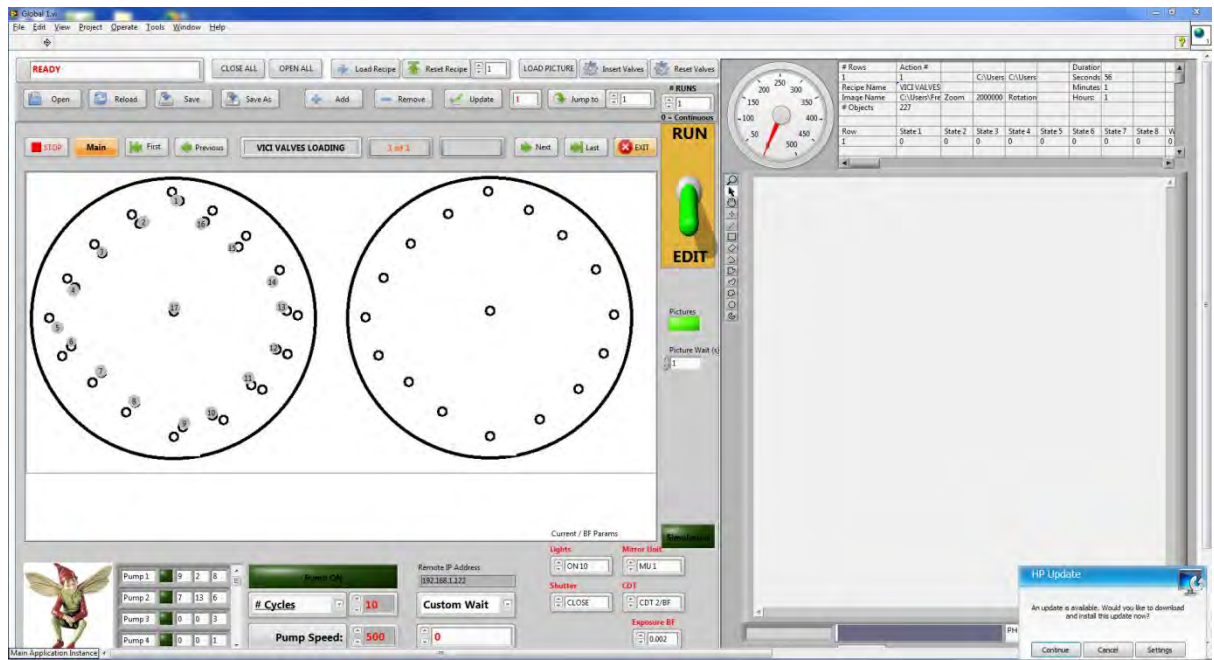


Figure 4.14: A screenshot image showing the front panel of the main LabVIEW VI (MagicElf) used for the SD and SF valve control.

AUTO-LOADING SYSTEM SD AND SF VALVE CONTROL DASHBOARD

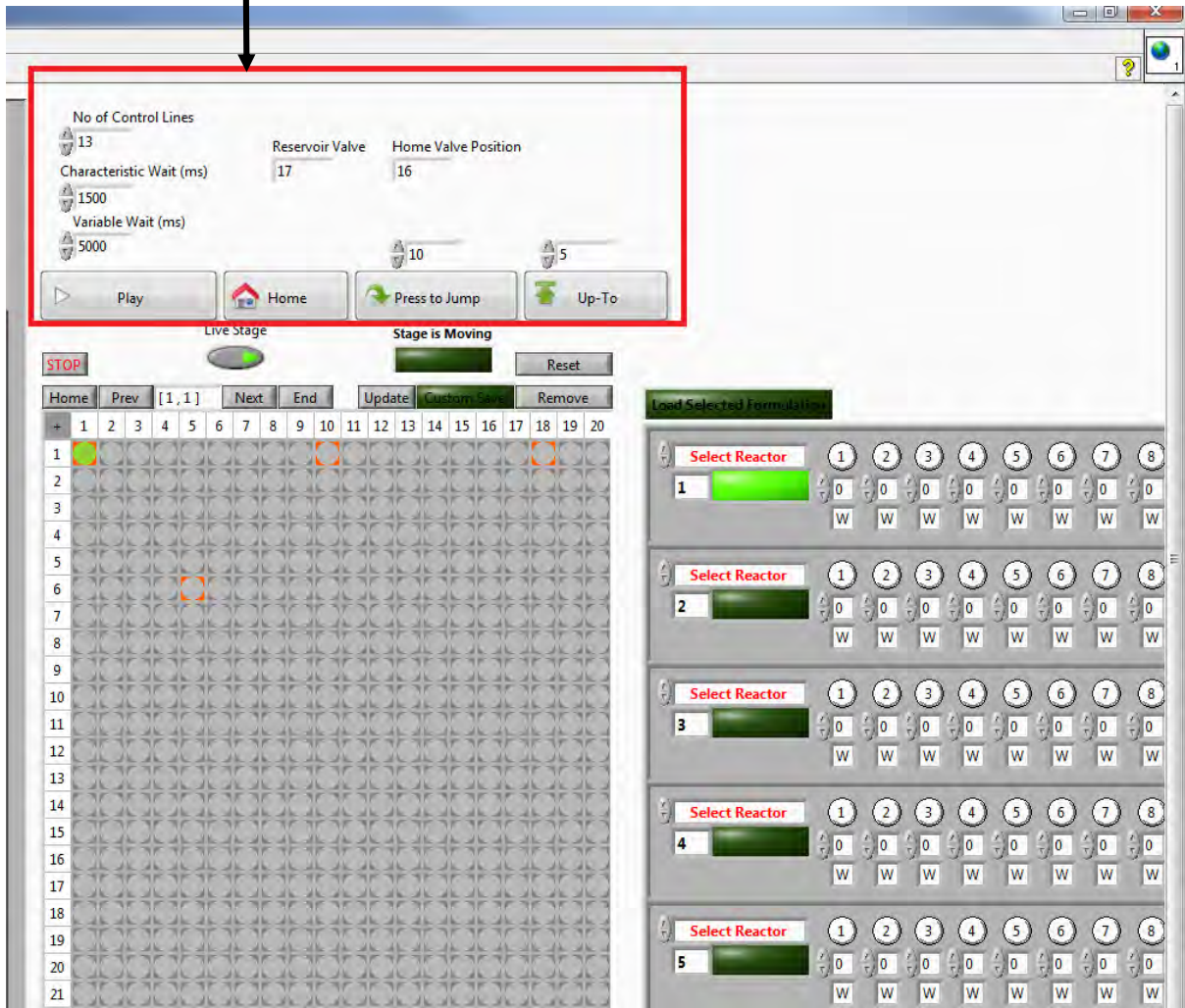


Figure 4.15: A screenshot image showing the sub-VI control board that controls the automated fluid transport system from off-chip to on-chip. This automation is performed by the aid of the SD and SF valves.

CHAPTER 5: RESULTS AND DISCUSSION

5.1 Microfluidic Plugs

One of the objectives of this project was to develop microfluidic plugs to relieve technicians from inserting pins into the microfluidic chip individually during the chip preparation step. These microfluidic plugs are supposed to be used in conjunction with an auto-loading system as off-chip to on-chip control channel interfaces. Two microfluidic plugs were developed and the following are the performance results of each of the fabricated plugs. Depending on the performance results and usability of the microfluidic plugs as off-chip to on-chip control channel interfaces, the same concept idea and design can be extended for use as off-chip to on-chip flow/reagent channel interfaces.

Polymethyldisiloxane (PDMS) Microfluidic Plug:

These microfluidic plugs were made from polymethyldisiloxane (PDMS). The fabricated device did not work as expected, the summary of the problems identified while using the device is given below:

The PDMS plug was not rigid enough (i.e. it was too soft/flexible) to be used as a plug. Because of the non-rigidity of the plug, it did not tightly hold the steel pins in place and it also made handling of the plug very difficult during the insertion of the plug into the microfluidic chip. Even when insertion of the plug into the chip was successful, during the process of removing the plug from the chip, the plug itself was destroyed as pins would either remain inserted into the chip or tear the PDMS block along the handled surfaces. This limited the plug to once-off use. We attempted to increase the rigidity of the plug by increasing the elastomeric stiffness (using different PDMS mixing ratios for the elastomer base to cross-linker base) and plastering it with epoxy adhesive and both attempts neither improved the rigidity nor the quality of the plug. We thus concluded that PDMS was an inappropriate material for fabricating microfluidic plugs.

Epoxy Adhesive Microfluidic Plug:

This microfluidic plug was made from epoxy adhesive. The fabricated device worked as expected, and became the first prototype plug for the auto-loading system. The device offered better rigidity (for holding the steel pins tightly in place) and handling than the PDMS plug. It also proved to be strong and durable for multiple uses over a period of time. Even though the epoxy plug worked as expected, as the first prototype, it exhibited some design flaws during operation which needed solutions in the foreseeable future. A summary of the problems identified while using the device is given below:

Often there was difficulty in inserting the plug into the microfluidic chip because of the slight misalignment of the plug's pins and the microfluidic chip's access ports. We identified the punching procedure during the microfluidic chip fabrication process as the main reason for the misaligned plug to chip connection. During the microfluidic chip fabrication process, each access port is punched one at a time using a punch. Precision is lost this way as it is nearly impossible to punch each of the access ports on different microfluidic chips, identically on the same exact spot. Also, since the epoxy plug is made using a microfluidic chip, it turns out that, the epoxy plug's pin separation is unique to the chip used during the fabrication process. An attempt to use the plug on a different microfluidic chip, resulted in a slight misalignment between the plug's pins and the access ports on the chip and delamination (i.e. separation of the bonded PDMS layers and the glass substrate) occurred during removal of the plug from the chip.

5.2 Auto-loading System Version 1.0

Auto-loading system version 1.0 (v1.0) was the first system developed to automate the loading process of the control channels on a microfluidic device. For this version of the system, the microfluidic device used was the ‘dual port’ microfluidic chip. This system is shown in Figure 5.1.

5.2.1 System Characterization.

The experimental set-up of the system was done according to the schematic illustration presented in Figure 5.1. The system is comprised of a 16 multi-position SF valve, 16 multi-position SD valve, fluid reservoir container, fluid waste container, pressure and valve control module, two microfluidic plugs, dual port microfluidic chip and a computer. The pressure and valve control module that shown in Figure 5.2 and is connected to the computer via an ethernet communication cable. This module comprises of a series of 8-port pneumatic pressure manifolds connected to pneumatic pressure regulators and a pneumatic pressure source (air compressor). The SF and SD valves are connected to the computer via RS-232 communication cables. The size of the tubing used for pressure and valve control module to the fluid reservoir container, fluid reservoir container to SF valve, SD valve to fluid waste container was 3/32” (ID) X 5/32” (OD). The connection between the SF valve to microfluidic plug and microfluidic plug to SD valve was done using 0.02” (OD) X 0.06” (ID) tygon tubing. The SF valve is used as a fluid injector device and the SD valve is used as a fluid receiver device. The microfluidic plugs connected to both the SF and SD valves have been inserted into the dual port microfluidic chip. Each control line on the microfluidic chip has its own individual stream/port on both the SF and SD valves.

The selectors on both the SF and SD valves have two inter-connected ports. For the SF valve, each stream has its inlet connected to the control channel on the microfluidic chip via the microfluidic plug and its individual outlet is used as an pressure inlet (the SF valve allows bidirectional flow between the inlet and its individual outlet) implying that it is connected to a port on the pressure manifold found on the pressure and valve control module. The SF valve’s selector will have one of its ports as a common fluid inlet (for fluid flow from the fluid reservoir container) and the other as an outlet in the case where stream/port selection has occurred. For the SD valve, each stream is connected to the corresponding control channel that is also connected to the SF valve via a microfluidic plug. The SD valve’s selector will have one of its ports as a fluid inlet in the case where stream/port has occurred and the other will be a common outlet (for flow to the fluid waste container). At rest position shown in the **red** state, there is no stream selection on both the SF and SD valves, for the SF valve, each stream is inter-connected to its own pneumatic pressure inlet and for the SD valve, the corresponding stream is dead-ended.

During the automation process, the developed user-friendly operating system (MagicElf) on the computer sends commands to the pressure and valve control module, SF and SD valves. MagicElf actuates the SF and SD valves for stream position change and actuates the individual solenoid valves residing in the pressure manifolds to open and close microvalves. In synchronization, the SF and SD valves actuate to a selected valve position and stream selection on matching streams on both the SF and SD valves occurs. Milliseconds later, pneumatic pressure from the pressure and valve control module is applied to the fluid reservoir container enabling flow of fluid from the container into the SF valve via the selector (shown in the **green** configuration in Figure 5.1) into the selected stream port and then flows into the chip's control line via the microfluidic plug. The introduced fluid in the control line will then flow through the chip and come out at the opposite end of the chip into the SD valve (shown in the **green** configuration in Figure 5.1) via another microfluidic plug. The fluid continues to flow through the SD valve until it reaches the fluid waste container. The instant fluid is collected in the fluid waste container, in synchronization, the SF and SD valve actuate to the next valve position. During the actuation of the SF and SD valves, the following happens at the SF and SD valves:

- i. The connection between the selector and a selected stream's inlet port is broken and the inter-connection between that inlet and its individual pneumatic pressure inlet is re-established and the corresponding port on the manifold is switched on allowing pneumatic pressure to be applied through that inlet into the microfluidic chip's control line.
- ii. While at the SD valve, the corresponding stream is dead-ended thus functionalizing the microfluidic chip's control line (i.e. ability to open and close valves in that control line).

When the SF and SD valves actuate to the next position, the process described above is repeated until all the control lines in the microfluidic chip have been functionalized. The operating pneumatic pressure was 20 pounds per square inch (psi). As a building step and for testing the prototype, the system actuates to the next valve position as instructed by an 'elapsed time' LabVIEW function that has been incorporated into the 'MagicElf' operating system. The actual elapsed time for valve actuation was manually measured using a stopwatch in one of the trial runs. It is the least measured and optimized time required for a control line to be functionalized specific to this current set-up. It can vary depending on tygon tubing length, operating pressure values, chip architecture and material properties of the liquid used (e.g. its viscosity).

5.2.2 Results and Discussion.

Auto-loading system version 1.0 was able to automate the loading process however this system proved to be inefficient when compared to the manual set-up process. This auto-loading system was operating at a rate of more than 30 minutes per control line. This translated to about 390 minutes (6 hours 30 minutes) for the 13 control line dual port microfluidic chip. The manual process for the same microfluidic chip has a rate of about 5 minutes per control line and depending on the mental and physical state of the technician the rate can decrease to about 10 minutes per control line for if the technician is mental fatigued. The manual process can take 65 minutes (1 hour 5 minutes) to 130 minutes (2 hours 10 minutes) for a 13 control line microfluidic dual port chip.

The key reason responsible for the inefficiency of the automated loading system was on-chip air introduction. We observed and determined that the auto-loading system was introducing air into the system (specifically to the microfluidic chip) ahead of the fluid. This air was being compressed in the tubing ahead of the fluid and then forced into the microfluidic chip and pushed all the way to the SD valve and into the fluid waste container. This process of compressing the air off-chip and forcibly funnelling it on-chip ahead of the fluid played a key part in increasing the loading time for the system.

At this point, a different approach to the auto-loading system was required or a quick and safe method of removing this introduced air in the system was required so as to have an efficient auto-loading system. One approach was to introduce robotic pipetting in the system in order to eliminate the chances of introducing air into the chip; however, this is a very expensive solution to the problem, one that is impractical if the auto-loading system is to be used along other microfluidic devices as point-of-care (POC) medical diagnostic devices.

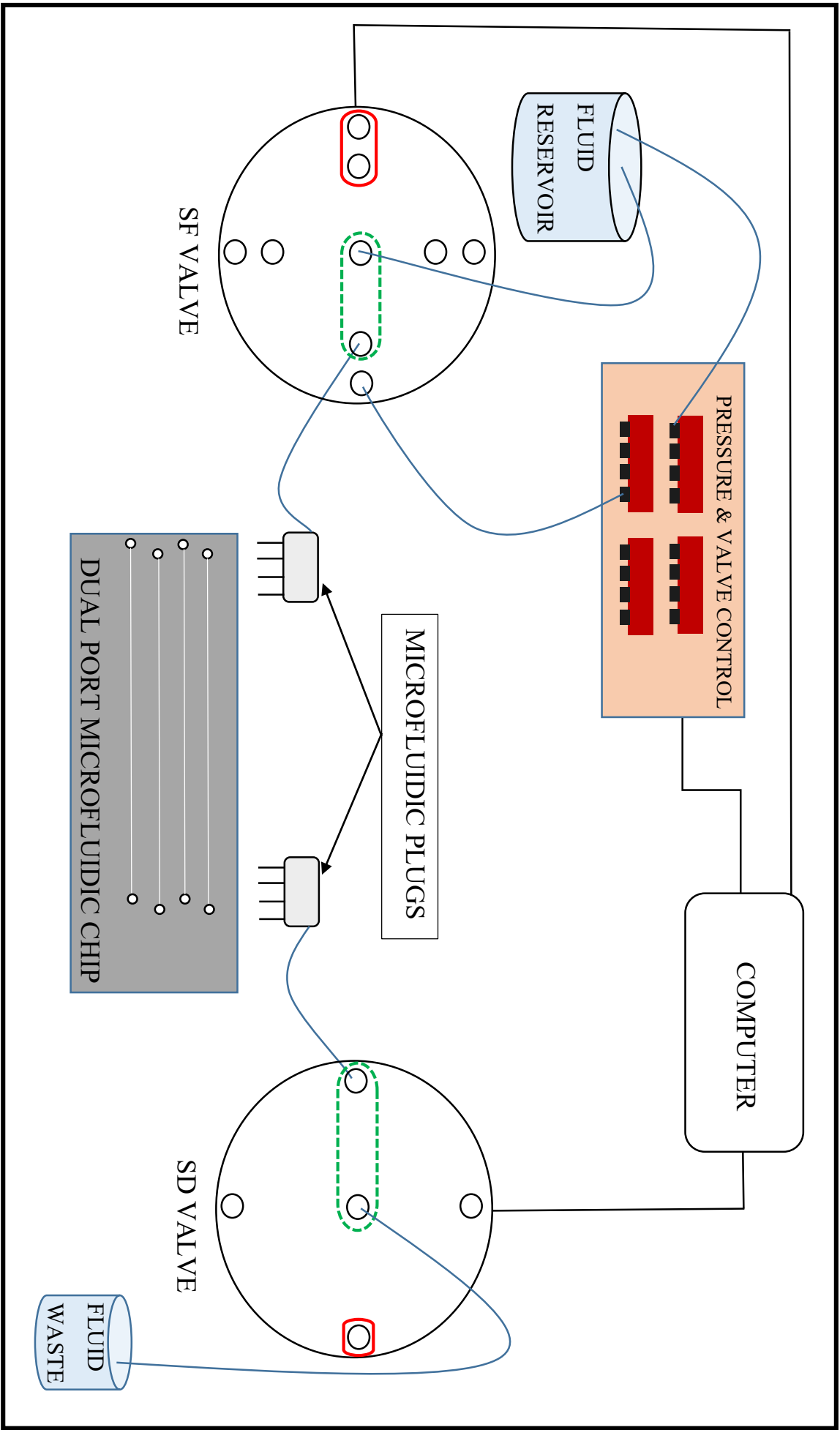


Figure 5.1: Simple schematic illustration of the Auto-loading System v1.0 using 4 multi-position SF and SD valves.

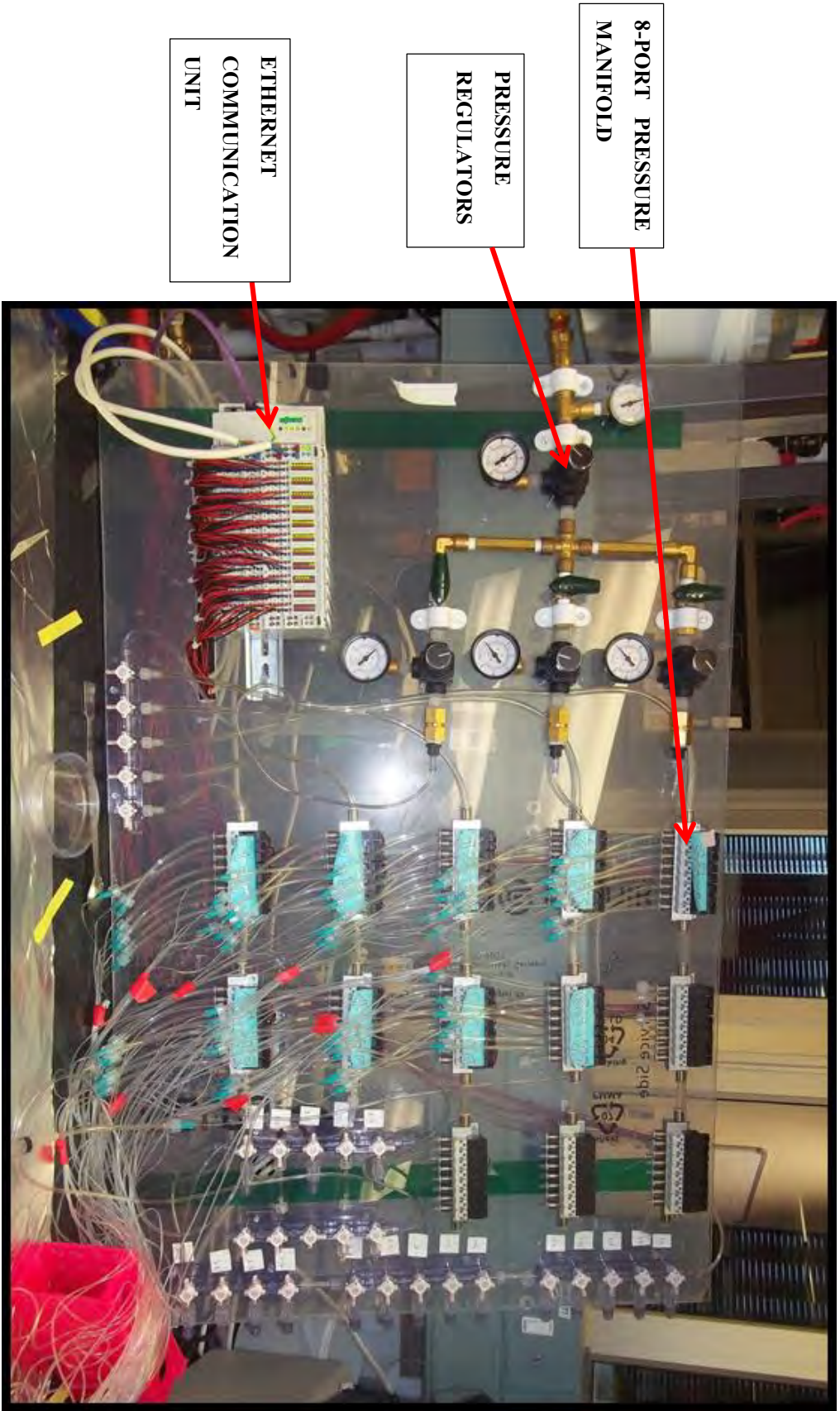


Figure 5.2: Pressure and valve control module.

5.3 Auto-loading System Version 2.0

Auto-loading system version 2.0 (v2.0) was the second system developed as the most economical solution to the problem of inefficiency identified in the auto-loading system v1.0. This new system was designed to remove a large approximate volume of air off-chip by introducing small branches in the flow path. These small branches were in the form of custom made ‘tee’ steel pins (0.025” OD X 0.013” ID X 1” long, Vita Needle Company, USA). For this version of the auto-loading system, tee-pins were used in place of microfluidic plugs because the nature of the pins made it difficult to make useable plugs. This system also made use of the ‘single port’ microfluidic chip. This system is shown in Figure 5.3.

5.3.1 System Characterization.

The experimental set-up of the system was done according to the schematic illustration presented in Figure 5.3. The system is almost identical to auto-loading system v1.0 but with the following differences:

- i. Tee-pins were used in place of microfluidic plugs.
- ii. Single port microfluidic chip used in place of the dual port microfluidic chip.
- iii. The automation process is slightly different and this is explained in more detail below.

During the automation process, the developed user-friendly operating system (MagicElf) on the computer sends commands to the pressure and valve control module, SF and SD valves. MagicElf actuates the SF and SD valves for stream position change and actuates the individual solenoid valves residing in the pressure manifolds to open and close microvalves. In synchronization, the SF and SD valves actuate to a selected valve position and stream selection on matching streams on both the SF and SD valves occurs. Milliseconds later, pneumatic pressure from the pressure and valve control module is applied to the fluid reservoir container enabling flow of fluid from the container into the SF valve via the selector (shown in the **green** configuration in Figure 5.3) and into the selected stream port and then flows to the tee-pin. At the tee-pin junction, the fluid and the air ahead of it flows to the SD valve. The reason for this occurrence is that, at the tee-junction, the flow path to the SD valve offers less resistance than the flow path to the microfluidic chip were it is compressed and forced into the chip. The introduced fluid and air will flow into the SD valve (shown in the **green** configuration in Figure 5.3). The fluid and air ahead of it continues to flow through the SD valve until it reaches the fluid waste container. The instant fluid is collected in the fluid waste container, only the SD valve will actuate to the next valve position. Since the SD valve has actuated, the flow path that had the fluid is now dead-ended. The dead-end increases resistance in the flow path to the SD valve on the tee-

junction, hence fluid (without air ahead of it) is then forced to flow into the microfluidic chip through the other end of the tee-pin that has been inserted into the chip. After the complete filling of the control line with fluid, the SF valve will then actuate to the next valve position. When the SF valve actuates, the connection between the selector and a selected stream's inlet port is broken and the interconnection between that inlet and its individual pneumatic pressure inlet is re-established. The corresponding port on the manifold is then switched on allowing pneumatic pressure to be applied through that inlet into the microfluidic chip's control line, thereby functionalizing the control line (i.e. ability to open and close valves in that control line). The functionalization of the microfluidic chip's control line happened as follows; since, the SD valve was first to be actuated to the next valve position before the SF valve, the corresponding stream was dead-ended, to functionalize the microfluidic chip's control line, the SF valve only needed to actuate to the next position and allow pneumatic pressure to be applied in that control line.

When the SF and SD valves actuate to the next position, the process described above is repeated until all the control lines in the microfluidic chip have been functionalized. The operating pneumatic pressure was 20 pounds per square inch (psi). The system actuates to the next valve position as instructed by an 'elapsed time' LabVIEW function that has been incorporated into the 'MagicElf' operating system. The actual elapsed time for valve actuation was manually measured using a stopwatch in one of the trial runs. It is the least measured and optimized time required for a control line to be functionalized specific to this current set-up. It can vary depending on tygon tubing length, operating pressure values, chip architecture and material properties of the liquid used (e.g. its viscosity).

5.3.2 Results and Discussion.

Auto-loading system version 2.0 was able to automate the loading of fluid off-chip to on-chip with efficiency when compared to auto-loading system v1.0 and the manual set-up process. This auto-loading system was operating at a rate of 1 minute 30 seconds per control line. This translated to about 21 minutes for the 13 control line single port chip. Comparing this system to the manual set-up, which takes about 65 minutes (1 hour 5 minutes) for a 13 control line microfluidic single port chip, this automated system was saving 68% of the time required to prepare the microfluidic chip. The auto-loading system v2.0 was saving 95% of the time taken by its predecessor, the auto-loading system v1.0.

The key reason responsible for the increased efficiency of the automated loading system was the successful removal of a large approximate volume of air off-chip before it was introduced on-chip. This was achieved by branching off the flow paths using tee-pins. The use of tee-pins did improve the automated loading system's efficiency; however the use of tee-pins invalidated the use of microfluidic plugs, mainly because it was difficult to fabricate microfluidic plugs using tee-pins. Figure 5.4 shows a picture of the tee-pins that have been inserted in the single port microfluidic chip. To bring back the practicality of using microfluidic large scale integration systems for point-of-care medical diagnostics, microfluidic plugs are essential in reducing the set-up time. This led to a need for the development of a new auto-loading system that worked in the manner the tee-pins did but making use of microfluidic plugs.

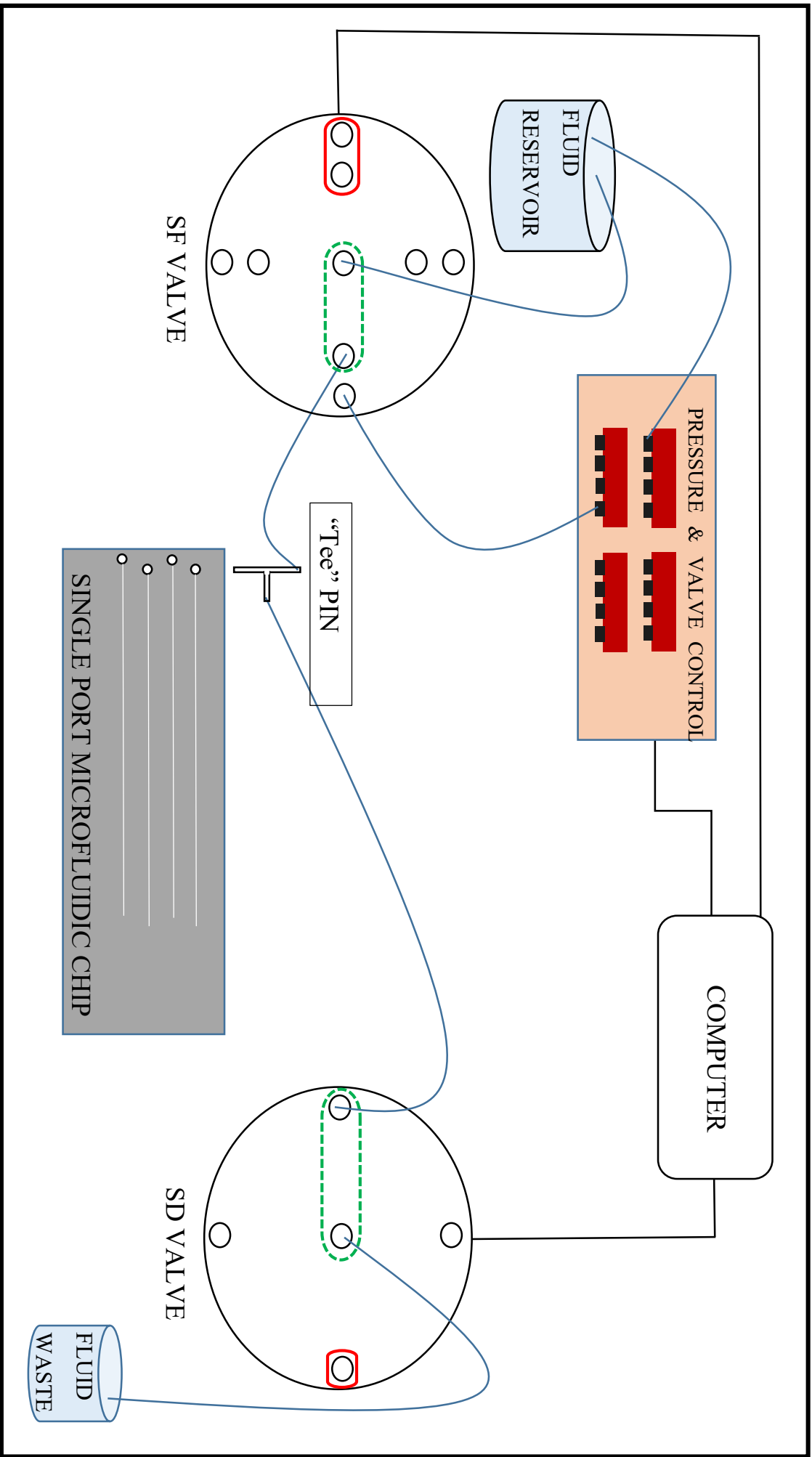


Figure 5.3: Simple schematic illustration of the Auto-loading System v2.0 using 4 multi-position SF and SD valves.

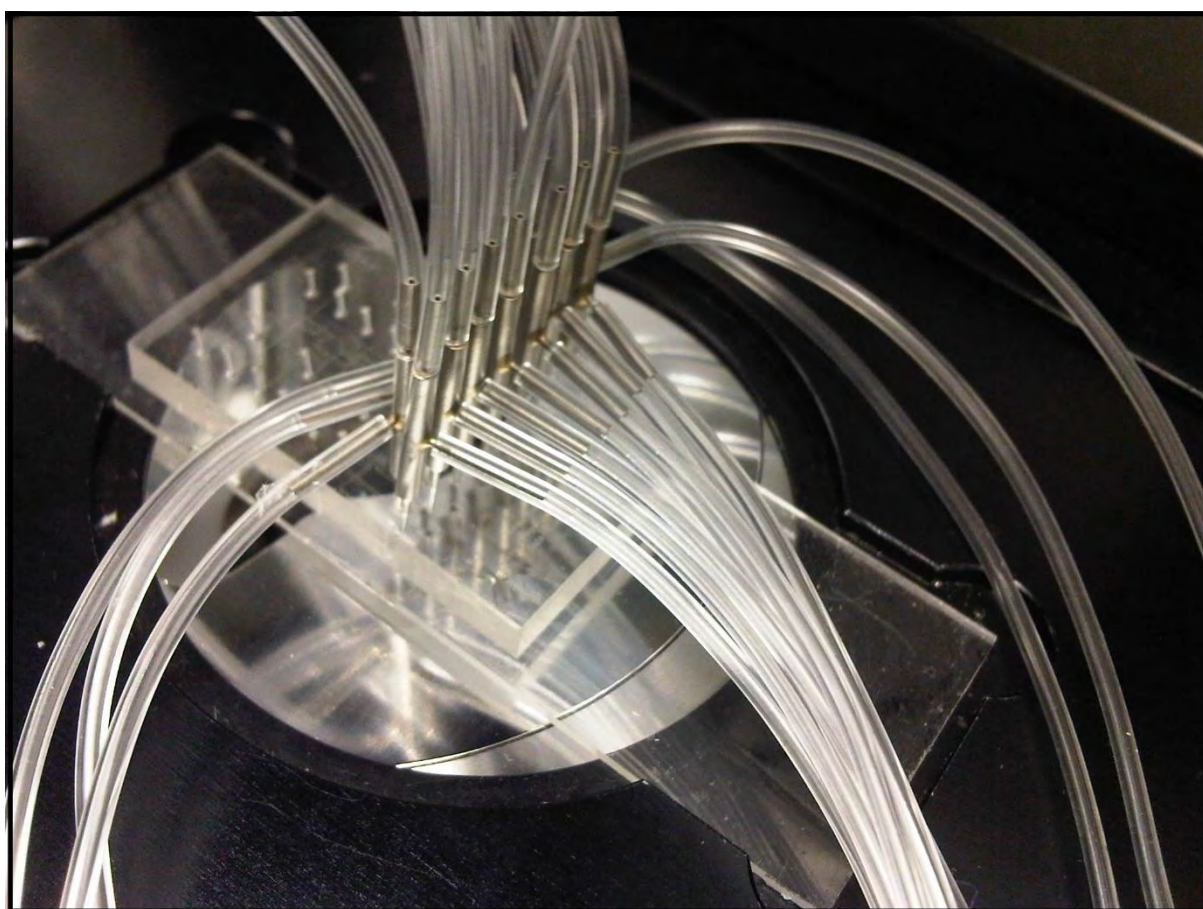


Figure 5.4: A picture showing the tee-pins inserted into the single port microfluidic chip.

5.4 Auto-loading System Version 3.0

Auto-loading system version 3.0 (v3.0) was the system developed to re-introduce the use of microfluidic plugs like those used in auto-loading system v1.0 and have the same air purging mechanism of auto-loading system v2.0 but without the use of tee-pins. For this version of the system, the microfluidic device used was the 'hybrid dual port' microfluidic chip. This system is shown in Figure 5.5.

5.4.1 System Characterization.

The experimental set-up of the system was done according to the schematic illustration presented in Figure 5.5. The system is almost identical to auto-loading system v2.0 but with the following differences:

- i. Microfluidic plugs were re-introduced in place of tee-pins.
- ii. Hybrid dual port microfluidic chip used in place of the single port microfluidic chip.

During the automation process, the developed user-friendly operating system (MagicElf) on the computer sends commands to the pressure and valve control module, SF and SD valves. MagicElf actuates the SF and SD valves for stream position change and actuates the individual solenoid valves residing in the pressure manifolds to open and close microvalves. In synchronization, the SF and SD valves actuate to a selected valve position and stream selection on matching streams on both the SF and SD valves occurs. Milliseconds later, pneumatic pressure from the pressure and valve control module is applied to the fluid reservoir container enabling flow of fluid from the container into the SF valve via the selector (shown in the **green** configuration in Figure 5.5) and into the selected stream port and then flows into the chip's control line via the microfluidic plug. The introduced fluid in the control line will then flow through the chip along the inter-port 'bridge' channel (shown in yellow on the microfluidic chip) that is between the two access ports. When it reaches the other access port, the same fluid movement observed in the case of branched flow paths using tee-pins occurs. The fluid will flow out of the chip via the other access port through the microfluidic plug and into the SD valve. The fluid and air ahead of it continues to flow through the SD valve (shown in the **green** configuration in Figure 5.5) until it reaches the fluid waste container. The instant fluid is collected in the fluid waste container, only the SD valve will actuate to the next valve position. Since the SD valve has actuated, the flow path that had the fluid is now dead-ended. The dead-end increases resistance in the flow path to the SD valve on the tee-junction, hence fluid (without air ahead of it) is then forced to flow into the microfluidic chip through the other end of the tee-pin that has been inserted into the chip. After the complete filling of the control line with fluid, the SF valve will then actuate to the next valve position.

When the SF valve actuates, the connection between the selector and a selected stream's inlet port is broken and the inter-connection between that inlet and its individual pneumatic pressure inlet is re-established and the corresponding port on the manifold is switched on allowing pneumatic pressure to be applied through that inlet into the microfluidic chip's control line, thereby functionalizing the control line (i.e. ability to open and close valves in that control line). The functionalization of the microfluidic chip's control line happened as follows; since, the SD valve was first to be actuated to the next valve position before the SF valve, the corresponding stream was dead-ended, to functionalize the microfluidic chip's control line, the SF valve only needed to actuate to next position and allow pneumatic pressure to be applied in that control line.

When the SF and SD valves actuate to the next position, the process described above is repeated until all the control lines in the microfluidic chip have been functionalized. The operating pneumatic pressure was 20 pounds per square inch (psi). The system actuates to the next valve position as instructed by an 'elapsed time' LabVIEW function that has been incorporated into the 'MagicElf' operating system. The actual elapsed time for valve actuation was manually measured using a stopwatch in one of the trial runs. It is the least measured and optimized time required for a control line to be functionalized specific to this current set-up. It can vary depending on tygon tubing length, operating pressure values, chip architecture and material properties of the liquid used (e.g. its viscosity).

5.4.2 Results and Discussion.

Auto-loading system version 3.0 was able to automate the loading of fluid off-chip to on-chip in the same manner as auto-loading system v2.0. This auto-loading system was operating at a rate of 2 minutes per control line. This translated to about 26 minutes for the 13 control line hybrid dual port chip. Comparing this system to the manual set-up, which takes about 65 minutes (1 hour 5 minutes) for a 13 control line microfluidic single port chip, this automated system was saving 60% of the time required to prepare the microfluidic chip. Although auto-loading system v2.0 was 30% more efficient than this system, auto-loading system v3.0 made use of microfluidic plugs, an essential component needed by the auto-loading system. The efficiency difference between auto-loading system v2.0 and auto-loading system v3.0 can be explained as follows:

- Assuming there is no flow of fluid, the ‘tee’ steel pins of dimensions (0.025” OD X 0.013” ID X 1” long) used in auto-loading system v2.0 can approximately hold a volume of 2.18 mm^3 whereas the rectangular interconnecting bridge channel in the ‘hybrid dual port’ microfluidic chip used in auto-loading system v3.0 has dimensions (10 μm high, 100 μm wide and 1000 μm long) thus it can approximately hold a volume of 0.001 mm^3 . We believe that this volume capacity difference in the sections of the auto-loading systems that aid the removal of trapped air, accounts for the difference in the efficiencies of these systems. We believe that even when flow of fluid is allowed, ‘tee’ pins of auto-loading system v2.0 allow more fluid to pass through than the interconnecting bridge channels of the ‘hybrid’ microfluidic chip hence making it more efficient than later.
- We believe that as fluid flows through the rectangular interconnecting bridge channel in the ‘hybrid dual port’ microfluidic chip used in auto-loading system v3.0, it encounters flow resistance in the form of friction between the fluid and channel surface. The same can be said for fluid flow in the ‘tee’ pins used in auto-loading system v2.0, however, we believe that the flow resistance and friction between the steel surface and the fluid is much smaller than that in auto-loading system v3.0 thus making auto-loading system v2.0 more efficient.

Even though auto-loading system v3.0 was 30% less efficient, we concluded that this system, auto-loading system v3.0 had met the objectives of the project because it made use of microfluidic plugs and automated the microfluidic chip loading process more efficiently than the manual set-up process.

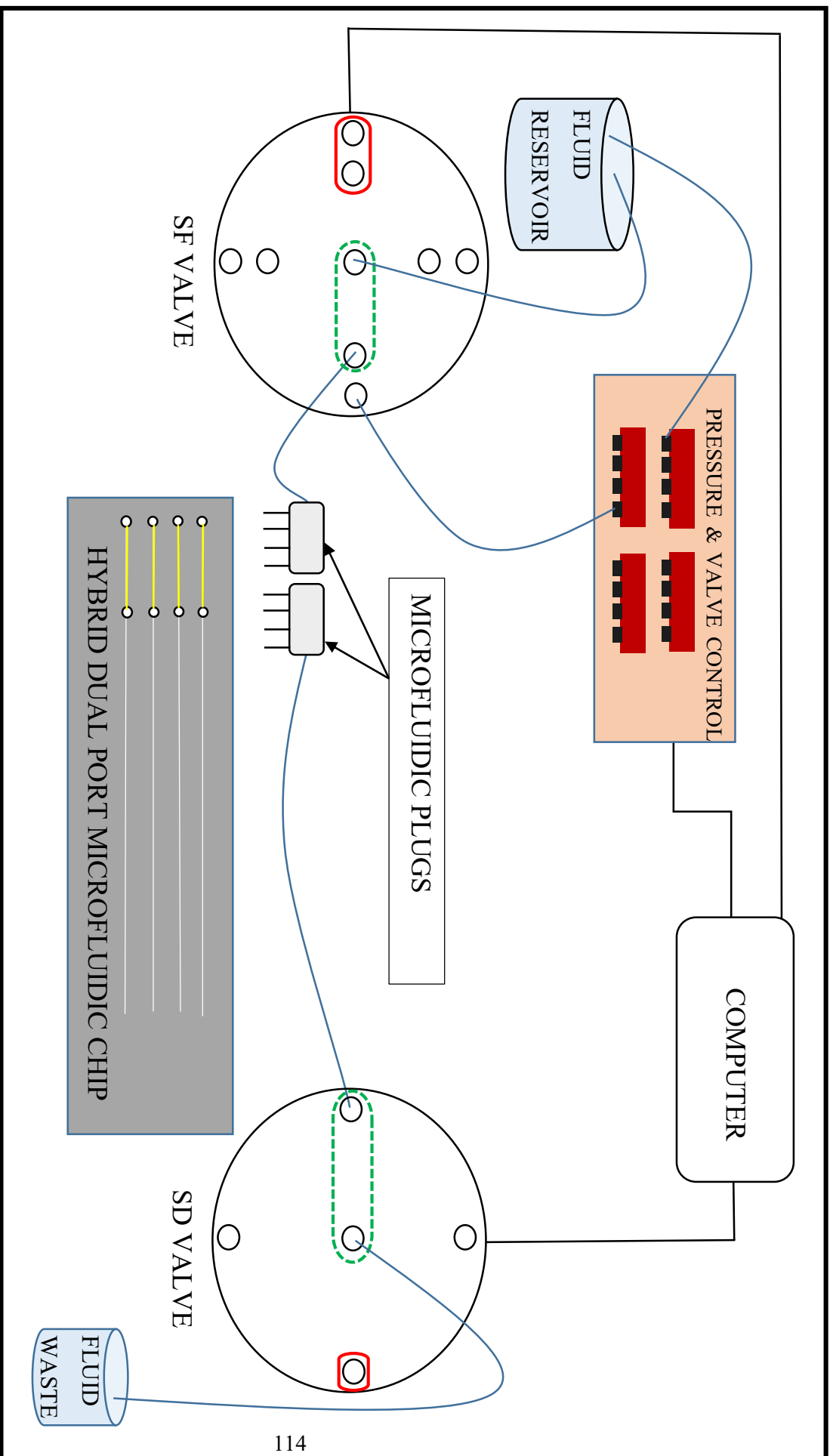


Figure 5.5: Simple schematic illustration of the Auto-loading System v3.0 using 4 multi-position SF and SD valves.

5.5 Microfluidic Chips

Important architectural features in the chip designs that were maintained in the microfluidic chips used in the auto-loading systems v1.0, v2.0 and v3.0 are the rotary pneumatic and linear peristaltic micropumps. The design images of these micropumps i.e. the rotary pneumatic and linear peristaltic micropumps were presented in Figure 4.3 (a) and Figure 4.3 (b) respectively. The figures below show these micropumps on working fabricated PDMS microfluidic chips. Figure 5.6 and Figure 5.7 show the rotary pneumatic and linear peristaltic micropumps respectively. Figure 5.8 and Figure 5.9 show examples of the open and closed state of microvalves in a working microfluidic chip respectively.

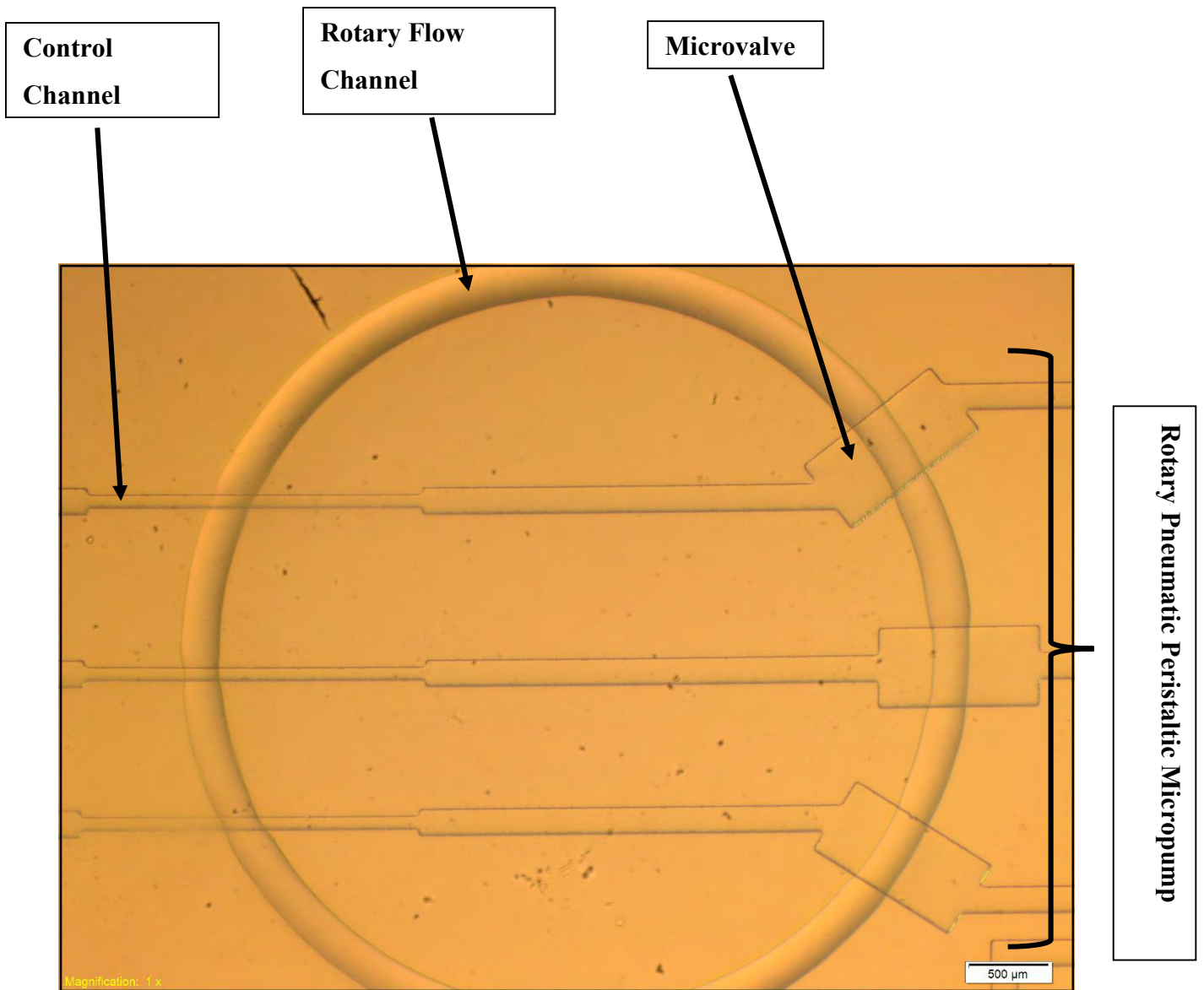


Figure 5.6: One of the rotary pneumatic peristaltic micropumps found in all the three designed microfluidic chips in this project, i.e. dual port, single port and hybrid dual port microfluidic chips. The image above shows a partial view of the rotary flow channel and the chip architectural geometry shown in Figure 4.4.

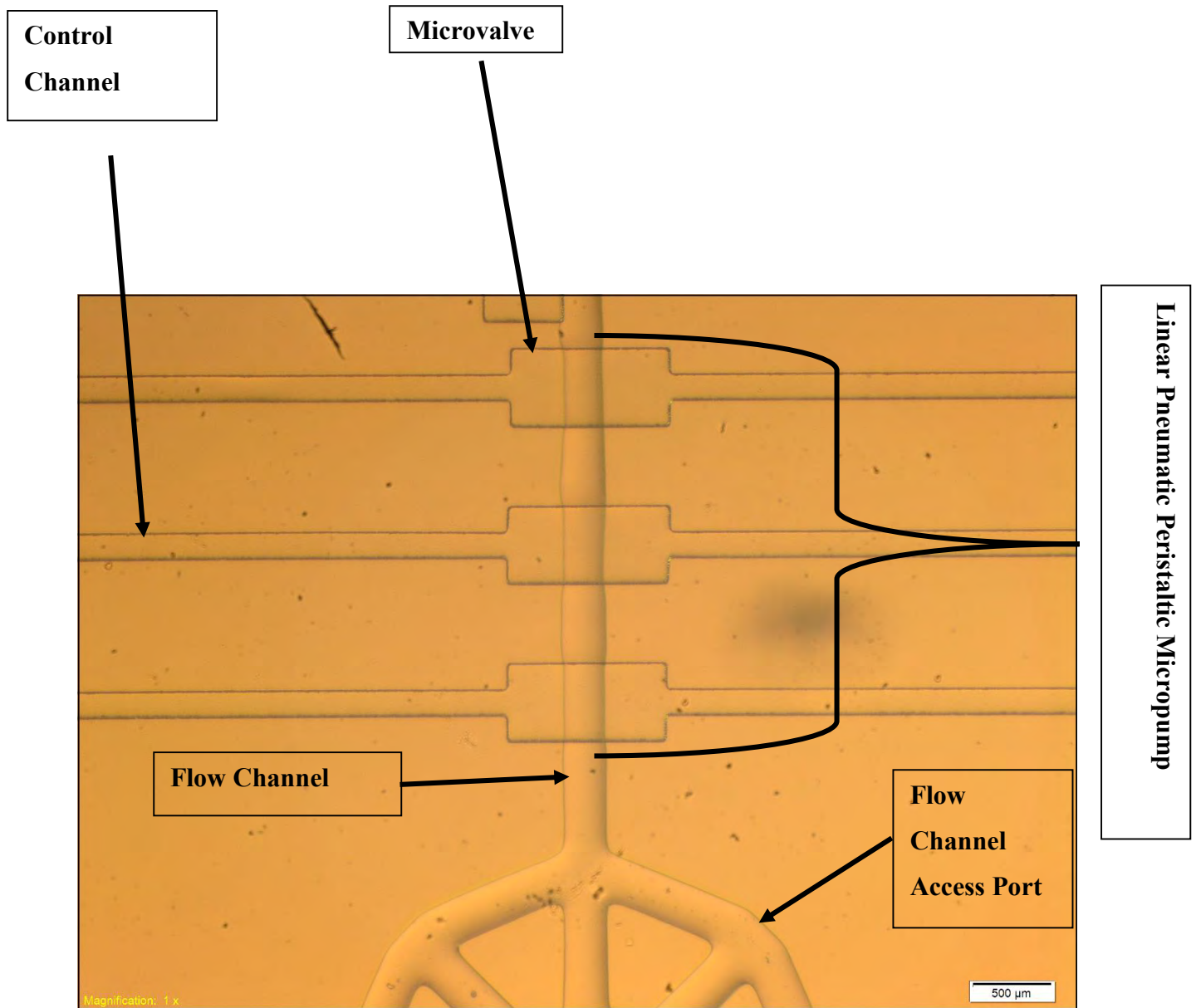


Figure 5.7: One of the linear pneumatic peristaltic micropumps found in all the three designed microfluidic chips in this project, i.e. dual port, single port and hybrid dual port microfluidic chips. The image above shows a partial view of the flow channel access port and the chip achitectural geometry shown in Figure 4.4.

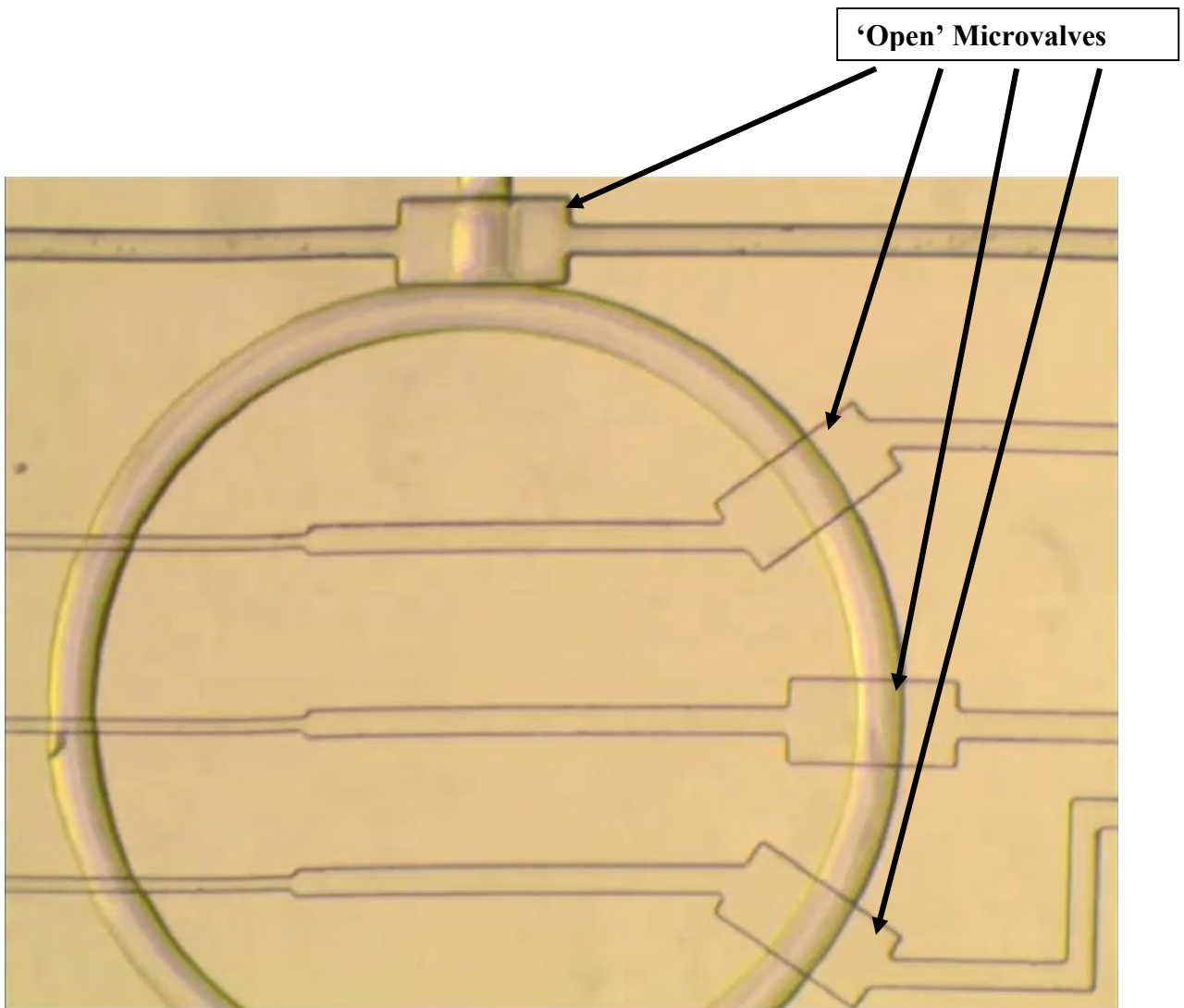


Figure 5.8: 'Open' microvalves in a working microfluidic chip. This image shows a partial view of the a rotary flow channel and its respective rotary pneumatic peristaltic micropump. In the image above, no pneumatic pressure is being applied in the control channels thus, all the microvalves are in the 'open' state i.e. they are allowing fluid flow in the flow channel.

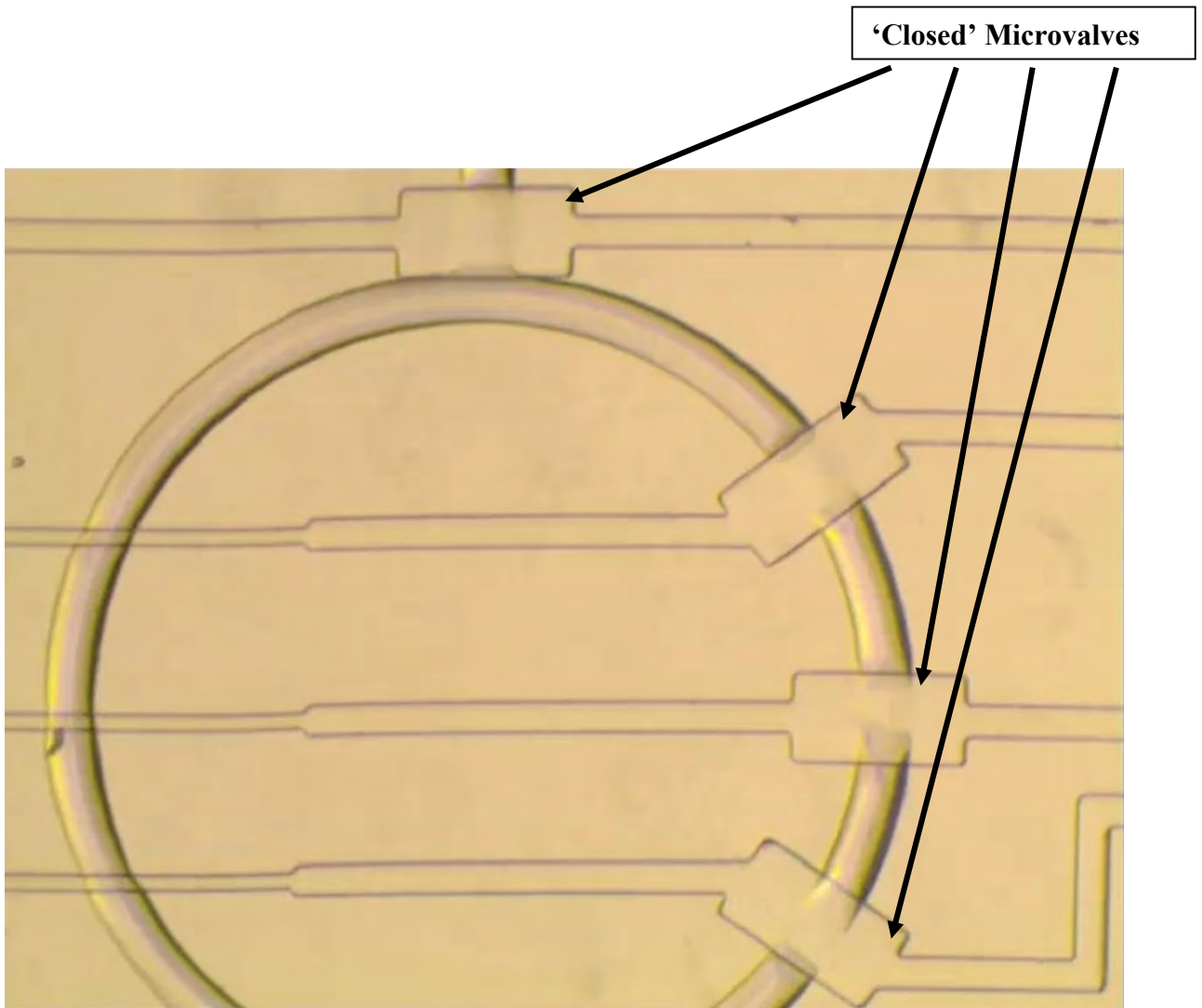


Figure 5.9: 'Closed' microvalves in a working microfluidic chip. This image shows a partial view of the a rotary flow channel and its respective rotary pneumatic peristaltic micropump. In the image above, pneumatic pressure is being applied in the control channels thus, all the microvalves are in the 'closed' state i.e. they are not allowing fluid flow in the flow channel. As seen in the image above, all the microvalves have pinched off the flow channels, this is illustrated by the gaps in-between the flow channels in the region the microvalves are located. The loading of the control lines with fluid and the 'opening' and 'closing' of the valves was automated i.e. there was no human involvement.

CHAPTER 6: CONCLUSION

We have developed a simple, reliable and automated microfluidic fluid introduction system for off-chip to on-chip fluid transport. The system makes use of relatively inexpensive hardware such as electrically actuated valves and microfluidic plugs. Based on the three versions of the automated systems developed, two showed to be more efficient than the manual set-up. The efficient versions were saving 60% - 68% of the time required to prepare the microfluidic system manually.

The introduction of a graphical user operating system (MagicElf) and the use of microfluidic plugs has enhanced the increase in user-friendliness of microfluidic system operation. These systems limited human involvement to only microfluidic plug insertion into a chip and system operation via the MagicElf dashboard. During the development of this project, I was able to successfully learn the principles of microfluidics technology. I learnt how to fabricate microfluidic devices using photolithography and soft-lithography from concept drawings. I also developed programming skills in the LabVIEW programming environment.

To a greater extent, the complete automation of the fluid transport, which was one of the aims of this project, has shown great potential as a one-of-a-kind solution to achieving the practicality of using microfluidic large scale integration platforms for point-of-care medical diagnostics. Going forward, the use of this system as proof of principle, improvements and optimizations is necessary to further develop this to the maturity required by international health standards. To compliment this proof of principle, we now aim to miniaturize the pressure and valve control module, such that the auto-loading system can become an enclosed, compact and portable unit.

CHAPTER 7: FUTURE WORK

Over the last decade, microdevices have generated vast interest in both academic and industrial laboratories [106]. Several challenges are yet to be overcome before these technologies can be translated into effective point-of-care medical diagnostic devices. A translation to point-of-care medical diagnostic devices requires the improvisation and optimization of all peripheral instrumentation associated with the system's development and operation. In order to achieve this goal, it is critical to innovate.

A study of African medical schools showed the extent at which innovation is emerging amongst academics [107]. The work described in this project is an example of innovation at play. This project has shown that it is possible to automate fluid transport off-chip to on-chip for microfluidic large scale integration systems. Moving forward, this project will involve optimizing the system and developing an enclosed, compact and portable versions of the system as a step towards decentralized health care and personalized medicine.

From the previous work performed in this project, we have drawn up possible solutions to some of the problems identified in our first prototype. One such proposal is re-design of the punch that is used during the microfluidic chip fabrication process. We aim to re-design the punch such that precision is conserved between the punching process of microfluidic chip access ports and microfluidic plug development. Once precision is maintained, the separation on the microfluidic plug's pins and the punched access ports on the microfluidic chip will be identical, thus removing the problem of microfluidic plug to chip misalignment. The new punch will be able to create 16 access ports at a time with the much needed accuracy. This punch will be highly suitable for use on the hybrid dual port microfluidic chip. The new proposed punch is a manual punch making it a cheaper solution to the existing problem than introducing an automated robotic punching system. The new punch will have an appearance as that shown in Figure 7.1.

Apart from optimizing the automation protocol of the auto-loading system, we have proposed a new microfluidic chip design that we expect will increase the efficiency of the system by removing the introduced air more rapidly. This proposed device is exactly the same as the hybrid dual port microfluidic chip; instead of the 10 μm high and 100 μm wide 'bridge', the inter-connected access ports have a 500 μm high and 500 μm wide 'bridge' channel, this is shown in *yellow* in Figure 7.2. The rest of the control lines are 10 μm high and 50 μm wide just like the old design.

We expect that the increased dimensions of the bridge channel will facilitate faster removal of air in the system thus making it more efficient. In the future as well, we hope to replace the ‘elapsed time’ LabVIEW function incorporated into the operating system with flow sensors. Flow sensors will detect fluid flow at the fluid waste container and will send signals to the SD and SF valves to actuate accordingly.

In brief, the plans for this project and the necessary steps to have it deployable in clinical settings are as follows:

1. Finish the prototype development as proof of principle. This process will involve the miniaturization of the pressure and valve control module that shown in Figure 5.2 and extending this auto-loading system to also cater for the flow channel sample loading. At the end of this stage, we hope to have a compact and portable automation kit similar to a desktop computer casing that houses the computer motherboard and electronics.
2. File for intellectual property and a patent protection (this is already underway).
3. Seek investment for the reduction to practise phase. This will involve making the system foolproof such that it has a repeatable performance and is foolproof. This stage will also increase the user-friendliness of the system.
4. Develop a prototype medical assay for POC testing (e.g. ELISA).
5. Optimize the medical assay to medically accepted standards in small scale clinical studies.
6. Seek approvals (e.g. ethics committees, national health councils etc.) for the system to be deployed into clinical practise.
7. Avail the system for clinical use.

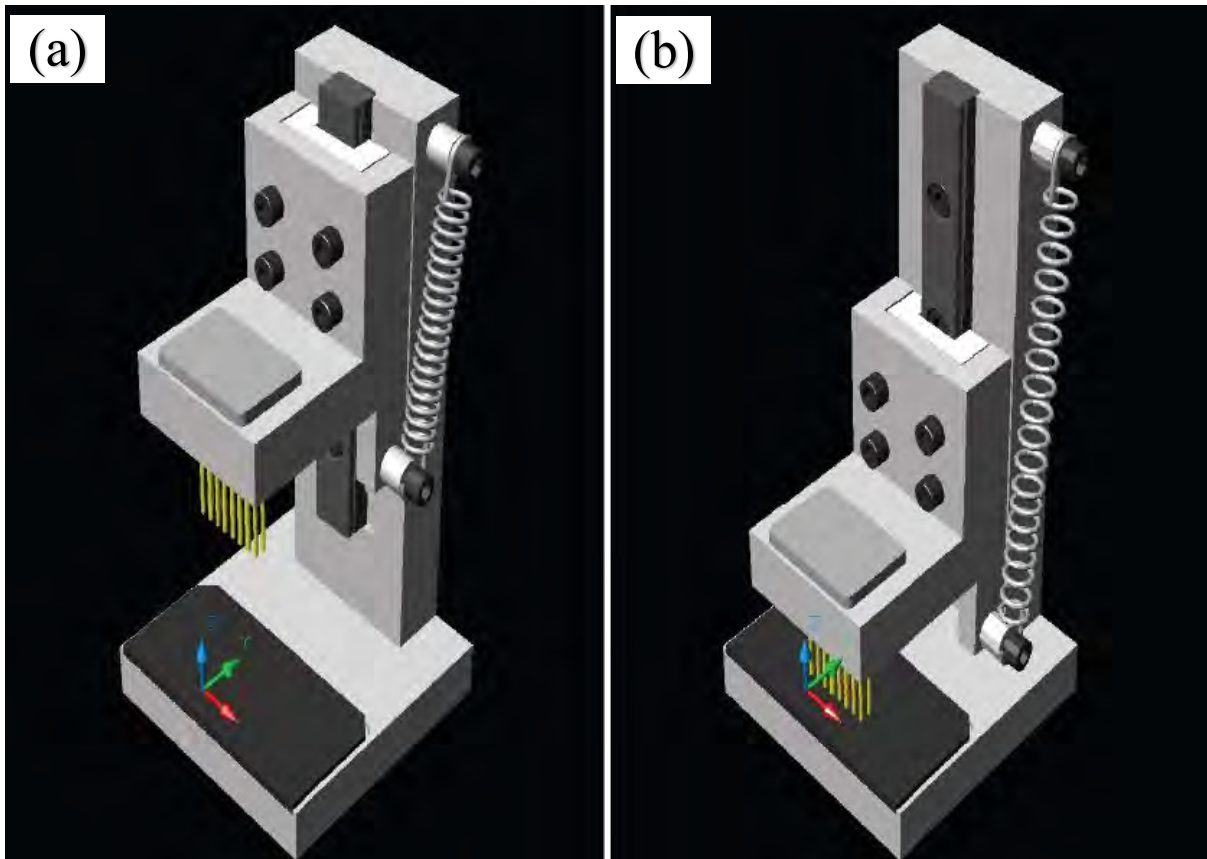


Figure 7.1: Proposed new punch; (a) punch press at rest position; (b) punch press at cutting/punching position. The new punch design aims to conserve/maintain precision between the punching process of microfluidic chip access ports and microfluidic plug development. Once precision is maintained, the separation on the microfluidic plug's pins and the punched access ports on the microfluidic chip will be identical, thus removing the problem of microfluidic plug to chip misalignment. The new punch will be able to create 16 access ports at a time with the much needed accuracy. This punch will be highly suitable for use on the hybrid dual port microfluidic chip. The new proposed punch is a manual punch making it a cheaper solution to the existing problem than introducing an automated robotic punching system.

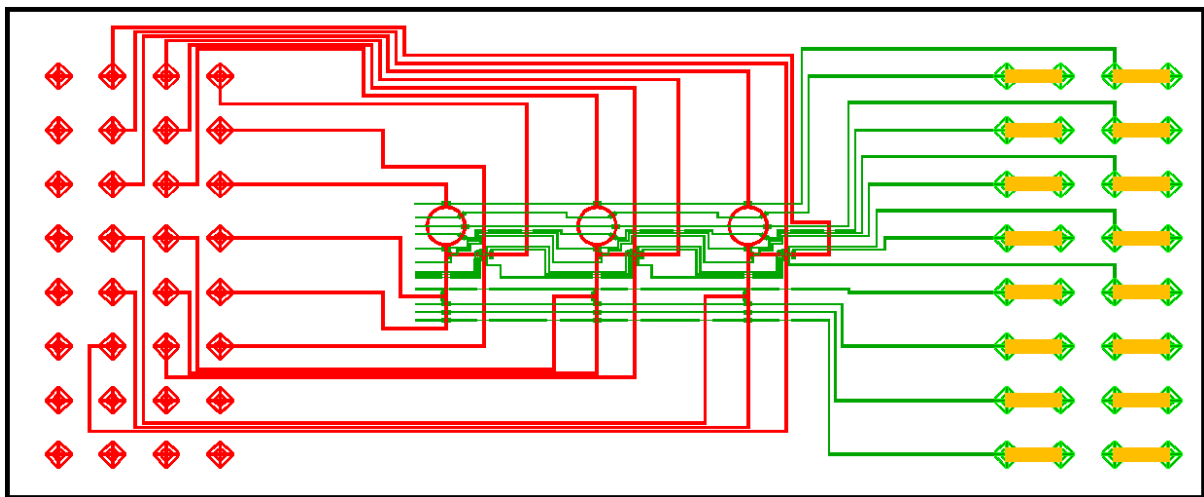


Figure 7.2: Proposed new hybrid dual port microfluidic device geometry. This proposed device is exactly the same as the old hybrid dual port microfluidic chip; instead of the 10 μm high and 100 μm wide ‘bridge’, the inter-connected access ports have a 500 μm high and 500 μm wide ‘bridge’ channel, this is shown in yellow. We expect this new design to increase the efficiency of the system by removing the introduced air more rapidly.

APPENDICES

Appendix A: Single Port, Dual Port, Hybrid Dual Port Microfluidic Device Master Mold Protocol and Single Port and Dual Port PDMS Microfluidic Device Fabrication Protocol

Rectangular channel: 10 μ m height

1.	SILANIZATION	None
2.	SPIN	Negative Photoresist: SU8-2010 Spin at 3000rpm, 1min, ACL = 130rpm/sec
3.	PRE-EXPOSURE BAKE	65 ⁰ C → 1min 95 ⁰ C → 2mins
4.	ALIGN	[if necessary]
5.	EXPOSE	1.5secs
6.	POST-EXPOSURE BAKE	65 ⁰ C → 1mins 95 ⁰ C → 3mins
7.	DEVELOP	Use Developer SU-8 Developer : 100% <ol style="list-style-type: none"> Develop for 1 – 2mins until a shiny surface engulfs the entire wafer Rinse in fresh SU-8 developer Spray with fresh SU-8 developer to flush out excess residue Dry gently with air gun
8.	PROFILE	[if necessary] ~ Mold will be rectangular at this point
9.	ROUNDING STEP	None
10.	PROFILE	None
11.	HARD BAKE	None
12.	PROFILE	None

Rounded channel: 10 μ m height

1.	SILANIZATION	HMDS for 2 mins
2.	SPIN	Positive Photoresist: MAP 1275 Spin at 1200rpm, 1min, ACL = 133rpm/sec
3.	PRE-EXPOSURE BAKE	95 ⁰ C → 90secs
4.	ALIGN	[if necessary]
5.	EXPOSE	15secs
6.	POST-EXPOSURE BAKE	None
7.	DEVELOP	Use Developer ma-D 531 : 100% <ul style="list-style-type: none"> e. Develop for 3 – 5mins until a shiny surface engulfs the entire wafer f. Rinse in fresh water g. Spray with fresh water to flush out excess developer h. Dry gently with air gun
8.	PROFILE	[if necessary] ~ Mold will be rectangular at this point
9.	ROUNDING STEP	Leave the rectangular mold overnight <u>Mold Reflow:</u> <div style="display: flex; align-items: center; justify-content: center;"> <div style="text-align: center;"> <p>65⁰C → 3mins</p> <p>115⁰C → 15mins</p> </div> <div style="font-size: 2em; margin: 0 10px;">}</div> <div style="text-align: left;"> <p>Directly on hot plate</p> </div> </div>
10.	PROFILE	Profile to ensure rounded cross-section. Mold will be rounded at this point. Single shiny line will be visible
11.	HARD BAKE	<u>[If layering on top]:</u> <ul style="list-style-type: none"> a. Set oven to 120⁰C b. Place mold in oven at 120⁰C c. Ramp oven to 180⁰C d. Leave in the oven for 1hr at 180⁰C e. Ramp down oven to 120⁰C
12.	PROFILE	Profile to ensure rounded cross-section

Single Port and Dual Port PDMS Microfluidic Device Fabrication Protocol

1. Cleaning molds:

- Wafers are to be silanized using TCMS vapours for 2 minutes in air tight container.

2. Flow layer PDMS casting:

- Prepare an 80grams:16grams PDMS mixture (5:1 elastomer base to cross-linker base) in a plastic cup. This gives a 4 – 5 mm thick layer.
- Perform a weight measurement of the PDMS containing cup and the mixer cup holder is done and the correct measurement is entered into the planetary centrifugal mixer machine for mixing.
- Planetary centrifugal mixer settings: Speed – 2200 rpm; Mixing time – 5 minutes; Defoaming time – 5 minutes.
- After PDMS mixing, pour the PDMS mixture onto the flow layer master mold which are in an aluminium foil covered petri dish.
- Place the flow layer master molds in a desiccator under vacuum for de-bubbling until all bubbles have risen to the surface of the PDMS.
- Remove the bubbles in the area on of concern (i.e. device pattern) using a spreader.
- Repeat the de-bubbling and bubble removal step until no bubbles are left covering the pattern.
- Place the flow layer containing petri dish in the oven for 40 minutes at 80 °C.

3. Control layer PDMS casting and glass slide/ cover slip coating:

- Prepare a 20grams:1grams PDMS mixture (20:1 elastomer base to cross-linker base) in a plastic cup.
- Perform a weight measurement of the PDMS containing cup and the mixer cup holder is done and the correct measurement is entered into the planetary centrifugal mixer machine for mixing.

- Planetary centrifugal mixer settings: Speed – 2200 rpm; Mixing time – 5 minutes; De-foaming time – 5 minutes.
- After PDMS mixing, spin coat the control layer master mold and the microscope glass slide in a spin coater.
- Spin coater settings: Speed – 1800 rpm; Time – 1 minute; Acceleration – 500rpm/second.
- After spin coating, let stand for 5 minutes then place the spin-coated components i.e. the control layer master mold and glass slide into oven for 40 minutes at 80 °C.

4. Alignment:

- After the baking of the flow layer master mold is complete.
- Peel off the PDMS flow layer from the master mold and cut to size using a razorblade or scalpel.
- Create flow channel access ports by punching the port patterns on the PDMS layer using a punch press.
- Align the flow layer PDMS layer onto the PDMS spin-coated and soft-baked control layer master mold. This can be aided by using a microscope.

5. PDMS bonding:

- After the alignment procedure is complete.
- Place the aligned device in oven for 40 minutes at 80 °C.
- After the baking is complete.
- Cut and peel off the bonded device off the control layer mold.
- Create control channel access ports by punching the port patterns on the PDMS layer using a punch press.

6. Substrate bonding:

- Place the multi-layered bonded onto on a cured PDMS coated glass slide.

- Place the microfluidic device in an oven at 80 °C for several hours (usually 9 – 12 hours) to allow the PDMS structures control layer to bond to the substrate.
- After the baking, the PDMS device is ready for use.

Appendix B: Hybrid Dual Port PDMS Microfluidic Device Fabrication Protocol

1. Cleaning molds:

- Wafers are to be silanized using TCMS vapours for 2 minutes in air tight container.

2. Control layer PDMS casting:

- Prepare an 80grams:16grams PDMS mixture (5:1 elastomer base to cross-linker base) in a plastic cup. This gives a 4 – 5 mm thick layer.
- Perform a weight measurement of the PDMS containing cup and the mixer cup holder is done and the correct measurement is entered into the planetary centrifugal mixer machine for mixing.
- Planetary centrifugal mixer settings: Speed – 2200 rpm; Mixing time – 5 minutes; Defoaming time – 5 minutes.
- After PDMS mixing, pour the PDMS mixture onto the control layer master mold which are in an aluminium foil covered petri dish.
- Place the control layer master molds in a desiccator under vacuum for de-bubbling until all bubbles have risen to the surface of the PDMS.
- Remove the bubbles in the area on of concern (i.e. device pattern) using a spreader.
- Repeat the de-bubbling and bubble removal step until no bubbles are left covering the pattern.
- Place the control layer containing petri dish in the oven for 40 minutes at 80 °C.

3. Flow layer PDMS casting and glass slide/ cover slip coating:

- Prepare a 20grams:1grams PDMS mixture (20:1 elastomer base to cross-linker base) in a plastic cup.
- Perform a weight measurement of the PDMS containing cup and the mixer cup holder is done and the correct measurement is entered into the planetary centrifugal mixer machine for mixing.

- Planetary centrifugal mixer settings: Speed – 2200 rpm; Mixing time – 5 minutes; De-foaming time – 5 minutes.
- After PDMS mixing, spin coat the flow layer master mold and the microscope glass slide in a spin coater.
- Spin coater settings: Speed – 1800 rpm; Time – 1 minute; Acceleration – 500rpm/second.
- After spin coating, let stand for 5 minutes then place the spin-coated components i.e. the flow layer master mold and glass slide into oven for 40 minutes at 80 °C.

4. Alignment:

- After the baking of the control layer master mold is complete.
- Peel off the PDMS control layer from the master mold and cut to size using a razorblade or scalpel.
- Create control channel access ports by punching the port patterns on the PDMS layer using a punch press.
- Align the control layer PDMS layer onto the PDMS spin-coated and soft-baked flow layer master mold. This can be aided by using a microscope.

5. PDMS bonding:

- After the alignment procedure is complete.
- Place the aligned device in oven for 40 minutes at 80 °C.
- After the baking is complete.
- Cut and peel off the bonded device off the flow layer mold.
- Create flow channel access ports by punching the port patterns on the PDMS layer using a punch press.

6. Substrate bonding:

- Place the multi-layered bonded onto on a cured PDMS coated glass slide.

- Place the microfluidic device in an oven at 80 °C for several hours (usually 9 – 12 hours) to allow the PDMS structures control layer to bond to the substrate.
- After the baking, the PDMS device is ready for use.

REFERENCES

1. Melin, J. and S.R. Quake, *Microfluidic large-scale integration: the evolution of design rules for biological automation*. Annu. Rev. Biophys. Biomol. Struct., 2007. **36**: p. 213-231.
2. Whitesides, G.M., *The origins and the future of microfluidics*. Nature, 2006. **442**(7101): p. 368-373.
3. Unger, M.A., et al., *Monolithic microfabricated valves and pumps by multilayer soft lithography*. Science, 2000. **288**(5463): p. 113-116.
4. Martinez-Duarte, R. and M. Madou, *SU-8 photolithography and its impact on microfluidics, in Microfluidics and Nanofluidics Handbook: Fabrication, Implementation and Applications*. 2010, p. 231-268.
5. Szlezák, N.A., et al., *The global health system: actors, norms, and expectations in transition*. PLoS Med, 2010. **7**(1): p. e1000183.
6. Aleku, G.A., M.P. Adoga, and S.M. Agwale, *HIV point-of-care diagnostics: meeting the special needs of sub-Saharan Africa*. The Journal of Infection in Developing Countries, 2014. **8**(10): p. 1231-1243.
7. Ki-moon, U.S.-G.B., *The Millennium Development Goals Report 2013*. United Nations Pubns, 2013.
8. WHO. *The 2014 Update, Global health Workforce Statistics Database*. 2014 [cited 2015 June 15]; Available from: <http://www.who.int/hrh/statistics/hwfstats>.
9. Nigel Crisp, M.A. and M.D. Lincoln Chen, *Global supply of health professionals*. The New England Journal of Medicine 2014. **370**(10).
10. Tawfik, L. and S. Kinoti, *The impact of HIV/AIDS on health systems and the health workforce in sub-Saharan Africa*. Washington (DC): SARA Project, USAID Bureau for Africa, 2003.

11. UNAIDS. *Fact Sheet 2014*. 2014 [cited 2015 June 11]; Available from: <http://www.unaids.org>.
12. Kaplan, J.E., et al., *The Impact of HIV Care and Support Interventions on Key Outcomes in Low-and Middle-Income Countries: A Literature Review—Introduction*. JAIDS Journal of Acquired Immune Deficiency Syndromes, 2015. **68**: p. S253-S256.
13. WHO., *Global Tuberculosis Report 2014*. 2014: World Health Organization.
14. Prüss-Üstün, A., E. Rapiti, and Y. Hutin, *Estimation of the global burden of disease attributable to contaminated sharps injuries among health-care workers*. American journal of industrial medicine, 2005. **48**(6): p. 482-490.
15. Shisana, O., et al., *HIV/AIDS prevalence among South African health workers: original article*. South African Medical Journal, 2004. **94**(10): p. p. 846-850.
16. Marchal, B., V.D. Brouwere, and G. Kegels, *Viewpoint: HIV/AIDS and the health workforce crisis: What are the next steps?* Tropical Medicine & International Health, 2005. **10**(4): p. 300-304.
17. Sharma, S., et al., *Point-of-Care Diagnostics in Low Resource Settings: Present Status and Future Role of Microfluidics*. Biosensors, 2015. **5**(3): p. 577-601.
18. Unger, A., T. Welz, and D. Haran. *The impact of HIV/AIDS on health care staff at a rural South African hospital, 1990–2001*. in *XIV International AIDS Conference*. 2002.
19. Yager, P., et al., *Microfluidic diagnostic technologies for global public health*. Nature, 2006. **442**(7101): p. 412-418.
20. Yager, P., G.J. Domingo, and J. Gerdes, *Point-of-care diagnostics for global health*. Annu. Rev. Biomed. Eng., 2008. **10**: p. 107-144.
21. Nichols, J.H., *Point of care testing*. Clinics in laboratory medicine, 2007. **27**(4): p. 893-908.

22. Peeling, R. and D. Mabey, *Point-of-care tests for diagnosing infections in the developing world*. *Clinical Microbiology and Infection*, 2010. **16**(8): p. 1062-1069.
23. Murtagh, M. *HIV/AIDS diagnostic technology landscape*. 2012 [cited 2015 June 17]; Available from: <http://www.unaids.org/en/about/market-approach/9-uncategorised/345-technical-reports>.
24. Leuvering, J.H., et al., *Sol particle immunoassay (SPIA)*. *Journal of immunoassay*, 1980. **1**(1): p. 77-91.
25. Shetty, S., et al., *Laboratory Tests for HIV: Diagnosing, monitoring and managing AIDS-an overview*. *International Journal of Oral and Maxillofacial Pathology*, 2011. **2**(1): p. 20-28.
26. Mark, D., et al., *Microfluidic lab-on-a-chip platforms: requirements, characteristics and applications*. *Chemical Society Reviews*, 2010. **39**(3): p. 1153-1182.
27. OrasureTechnologies. [cited 2016 February 01]; Available from: <http://www.orasure.com/products-infectious/products-infectious-oraquick.asp>.
28. MedMira. [cited 2016 February 01]; Available from: <http://medmira.com/products/hiv/reveal-g3>.
29. TrinityBiotech. [cited 2016 February 01]; Available from: <http://www.trinitybiotech.com/products/uni-gold-hiv/>.
30. Delaney, K.P., et al., *Evaluation of the performance characteristics of 6 rapid HIV antibody tests*. *Clinical Infectious Diseases*, 2011. **52**(2): p. 257-263.
31. Klarkowski, D.B., et al., *The evaluation of a rapid in situ HIV confirmation test in a programme with a high failure rate of the WHO HIV two-test diagnostic algorithm*. *PLoS One*, 2009. **4**(2): p. e4351.

32. Choko, A.T., et al., *The uptake and accuracy of oral kits for HIV self-testing in high HIV prevalence setting: a cross-sectional feasibility study in Blantyre, Malawi*. PLoS Med, 2011. **8**(10): p. e1001102.
33. Pai, N.P. and M. Pai, *Point-of-care diagnostics for HIV and tuberculosis: landscape, pipeline, and unmet needs*. Discovery medicine, 2012. **13**(68): p. 35-45.
34. Perkins, M.D. and J. Cunningham, *Facing the crisis: improving the diagnosis of tuberculosis in the HIV era*. Journal of Infectious Diseases, 2007. **196**(Supplement 1): p. S15-S27.
35. Rie, A.V., et al., *Xpert® MTB/RIF for point-of-care diagnosis of TB in high-HIV burden, resource-limited countries: hype or hope?* Expert Rev. Mol. Diagn., 2010. **10**(7): p. 937-946.
36. Carr, J.H. *Gram-positive Mycobacterium tuberculosis bacteria*. . 2006 [cited 2016 January 27]; Available from: <http://phil.cdc.gov/phil/details.asp?pid=9997>.
37. Eirik. *Who's in Control: The Human Host or the Microbiome?* 2014 [cited 2016 January 27]; Available from: <http://darwinian-medicine.com/whos-in-control-the-human-host-or-the-microbiome/>.
38. Dearden, L. *Warning at Manchester University after student, 19, dies of meningitis*. 2014 [cited 2016 January 27]; Available from: <http://imgbuddy.com/haemophilus-influenzae.asp> & <http://www.independent.co.uk/news/uk/home-news/warning-at-manchester-university-after-student-19-dies-of-meningitis-9838880.html>.
39. Unknown. *The Immune System - Overview*. 2004 [cited 2016 January 27]; Nobel Media AB 2014]. Available from: <http://www.nobelprize.org/educational/medicine/immunity/immune-overview.html>.
40. Unknown. *The Human Defence System*. [cited 2016 January 27]; Available from: <http://leavingbio.net/the%20human%20defence%20system-web-2.htm>.

41. Unknown. *Rapid colorimetric drug susceptibility test (DST)*. [cited 2016 January 27]; MDRTB grew in detection, isoniazid and rifampicin containing quadrants, but the quinolone (blue) prevented TB growth, ruling out XDRTB.]. Available from: http://www.finddiagnostics.org/programs/tb/find_activities/rapid_colorimetric_dst.html.
42. Unknown. 2015 [cited 2016 January 27]; Available from: <http://www.gasdetectorsafety.com/top-5-dangerous-volatile-organic-compounds/>.
43. Cisbio. *Human IL6 & Mouse IL6 Assay Kits*. [cited 2016 January 27]; Available from: <http://www.cisbio.com/usa/drug-discovery/human-il6-mouse-il6-assay-kits>.
44. Classroomclipart. [cited 2016 January 27]; Available from: http://classroomclipart.com/images/gallery/Clipart/Occupation/bologist_with_microscope.jpg.
45. Shaikh, S. *Suburban Diagnostics is revolutionizing Microbiology with the help of advanced machinery and speedy diagnosis*. [cited 2016 January 27]; Genexpert / MTB / RIF]. Available from: <http://www.suburbandiagnosics.com/microbiology-test>.
46. Unknown. [cited 2016 January 27]; Available from: http://schools-wikipedia.org/wp/i/Immune_system.htm.
47. Pai, M. and R. O'Brien. *New diagnostics for latent and active tuberculosis: state of the art and future prospects*. in *Seminars in respiratory and critical care medicine*. 2008.
48. Mao, X. and T.J. Huang, *Microfluidic diagnostics for the developing world*. *Lab on a Chip*, 2012. **12**(8): p. 1412-1416.
49. United, S., *An act to provide assistance to foreign countries to combat HIV/AIDS, tuberculosis, and malaria, and for other purposes. United States Leadership Against HIV/AIDS, Tuberculosis, and Malaria Act of 2003. Public Law 108-25*. United States statutes at large, 2003. **117**: p. 711.

50. PEPFAR. *PEPFAR Overview*. [cited 2015 July 02]; Available from: <http://www.pepfar.gov/documents/organization/189671.pdf>.
51. Batz, H.-G., G.S. Cooke, and S.D. Reid, *Towards lab-free tuberculosis diagnosis*. Treatment Action Group, the TB/HIV Working Group of the Stop TB Partnership, Imperial College, MSF. Geneva, 2011.
52. Anderson, J.R., et al., *Fabrication of microfluidic systems in poly (dimethylsiloxane)*. *Electrophoresis*, 2000. **21**(1): p. 27-40.
53. Terry, S.C., J.H. Jerman, and J.B. Angell, *A gas chromatographic air analyzer fabricated on a silicon wafer*. *Electron Devices, IEEE Transactions on*, 1979. **26**(12): p. 1880-1886.
54. Manz, A., et al., *Design of an open-tubular column liquid chromatograph using silicon chip technology*. *Sensors and actuators B: Chemical*, 1990. **1**(1): p. 249-255.
55. Hindson, B.J., et al., *APDS: the autonomous pathogen detection system*. *Biosensors and Bioelectronics*, 2005. **20**(10): p. 1925-1931.
56. Brody, J.P., et al., *Biotechnology at low Reynolds numbers*. *Biophysical journal*, 1996. **71**(6): p. 3430-3441.
57. Radenovic, A., *MICROFLUIDICS LAB ON CHIP*. *Advanced Bioengineering methods laboratory*: p. 1-27.
58. Stone, H.A., A.D. Stroock, and A. Ajdari, *Engineering flows in small devices: microfluidics toward a lab-on-a-chip*. *Annu. Rev. Fluid Mech.*, 2004. **36**: p. 381-411.
59. Squires, T.M. and S.R. Quake, *Microfluidics: Fluid physics at the nanoliter scale*. *Reviews of modern physics*, 2005. **77**(3): p. 977.
60. Vaid, A., R. Singh, and P. Lehana, *DEVELOPEMENT OF MICROCHANNEL FABRICATION TECHNIQUE AND METHOD TO INCREASE TRENCH DEPTH ON PDMS*.

International Journal of Advanced Research in Computer and Communication Engineering, 2013. **2**(12): p. 4856-4861.

61. Pennathur, S., C.D. Meinhart, and H.T. Soh, *How to exploit the features of microfluidics technology*. Lab on a Chip, 2008. **8**(1): p. 20-22.
62. Beebe, D.J., G.A. Mensing, and G.M. Walker, *Physics and applications of microfluidics in biology*. Annual review of biomedical engineering, 2002. **4**(1): p. 261-286.
63. Haeberle, S., et al., *Centrifugal micromixery*. Chemical engineering & technology, 2005. **28**(5): p. 613-616.
64. Duffy, D.C., et al., *Microfabricated centrifugal microfluidic systems: characterization and multiple enzymatic assays*. Analytical Chemistry, 1999. **71**(20): p. 4669-4678.
65. Honda, N., et al., *Simultaneous multiple immunoassays in a compact disc-shaped microfluidic device based on centrifugal force*. Clinical Chemistry, 2005. **51**(10): p. 1955-1961.
66. Mark, D., et al., *Centrifugo-pneumatic valve for metering of highly wetting liquids on centrifugal microfluidic platforms*. Lab on a Chip, 2009. **9**(24): p. 3599-3603.
67. Ducrée, J., et al., *The centrifugal microfluidic Bio-Disk platform*. Journal of Micromechanics and Microengineering, 2007. **17**(7): p. S103.
68. Hugo, S., et al., *A centrifugal microfluidic platform for point-of-care diagnostic applications*. South African Journal of Science, 2014. **110**(1-2): p. 1-7.
69. Smith, S., et al., *CD-Based Microfluidics for Primary Care in Extreme Point-of-Care Settings*. Micromachines, 2016. **7**(2): p. 22.
70. Chanmanwar, R., R. Balasubramaniam, and L. Wankhade, *Application and manufacturing of microfluidic devices: review*. IJMER, 2013. **3**: p. 849-856.

71. Dragoi, V., E. Cakmak, and E. Pabo, *Metal wafer bonding for MEMS devices*. Romanian J. Inf. Sci. Technol, 2010. **13**(1): p. 65-72.
72. Bubendorfer, A., X. Liu, and A.V. Ellis, *Microfabrication of PDMS microchannels using SU-8/PMMA moldings and their sealing to polystyrene substrates*. Smart Materials and Structures, 2007. **16**(2): p. 367.
73. Loke, Y., et al. *Micro injection-molding of cyclic olefin copolymer using metallic glass insert*. 2007 [cited 2016 January 27]; Available from: <http://hdl.handle.net/1721.1/35813>.
74. Nunes, P.S., et al., *Cyclic olefin polymers: emerging materials for lab-on-a-chip applications*. Microfluidics and nanofluidics, 2010. **9**(2-3): p. 145-161.
75. Capanu, M., J.G. Boyd IV, and P.J. Hesketh, *Design, fabrication, and testing of a bistable electromagnetically actuated microvalve*. Microelectromechanical Systems, Journal of, 2000. **9**(2): p. 181-189.
76. Hasegawa, T., et al., *Multi-directional micro-switching valve chip with rotary mechanism*. Sensors and Actuators A: Physical, 2008. **143**(2): p. 390-398.
77. Shoji, S. and M. Esashi, *Microflow devices and systems*. Journal of Micromechanics and Microengineering, 1994. **4**(4): p. 157.
78. Oh, K.W. and C.H. Ahn, *A review of microvalves*. Journal of micromechanics and microengineering, 2006. **16**(5): p. R13.
79. Zhang, C., D. Xing, and Y. Li, *Micropumps, microvalves, and micromixers within PCR microfluidic chips: advances and trends*. Biotechnology advances, 2007. **25**(5): p. 483-514.
80. Smits, J.G., *Piezoelectric micropump with three valves working peristaltically*. Sensors and Actuators A: Physical, 1990. **21**(1): p. 203-206.

81. Krutzch, W. and P. Cooper, *Introduction: classification and selection of pumps Pump Handbook ed IJ Karassik et al.* 2001, New York: McGraw-Hill.
82. Laser, D. and J. Santiago, *A review of micropumps.* Journal of micromechanics and microengineering, 2004. **14**(6): p. R35.
83. Kumar, A. and G.M. Whitesides, *Features of gold having micrometer to centimeter dimensions can be formed through a combination of stamping with an elastomeric stamp and an alkanethiol 'ink' followed by chemical etching.* Applied Physics Letters, 1993. **63**(14): p. 2002-2004.
84. Abbott, N.L., A. Kumar, and G.M. Whitesides, *Using micromachining, molecular self-assembly, and wet etching to fabricate 0.1-1- μ m-scale structures of gold and silicon.* Chemistry of materials, 1994. **6**(5): p. 596-602.
85. Singhvi, R., et al., *Engineering cell shape and function.* Science, 1994. **264**(5159): p. 696-698.
86. Wilbur, J.L., et al., *Lithographic molding: A convenient route to structures with sub-micrometer dimensions**.* Advanced Materials, 1995. **7**(7): p. 649-652.
87. Xia, Y. and G.M. Whitesides, *Soft lithography.* Annual review of materials science, 1998. **28**(1): p. 153-184.
88. Voldman, J., M.L. Gray, and M.A. Schmidt, *Microfabrication in biology and medicine.* Annual review of biomedical engineering, 1999. **1**(1): p. 401-425.
89. Sia, S.K. and G.M. Whitesides, *Microfluidic devices fabricated in poly (dimethylsiloxane) for biological studies.* Electrophoresis, 2003. **24**(21): p. 3563-3576.

90. Unknown. *Tutorial Lithography Nanopatterning*. [cited 2015 August 03]; Available from: <http://www.sigmaaldrich.com/materials-science/micro-and-nanoelectronics/lithography-nanopatterning/tutorial.html>.
91. Pearson, R. and R. Dyson, *Specialty polymers*. Dyson, RW, Ed, 1987: p. 150.
92. San-Miguel, A. and H. Lu. *Microfluidics as a tool for C. elegans research*. 2005 [cited 2016 January 27]; Available from: <http://www.ncbi.nlm.nih.gov/books/NBK174829/>.
93. Wolfe, D.B., D. Qin, and G.M. Whitesides, *Rapid prototyping of microstructures by soft lithography for biotechnology*, in *Microengineering in Biotechnology*. 2010, Springer. p. 81-107.
94. Quake, S.R. and A. Scherer, *From micro-to nanofabrication with soft materials*. *Science*, 2000. **290**(5496): p. 1536-1540.
95. Fordyce, P., et al., *Systematic characterization of feature dimensions and closing pressures for microfluidic valves produced via photoresist reflow*. *Lab on a Chip*, 2012. **12**(21): p. 4287-4295.
96. Pai, N.P., et al., *Point-of-care testing for infectious diseases: diversity, complexity, and barriers in low-and middle-income countries*. *PLoS Med*, 2012. **9**(9): p. e1001306.
97. Chin, C.D., et al., *Microfluidics-based diagnostics of infectious diseases in the developing world*. *Nature medicine*, 2011. **17**(8): p. 1015-1019.
98. Luthuli, B.B., G.E. Purdy, and F.K. Balagaddé, *Confinement-Induced Drug-Tolerance in Mycobacteria Mediated by an Efflux Mechanism*. *PloS one*, 2015. **10**(8): p. e0136231.
99. OLYMPUS. *Olympus Products/Digital Cameras*. [cited 2015 August 31]; Available from: <http://www.olympus-ims.com/en/microscope/sc30/> & <http://www.olympus-ims.com/en/microscope/sc100/>

100. Unknown. [cited 2015 August 31]; Available from: <http://web.stanford.edu/group/foundry/index.html>.
101. LT Jr, C.S., *An automatic method for colorimetric analysis*. Amer. J. Clin. Pathol, 1957. **28**: p. 311-22.
102. Jensen, E.C., *Fluidic Microvalve Digital Processors for Automated Biochemical Analysis*. 2011, UC Berkeley Electronic Theses and Dissertations.
103. Feng, J., et al., *An Automated Fluid-transport Device for a Microfluidic System*. Analytical Sciences, 2011. **27**(10): p. 1057.
104. VICI. [cited 2015 September 28]; Available from: <http://www.vici.com/vval/sd.php> & <http://www.vici.com/vval/sf.php>.
105. Elliott, C., et al., *National instruments LabVIEW: a programming environment for laboratory automation and measurement*. Journal of the Association for Laboratory Automation, 2007. **12**(1): p. 17-24.
106. D.Chin, C., et al., *Low-Cost Microdevices for Point-of-Care Testing*. Point-of-Care Diagnostics on a Chip, 2013.
107. Mullan, F., et al., *Medical schools in sub-Saharan Africa*. The Lancet, 2011. **377**(9771): p. 1113-1121.